Vol. 4 No. 2 2019
ISSN:1390-9347

Bionatura

Latin American journal of Biotechnology and Life Sciences

Will our next revolution support or obstruct the achievement of the Sustainable Development Goals?

Effectiveness of chitosan as natural coagulant in treating turbid waters
The structure of Neurexin 1α (n1α) and its role as synaptic organizer

UCO Universidad Católica de Oriente
clinicalbiotec.com
UNIVERSIDAD YACHAY TECH
CBB

http://www.revistabionatura.com/ https://www.facebook.com/bionaturajournal/ https://twitter.com/rbionatura

Vol. 4 No. 2 2019

Bionatura

La Revista Bionatura publica trimestral en español o inglés trabajos inéditos de investigaciones básicas y aplicadas en el campo de la Biotecnología, la Inmunología, la Bioquímica, Ensayos Clínicos y otras disciplinas afines a las ciencias biologícas, dirigidas a la obtención de nuevos conocimientos, evaluación y desarrollo de nuevas tecnologías, productos y procedimientos de trabajo con un impacto a nivel mundial.

Equipo editorial

latindex

Index in directory of open access journals

Instrucciones para los Autores

Los Trabajos serán Inéditos: Una vez aprobados, no podrán someterse a la consideración de otra revista, con vistas a una publicación múltiple, sin la debida autorización del Comité Editorial de la Revista. La extensión máxima será 8 cuartillas para los trabajos originales, 12 las revisiones y 4 las comunicaciones breves e informes de casos, incluidas las tablas y figuras. Los artículos se presentarán impresos (dos ejemplares). Todas las páginas se numerarán con arábigos y consecutivamente a partir de la primera. Estos deben acompañarse de una versión digital (correo electrónico o CD) en lenguaje Microsoft Word, sin sangrías, tabuladores o cualquier otro atributo de diseño (títulos centrados, justificaciones, espacios entre párrafos, etc.). Siempre se ha de adjuntar la carta del consejo científico que avala la publicación y una declaración jurada de los autores.

Referencias Bibliográficas. Se numerarán según el orden de mención en el texto y deberán identificarse mediante arábigos en forma exponencial. Los trabajos originales no sobrepasarán las 20 citas; las revisiones, de 25 a 50 y las comunicaciones breves e informes de casos.

En las Referencias en caso de que las publicaciones revisadas esten online se debe proveer un enlace consistente para su localización en Internet. Actualmente, no todos los documentos tienen DOI, pero si lo tienen se debe incluir como parte de la referencias. Si no tuviese DOI, incluir la URL.

Tablas, modelos y anexos: Se presentarán en hojas aparte (no se intercalarán en el artículo) y en forma vertical numeradas consecutivamente y mencionadas en el texto. Las tablas se ajustarán al formato de la publicación se podrán modificar si presentan dificultades técnicas.

Figuras: Las fotografías, gráficos, dibujos, esquemas, mapas, salidas de computadora, otras representaciones gráficas y fórmulas no lineales, se denominarán figuras y tendrán numeración arábiga consecutiva. Se presentarán impresas en el artículo en páginas independientes y en formato digital con una resolución de 300 dpi. Todas se mencionarán en el texto. Los pies de figuras se colocarán en página aparte. El total de las figuras y tablas ascenderá a 5 para los trabajos originales y de revisión y 3 para las comunicaciones breves e informes de casos.

Abreviaturas y siglas: Las precederá su nombre completo la primera vez que aparezcan en el texto. No figurarán en títulos ni resúmenes. Se emplearán las de uso internacional.

Sistema Internacional de Unidades (SI): Todos los resultados de laboratorio clínico se informarán en unidades del SI o permitidas por este. Si se desea añadir las unidades tradicionales, se escribirán entre paréntesis. Ejemplo: glicemia: 5,55 mmol/L (100 mg/100 mL).

Para facilitar la elaboración de los originales, se orienta a los autores consultar los requisitos uniformes antes señalados disponibles en: http://www. fisterra.com/recursos_web/mbelvancouver.htm#ilustraciones%20 (figura)

Los trabajos que no se ajusten a estas instrucciones, se devolverán a los autores. Los aceptados se procesarán según las normas establecidas por el Comité Editorial. El arbitraje se realizará por pares y a doble ciego en un período no mayor de 60 días. Los autores podrán disponer de no más de 45 días para enviar el artículo con correcciones, se aceptan hasta tres reenvíos. El Consejo de Redacción se reserva el derecho de introducir modificaciones de estilo y /o acotar los textos que lo precisen, comprometiéndose a respetar el contenido original.

El Comité Editorial de la Revista se reserva todos los derechos sobre los trabajos originales publicados en esta.

Bionatura

La Revista Bionatura es un medio especializado, interinstitucional e interdisciplinario, para la divulgación de desarrollos científicos y técnicos, innovaciones tecnológicas, y en general, los diversos tópicos relativos a los sectores involucrados en la biotecnología, tanto en Ecuador como en el exterior; así mismo, la revista se constituye en un mecanismo eficaz de comunicación entre los diferentes profesionales de la biotecnología.

Es una publicación sin ánimo de lucro. Los ingresos obtenidos por publicidad o servicios prestados serán destinados para su funcionamiento y desarrollo de su calidad de edición. (http://revistabionatura.com/media-kit.html)

Es una revista trimestral, especializada en temas concernientes al desarrollo teórico, aplicado y de mercado en la biotecnología.

Publica artículos originales de investigación y otros tipos de artículos científicos a consideración de su consejo editorial, previo proceso de evaluación por pares (peer review) sin tener en cuenta el país de origen.

Los idiomas de publicación son el Español e Inglés.

Esta revista utiliza Open Journal Systems, que es un gestor de revistas de acceso abierto y un software desarrollado, financiado y distribuido de forma gratuita por el proyecto Public Knowledge Project sujeto a la Licencia General Pública de GNU.

Nuestros contactos deben ser dirigidos a:
Revista Bionatura: editor@revistabionatura.com

ISSN: 1390-9347 (Versión impresa)
Formato: 21 x 29,7 cm
ISSN: 1390-9355 (Versión electrónica)
Sitio web: **http://www.revistabionatura.com**

Publicación periódica trimestral
Esta revista utiliza el sistema peer review para la evaluación de los manuscritos enviados.

Instrucciones a los autores en:
http://revistabionatura.com/instrucciones.html

Asistente de publicación / Publication assistant
Evelyn Padilla Rodriguez (sales@revistabionatura.com)

ÍNDICE / INDEX

CASE REPORTS / REPORTE DE CASOS

REVIEWS / REVISIONES

NEWS AND VIEWS / NOTICIA Y OPINIONES

ZURITA & ZURITA Laboratorios

LABORATORIO CLÍNICO

Desde 1959

Investigación
Docencia
Servicio

CERTIFIED IQNet MANAGEMENT SYSTEM

ISO 9001 icontec internacional SC6659-1

REALIZAMOS PRUEBAS EN:

- Microbiología
- Parasitología
- Marcadores Tumorales
- Biología Molecula
- Citología Vaginal
- Coagulación y Hemostasia
- Endocrinología
- Hematología
- Inmunología
- Bioquímica Clínica
- Uroanálisis
- Toxicología y Drogas
- Citometría de Flujo
- Micología

PBX.: 3 945 120

INVESTIGACIÓN + DOCENCIA + SERVICIO

www.zuritalaboratorios.com

contacto@zuritalaboratorios.com

EDITORIAL

The First Geopark in Ecuador: Imbabura.

Yaniel Misael Vázquez Taset and Andrea Belén Tonato Ñacato

DOI. 10.21931/RB/2019.04.01.1

The UNESCO Global Geoparks are created in the nineties as a European regional initiative to respond the increasing need for enhancing and preserving the geological heritage of our planet [1], based on the geological record of determined areas. These geographic sites are part of the evidence of the 4600 Ma of Earth's evolution. This initiative is based on three essential pillars [2]: preservation, education and geo – tourism designed to reach the sustainable economic development based on the harnessing of the geological heritage. These main thrusts are the guidelines to manage Geoparks, and give the possibility to develop economic and touristic activities which increase the economic income in communities. As a consequence, the settler's life's quality is positively affected.

At the beginning, the Geoparks Network was totally integrated by European members (France, Germany, Greece and Spain) [2]. As the initiative started to be known around the world, other regions showed interest in being part of, and joined to the initiative. Among these are: South America which only had four Geoparks (Araripe in Brazil, Grutas del Palacio in Uruguay, and Comarca Minera and Mixteca Alta in México) until the last week (17th April, 2019) when the Executive Board, United Nations Educational, Scientific and Cultural Organization (UNESCO) decided to give the nomination of Global Geoparks to 7 from 23 candidates, including three Latin American applicants (Valle del Colca and Volcanes de Andagua in Peru, Kütralkura in Chile, and Imbabura in Ecuador). With these new additions, there are 147 members of the Global Geoparks Network distributed in 41 countries [3].

Geoparks composed specific geographic areas that show particular and relevant geological features of our planet's history (UNESCO [4]). In South America, and principally in the Andean zone, the evidence associated to the convergence and subduction of the Nazca Plate and South American Plate is well preserved. For this reason, there is a wide variety of natural and geological attractions (ranges of different ages, valleys, volcanoes, geothermal systems, sedimentary basins, faults, rocks, minerals, fossils, etc.). The beauty and the showiness of the region have motivated the launching of various Geopark proposals, for example: Napo – Sumaco in the Amazon Region, Península Santa Elena and Jama – Pedernales in the Coast, Galápagos in the Insular Region, and Volcán Tungurahua and Imbabura in the Sierra Region; all of them, in Ecuador [5].

Imbabura Geopark occupies all the surface of the homonym province (4,599 km2), and is located in the northern part of Ecuador. Imbabura is surrounded by the Carchi province to the north, Pichincha to the south, Sucumbíos to the east and Esmeraldas to the West. Inside Imbabura Geopark, it is possible to recognize the two mountain ranges, the Cordillera Real and Western Cordillera, separated by the Interandean Valley, all oriented in a general NE – SW direction. These are the principal geological structures that typify the Andean orogeny. The units of the Cordillera Real and Western Cordillera occur to the east and to the west of the Geopark, respectively. The Interandean Valley is the depression located between both ranges. The Geological heritage of the Imbabura Geopark is equally distributed in the ranges as in the Interandean valley. Prominent geoheritage sites are volcanoes

Figure 2. Panoramic view of Cuicocha Lake taken from the north. It is located in the eastern part of the Western Cordillera, 10 km west of Cotacachi ci
It was formed through a crater collapse of the Cuicocha dome which is part of the Cotacachi – Cuicocha Volcanic Complex. Inside the crater lake, NE –
is one of the most important and beautiful geosites of Imbabura Geopark, and it receives the greatest inflow of tourists per year in this area.

Yaniel Misael Vázquez Taset and Andrea Belén Tonato Ñacato, Escuela de Ciencias de la Tierra, Energía y Ambiente, Yachay Tech
Corresponding author: yvazquez@yachaytech.edu.ec

Figure 1. Western view of Imbabura Volcano and San Pablo Lake. Both constitute geosites of the Imbabura Geopark, and are located in the Inter-Andean Valley. The Imbabura Volcano is a compound stratovolcano that reaches 4621 6 meters high, on the summit of Taita Imbabura. In its foothills settle major populations, such as the cities of Ibarra and Otavalo. San Pablo Lake is located south of Otavalo city and its origin is not yet clear. As hypothesis, the glacial origin and the damming by a debris flow from the Imbabura Volcano have been proposed.

(Imbabura Fig. 1, Yanahurco, Cubilche, Cotacachi – Cuicocha), lagoons and lakes (San Pablo Fig. 1, Yahuarcocha, Piñan, Cuicocha), valleys (Chota and Intag), Geothermal complexes (Chachimbiro, Timbuyacu, Nangulví), mineral resources, archeological sites (Urcuquí, among others) and sedimentary basin (Chota), among others. Due to their scenic beauty, these geosites are mandatory visiting points in the province. For example, Cuicocha Lake (Fig. 1) is one of the most visited geosites in Imbabura, and in northern Ecuador. The rich geological history makes Imbabura a potential area to develop touristic and educative activities, which will guarantee the increase of geotourism. Additionally, it is important to mention that many of the geosites are areas where students and investigators from the School of Earth's Science, Energy and Environment of Yachay Tech, and from other Ecuadorian universities develop academic activities and fieldwork. This academic work is a key component supporting the Unesco Imbabura Geopark.

ty, Imbabura. It is a lake of approximately 180 m depth, and 3.5 km of diameter [7]. – SE directed, are two camel-back domes Yeroví (left) and Wolf (right). Cuicocha

References

1.http://www.exteriores.gob.es/RepresentacionesPermanentes/unesco/es/unescoenespa%C3%B1a/Inscripciones/Paginas/Geoparques.aspx

2.http://www.exteriores.gob.es/RepresentacionesPermanentes/unesco/es/unescoenespa%C3%B1a/Inscripciones/Paginas/Geoparques.aspx

3.https://es.unesco.org/news/once-sitios-asia-america-del-y-europa-designados-geoparques-mundiales-unesco

4.https://unesdoc.unesco.org/ark:/48223/pf0000243650_spa

5.http://www.unesco.org/new/fileadmin/MULTIMEDIA/FIELD/Quito/pdf/Texto_Declaracion_Tena.pdf

6.https://www.igepn.edu.ec/Cuicocha

7.https://deskgram.net/explore/tags/conociendoimbabura

LETTER TO EDITOR / CARTA AL EDITOR

Will our next revolution support or obstruct the achievement of the Sustainable Development Goals?

Nicolas Serrano-Palacio[1] and Jorge Gómez-Paredes[2]

DOI. 10.21931/RB/2019.04.01.2

The so-called "Fourth Industrial Revolution" (4IR) [1], is an emerging phenomenon which will likely transform our lives and affect multiple sectors of society. This new revolution encompasses and combines a wide range of new technologies, such as quantum computing, nano and biotechnology, artificial intelligence (AI), the internet of things (IoT), and advanced automation. Foreseeing all the impacts and ripple effects that these technologies will have in our societies, in the next years, is a sizeable and challenging task. Much of the debate has usually been focused on automation, which the Cambridge Dictionary defines as "the use of machines or computers instead of people to do a job, especially in a factory or office" [2]. The ongoing debate focuses, on the potential of automation to generate production efficiency benefits vs. the threat to increase unemployment lines. However, the actual effects (positive and negative) of this revolution may be much broader and deeper, including social and environmental impacts closely related to sustainable development. Following, we present a brief non-exhaustive commentary on some of the potential advantages and disadvantages of the 4IR from the perspective of the 17 goals adopted by all parties to the United Nations on September 2015, as part of an agenda to tackle global problems and reach sustainable development[3].

In the United Nations 2030 Agenda[3], "end poverty in all its forms everywhere" is the first Sustainable Development Goal (SDG 1). In this regard, automation can have a negative effect by creating job losses, particularly in low-income groups, reducing social mobility, and increasing income and wealth inequalities (thus affecting to the SDG 10: "Reduce inequality within and among countries"). This, in a world where there is a gender gap in employment[4], may disproportionately affect women (thus also hindering the SDG 5: "Achieve gender equality and empower all women and girls"). As Friedrich Soltau explains, the threat to human employment is based on the fast pace of change in production systems which will "displace humans faster that they can adapt, through the acquisition of new skills and education"[4]. However, a counter argument to all this is that technology development will foster the creation of new businesses, which in turn may bring new and better jobs, thus promoting "sustained, inclusive and sustainable economic growth, full and productive employment and decent work for all" (SDG 8). This, however, clearly depends firstly on whether or not these businesses' socio-environmental impacts also "ensure sustainable consumption and production patterns" (SDG 12), and secondly on their capacity to re-employ those affected, which in itself poses a challenge given that most new jobs will likely require advanced technical knowledge and skills that are not common in low-income populations[5]. The wide range and growing amount of online educational tools could be part of the solution to this problem. Massive Open Online Courses (MOOC), tutorials, and the vast amount of online freely available information allow people to learn from experts around the world, overcoming the obstacle of physical distance. However, connectivity is a requirement for the spread of online education. That is being addressed by projects such as Amazon Project Kuiper[6], SpaceX Project Starlink[7], among others[8]. Thus, automation may help in the goal of ensuring "inclusive and equitable quality education and promote lifelong learning opportunities for all" (SDG 4). However, going back to jobs, whether these educational tools will help the unemployed to seize opportunities in emerging labor markets will depend on them having access to technology and on having minimal training and knowledge (and, of course, also some spared time). Sadly, this is unlikely to be the case without some government or another kind of support programs, as most of the people whose jobs would be automated do not usually have strong initial education or enough motivation to catch up with the steepest learning curves of emerging jobs such as programming or graphic design[9].

Beyond jobs, one of the leading global challenges that humanity is facing, and will increasingly face in the incoming years, is "end hunger, achieve food security and improved nutrition and promote sustainable agriculture" (SDG 2). The use of machines and technology on agriculture has increased food production in the past, hence the belief of some people on the potential benefits of applying aspects of the 4IR on agriculture[10]. One of these benefits could be improving inefficient distribution system and reducing food loss. For instance, software systems are being developed to monitor and analyze data in order to predict the best time to dispatch food production to local markets. Blockchain technology, in turn, offers opportunities to track products along supply chains and validate fair trade schemes[11]. Here, again, the positive impact of these technologies will largely be determined by technology transfer and support for small farmers and applications in remote locations, since "family farms makeup 90 percent of the world's farms and produce over 80 percent of the world's food"[12].

"Ensure healthy lives and promote well-being for all at all ages" (SDG 3) may also be influenced by the 4IR. New software applications and technologies using AI seem promising in terms of expanding the reach of medical diagnosis[13], improving patients' treatments[14], improving medical records keeping systems[15], among others. The IoT may also play a role in health, by collecting and analyzing significant amounts of data from different patient scenarios[16]. On the negative side, the IoT's extensive data collection (which goes beyond personal health data) may compromise our privacy[17] and security[18]. Here too, blockchain technology has been proposed as a way to decentralize information and hinder incorrect practices by central entities[19]; yet, it is clear that having access to such "big data" is in the interest of many groups of individuals whom may not have the health and wellbeing of all in mind.

Since the majority of the human population lives in urban areas[20], cities are at the heart of sustainable development. "Making cities and human settlements inclusive, safe, resilient and sustainable" (SDG 11) is yet another personal challenge that the proponents of the 4IR say that it can address[21] along and aligned with efforts to "build resilient infrastructure, promote inclusive and sustainable industrialization and foster innovation" (SDG 9). Smart city models promise that the application 4IR's technologies, through around-the-clock active sensors, video surveillance cameras, and data collection, will advance good governance and enhance public

[1]Student at Yachay Tech and Coordinator of the SDSN Andes Youth Network. corresponding author: nicolas.serrano@yachaytech.edu.ec
[2]Lecturer at Yachay Tech and Manager of the SDSN Andes

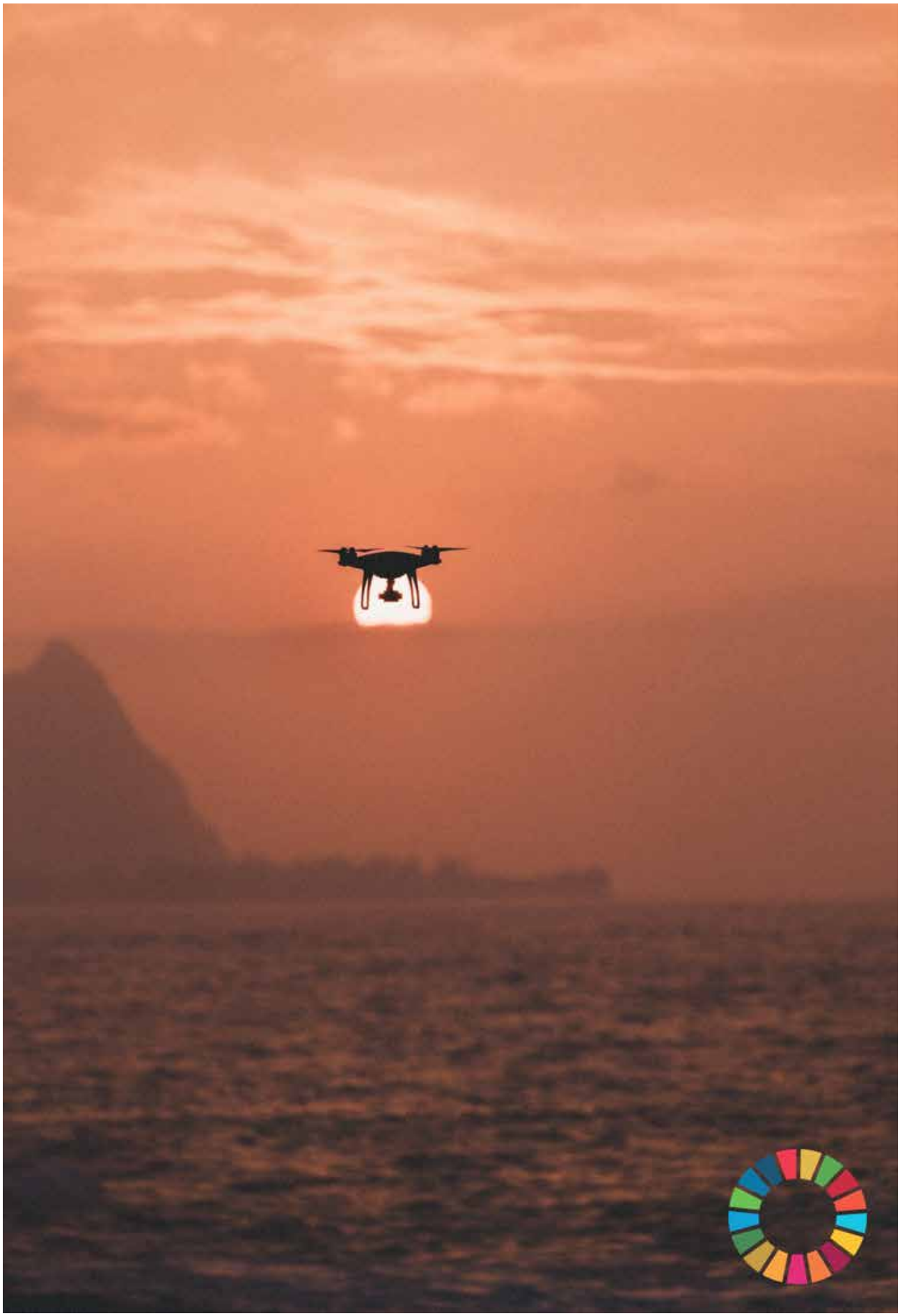

unplash.com, Photo by: Jakob Owens

safety[22]. Also, there is the claim that data analysis could address air quality, traffic distribution, electricity supply (thus contributing to SDG 7: "Ensure access to affordable, reliable, sustainable and modern energy for all"), and even water and sanitation (thus also contributing to SDG 6: "Ensure availability and sustainable management of water and sanitation for all")[23]. Here, again, concerns include safety issues. As Kitchin and Dodge[24] mention, by having everything centralized, we may be more prone to cyber-attacks targeting critical urban systems, such as water supply and electricity grids. In any case, considering that global urban population growth will take place in cities of all sizes, yet the fastest growth will take place in medium-to-small cities mostly located in the global south[20], if we assume that 4IR's technology will effectively contribute to achieving the aforementioned SDGs, technology transfer will be a significant determining factor.

The need to promote "peaceful and inclusive societies for sustainable development, provide access to justice for all and build effective, accountable and inclusive institutions at all levels" (SDG 16) is another fundamental step towards a better future. Here, more secure, transparent, and efficient software, combined with the automation of some bureaucratic tasks, could bring about more trustable and accountable organizations, for example by reducing human error[25], and by implementing tamper-evident and less-susceptible-to-modify ledgers that could reduce cases of corruption[26].

This, of course, is only a brief glimpse of the large number of possible applications and implications of the 4IR. However, are we assessing these opportunities and risks accurately? Alternatively, are we fetishizing technology?[27]. Part of answering these questions is to avoid assuming a cornucopian stance and to acknowledge that all these technologies (alike current technologies) will demand from nature continuous flows of energy and materials, which particularly under our current fossil-fuel-based energy systems and material-extraction practices, will likely imply GHG emissions (thus hindering efforts aimed at achieving SDG 13: "Take urgent action to combat climate change and its impacts")[28], as well as the further destruction of ecosystems and associated extinction of species[29]. In addition to that, our consumption patterns may quickly transform new products into new waste. The IoT, for instance, maybe causing an "internet of trash" situation where IoT electronic components are disposed after 5 years or less, adding to the problem of e-waste[30, 31], water and soil pollution. All these effects combined, and their ramifications, will in turn hinder our efforts to "conserve and sustainably use the oceans, seas and marine resources for sustainable development" (SDG 14) and to "protect, restore and promote sustainable use of terrestrial ecosystems, sustainably manage forests, combat desertification, and halt and reverse land degradation and halt biodiversity loss" (SDG 15).

Urgently addressing these fundamental questions and challenges is the responsibility of all, at all levels and sectors of society. Besides, effective action requires us to "strengthen the means of implementation and revitalize the Global Partnership for Sustainable Development" (SDG 17). In this line, the Sustainable Development Solutions Network (SDSN), a global initiative working under the auspices of the United Nations Secretary-General, seeks to bring together academia, civil society, public and private sectors in order to work for the achievement of the SDGs[32]. The SDSN has multiple regional and national chapters around the world; among them is the SDSN Andes, currently hosted by Yachay Tech, which seeks to mobilize and connect different sectors of society in order to jointly contribute to the achievement of the SDGs in the Andean Region (Argentina, Bolivia, Colombia, Chile, Ecuador, Peru, and Venezuela).

Will the 4IR be aligned with the sustainable development revolution that we so desperately need? As SDSN Andes, we invite you to think and explore these questions, and ultimately to work on solutions, for your sake and the sake of humanity.

References

1 Schwab, Klaus. 2017. The fourth industrial revolution.

2 "Cambridge Dictionary," 2019. [Online]. Available: https://dictionary.cambridge.org/dictionary/english/automation.

3 United Nations General Assembly. Transforming our world: the 2030 Agenda for Sustainable Development. New York, 2015.

4 ILO, "The gender gap in employment: What's holding women back?," 2019. [Online]. Available: https://www.ilo.org/infostories/en-GB/Stories/Employment/barriers-women#persistent-barriers.

5 F. Soltau, "Automation and artificial intelligence – what could it mean for sustainable development ?," United Nations Dep. Econ. Soc. Aff., pp. 1–4, 2016.

6 Amazon, "Project Kuiper," Low Earth Orbit satellites, 2019. [Online]. Available: https://www.amazon.jobs/en/teams/projectkuiper.

7 M. Handley, "Delay is Not an Option," pp. 85–91, 2018.

8 UNHCR, "Connectivity for Everyone," 2016.

9 L. Rainie and J. Anderson, "The Future of Jobs and Job Training," no. May, 2017.

10 G. (WEF) Dixie, "The Fourth Industrial Revolution must not leave farming behind," 2018. [Online]. Available: https://www.weforum.org/agenda/2018/08/the-fourth-industrial-revolution-must-not-leave-farming-behind/.

11 D. Galvin, "IBM and Walmart: Blockchain for Food Safety," Ibm, 2017.

12 FAO. Innovating for our future of food and agriculture. http://www.fao.org/fao-stories/article/en/c/1170362/.

13 "HealthTap," 2010. [Online]. Available: https://www.healthtap.com/.

14 M. Boaz, K. Hellman, and J. Wainstein, "An Automated Telemedicine System Improves Patient-Reported Well-Being," Diabetes Technol. Ther., vol. 11, no. 3, pp. 181–186, 2009.

15 A. Sunyaev, "Evaluation of Microsoft HealthVault and Google Health personal health records," Health Technol. (Berl)., vol. 3, no. 1, pp. 3–10, 2013.

16 H. J. A. Van Os et al., "The Internet of Things for Health Care: A Comprehensive Survey," Int. J. Stroke, vol. 10, p. 217, 2015.

17 M. Meingast, T. Roosta, and S. Sastry, "Security and Privacy Issues with Healthcare Information Technology."

18 Sadeeq MAM, Zeebaree SRM, Qashi R, Ahmed SH, Jacksi K. Internet of Things Security: A Survey. Int Conf Adv Sci Eng 2018; 88: 162–166. doi:10.1109/ICOASE.2018.8548785.

19 AIDTech, "Empowering Through Transparency: Transparency As A Service Token (TaaST)," 2018.

20 United Nations, Department of Economic and Social Affairs, Population Division (2014). World Urbanization Prospects: The 2014 Revision, Highlights (ST/ESA/SER.A/352)

21 Joshi-Ghani A, Ratti C. A Glimpse into the Future. 2018. https://www.weforum.org/agenda/2018/07/podcast-a-glimpse-into-the-future-of-cities-and-urbanization/.

22 B. S. P. Mohanty, U. Choppali, and E. Kougianos, "Everything You Wanted to Know About Smart Cities," no. JULY 2016.

23 Neirotti P, De Marco A, Cagliano AC, Mangano G, Scorrano F. Current trends in smart city initiatives: Some stylised facts. Cities 2014; 38: 25–36. doi:10.1016/j.cities.2013.12.010.

24 R. Kitchin and M. Dodge, "The (In)Security of Smart Cities: Vulnerabilities, Risks, Mitigation, and Prevention," J. Urban Technol., vol. 0, no. 0, pp. 1–19, 2017.

25 D. Landsbergen and G. Wolken, "Realizing the promise : Government information systems and the fourth generation of information technology," Public Adm. Rev., vol. 61, no. 2, p. 206, 2001.

26 H. Hou, "The application of blockchain technology in E-government in China," 2017 26th Int. Conf. Comput. Commun. Networks, ICCCN 2017, 2017.

27 Hornborg A. Machine fetishism and the consumer's burden. Anthropol Today 2008; 24: 4–5. doi:10.1111/j.1467-8322.2008.00610.x.

28 C. Mora et al., "Bitcoin emissions alone could push global warming above 2°C," Nat. Clim. Chang., vol. 8, no. 11, pp. 931–933, 2018.

29 Tollefson J. One million species face extinction. Nature. 2019; : 9. http://sci-hub.tw/https://www.nature.com/articles/d41586-019-01448-4#.

30 United Nations Environmental Management Group, "United Nations System-wide Response to Tackling E-waste," 2017.

31 B. Ellis, "Environmental issues in electronics manufacturing : a review," pp. 17–21, 2000.

32 "SDSN Andes," 2015. [Online]. Available: http://unsdsn.org/about-us/vision-and-organization/.

RESEARCHS / INVESTIGACIÓN

Polypharmacological study of Ceritinib using a structure based *in silico* approach

Tammanna R. Sahrawat[1] and Prabhjeet Kaur[2]

DOI. 10.21931/RB/2019.04.02.3

Abstract: Drug repurposing has gained mass recognition over the past few years as it has paved new therapeutic applications for already approved FDA drugs. It focuses on finding new molecular targets of drugs for medical uses different than the one originally proposed. Ceritinib, an Anaplastic Lymphoma Kinase (ALK) inhibitor is given orally in the treatment of non-small cell lung cancer (NSCLC). This treatment has been reported to be associated with a number of side effects such as hyperglycemia, convulsion, pneumonitis etc. The side effects are usually due to the unintended interaction of the drug with other protein targets. *In silico* polypharmacological studies of Ceritinib suggests that it binds to multiple targets other than the intended one which may largely be due to different proteins possessing similar binding sites. ProBis server was used to retrieve probable off-targets of Ceritinib based on presence of structurally similar protein binding sites as that of ALK. Ceritinib was found to bind effectively to three proteins namely Lymphocyte Cell-Specific Protein-Tyrosine Kinase, Tropomyosin receptor kinase B and Aurora kinase B having favorable binding energies and inhibition constants, with no reported side-effects as compared to their marketed drugs. Therefore, it is concluded from the present study that Ceritinib may act as an effective therapeutic target against its polypharmacological targets.

Keywords: Polypharmacology, repurposing, molecular docking, protein binding similarity search.

.

Introduction

Conventional drug discovery processes require huge time and a hefty amount of money to bring a single drug into the market. Hence, in silico methods play a vital role in drug discovery and development by offering an enhanced efficiency to the pharmaceutical industry[1]. Over the last four decades, the drug manufacturing companies have shifted their focus from the reductionist approach towards 'one drug, multiple targets' also known as polypharmacology. Polypharmacology has been defined as the ability of small molecules to interact simultaneously and specifically with multiple targets[2]. Polypharmacology can be broadly characterized into two types: adverse polypharmacology (which involves off–target binding) and therapeutic polypharmacology (which involves repurposing of drugs i.e. the process of searching new therapeutic applications for existing drugs also known as drug repositioning)[3].

Polypharmacology thus offers to be a promising approach for identifying novel therapeutic uses for already known drugs against complex diseases. It has been previously reported that effect of a drug on an unintended target might suggest new uses for an existing drug (i.e. multi-target drugs)[4]. Moreover, drugs which failed to provide the intended benefit can also be considered for repurposing for the treatment of other diseases. A classic example is the anti-cancer drug Zidovudine which failed in intended treatment of cancer however it was found to be effective against HIV and in 1987 was approved by FDA for HIV treatment[5].

Polypharmacological drugs are expected to have relatively lower chances for developing drug resistance as they target multiple drug targets and are considered to show better efficacy than drugs for a single target[6,7]. Several drugs have already been successfully repurposed for new diseases, outside the original medical scope. For example, the blockbuster drug Sildenafil (Viagra), a phosphodiesterase (PDE) inhibitor was first developed for treating hypertension and ischemic heart disease. During the phase I clinical trials, Sildenafil was found to induce penile erections as a side effect and after phase II clinical trial failure, sildenafil was repositioned for the treatment of erectile dysfunction and approved by the FDA[8].

Ceritinib (formerly known as LDK378 and marketed as Zykadia™), an inhibitor of Anaplastic lymphoma kinase is used to treat non-small cell lung cancer (NSCLC). It acts to inhibit the autophosphorylation of Anaplastic Lymphoma Kinase (ALK) and its downstream signaling protein STAT3 thereby preventing the proliferation of ALK-dependent cancer cells[9].

In silico computational methods are of high biological and pharmacological value as they predict new targets for existing small-molecule compounds[2]. In our previous in silico polypharmacological study, it was found that hyperglycemia caused in patients after Ceritinib treatment could be due to the off-target binding of Ceritinib to dual specificity protein kinase CDC Like Kinase 2 (CLK2) (PDB ID: 3NR9) along with its actual target Anaplastic Lymphoma Kinase[10]. Therefore, in the present study, we further investigated the polypharmacological-targets of ceritinib to identify its probable repurposing potential.

Materials and methods

Data mining of target protein of Ceritinib

The Drugs and Drug Targets mapping tool of the Protein Data Bank (PDB) was utilized to obtain the crystal structure of the target protein Anaplastic lymphoma tyrosine kinase (ALK) bound with Ceritinib (PDB ID: 4MKC)[11].

Identification of proteins with similar binding sites

The ProBis server was used to detect structurally similar protein binding sites in ALK tyrosine kinase (PDB ID: 4MKC). ProBis employs a fast maximum clique algorithm to detect similar protein binding sites independent of the sequence or the fold present in proteins[12]. Therefore, using ProBis proteins having similar geometrical and physicochemical properties to Ceritinib target ALK were retrieved.

[1]Assistant Professor, 2Post-graduate student
[1, 2] Centre for Systems Biology & Bioinformatics, UIEAST Panjab University, Chandigarh, India
Corresponding Author: Dr. Tammanna R. Sahrawat* Ph.D. Email: tammanna@pu.ac.in

Docking studies of Ceritinib with probable polypharmacological/off-targets

To investigate the binding affinity of Ceritinib with proteins other than its actual target ALK tyrosine kinase, Autodock tool was used to perform drug-protein docking[13]. The binding energies and inhibition constants of polypharmacological-targets with Ceritinib and their bound ligands were tabulated and compared.

Literature mining

The probable polypharmacological-targets of Ceritinib were studied for their role in disease pathways and therapeutics in order to predict its repurposing prospects.

Results and discussion

Repurposing studies involve investigating multiple targets of drugs to enhance their biological activities as well as reduce their toxicities. In order to find polypharmacological targets of Ceritinib, the drug was docked with 33 probable off-targets obtained from ProBis server. Literature studies also revealed that these polypharmacological targets may be critical therapeutic targets in various other complex diseases such as breast cancer, Acute Lymphoblastic Leukemia (ALL) and CNS disorders. Sahrawat and Kaur (2018) while investigating the polypharmacology of Certinib have reported that proteins having similar binding sites to the actual target of Certinib i.e. ALK , retrieved from ProBis server, namely Ribosomal protein S6 kinase alpha-1 (RSK1) (PDB ID: 2Z7R), Lymphocyte Cell-Specific Protein-Tyrosine Kinase (LCK) (PDB ID: 1QPC), Tropomyosin receptor kinase B (TRKB) (PDB ID: 4AT5) and Aurora kinase B (AURKB) (PDB ID: 4AF3) had a significant Z-score > 2.0. Z-score is the measure of similarity between two protein binding sites[12] due to which different proteins may interact with same drug molecules. Further, the docking analysis of these proteins with the drug Ceritinib, revealed binding energies and inhibition constants comparable to the actual target i.e. ALK, with no reported side-effects on binding to Ceritinib[10]. Therefore, the proteins which were identified as off-targets of Ceritinib, were further investigated for repurposing of Ceritinib, so as to identify other probable usage of the drug.

The results obtained from docking server, Autodock is in terms of binding energy and inhibition constant (K_i) at temperature 298.15 K. Binding energy is the affinity of the ligand with which it binds to the target protein. More negative binding energy, higher is the affinity of the ligand to bind the receptor protein. Inhibition constant of a drug is the concentration required to produce half maximum inhibition on binding the receptor, therefore, lower the inhibition constant value lesser is the amount of drug concentration needed to produce an effect[13].

The docking studies indicated that the binding energy of Ceritinib with its actual target, ALK (PDB ID: 4MKC) was -5.62 kcal/mol with an inhibition constant of 75.9 μM μM. In addition, the docking studies of Ceritinib with proteins Ribosomal protein S6 kinase alpha-1 (RSK1) (PDB ID: 2Z7R), Lymphocyte Cell-Specific Protein-Tyrosine Kinase (LCK) (PDB ID: 1QPC), Tropomyosin receptor kinase B (TRKB) (PDB ID: 4AT5) and Aurora kinase B (AURKB) (PDB ID: 4AF3) revealed that they had higher binding affinities and lower inhibition constant for Ceritinib than its actual target ALK (PDB ID: 4KMC)[10] as shown in Table 1.

Ribosomal protein S6 Kinase alpha-1 (PDB ID: 2Z7R) retrieved from ProBis server had binding energy of -7.83 kcal/mol with Ceritinib while its marketed therapeutic agent Staurosporine (Drugbank ID: DB02010) had a higher binding energy of -10.3 kcal/mol. Further, RSK1 had a favorable inhibition constant for Staurosoporine, which has been used for treating triple negative breast cancer[14,15] (Table 1). Our results are also supported by the report of Kuenzi et al. (2017) in an integrated functional proteomics study for repurposing of the anaplastic lymphoma kinase (ALK) inhibitor Ceritinib, wherein it was reported that IGF1R, RSK1, RSK2 and FAK1 are potential off-targets of Ceritinib[16].

LCK is a potential target in the treatment of T-cell Acute Lymphoblastic Leukemia (ALL) and its marketed drug is Dasatinib (D number: D03658)[17, 18]. Moreover, for the treatment of Central nervous system (CNS) disorders and various tumors including NSCLC, TRKB has been used as a potential therapeutic target and Entrectinib (D number: D10926) is prescribed for its treatment[19,20]. The probable polypharmacological targets of Ceritinib, namely LCK protein (PDB ID: 1QPC) and TRKB (PDB ID: 4AT5) had higher binding affinity and lower inhibition constant for Ceritinib as compared to their marketed therapeutic agents Dasatinib and Entrectinib, respectively (Table 1).

S.No.	Protein	Drug*	PDB ID	Binding energy (kcal/mol)		Inhibition constant (μM)	
				Ceritinib	Drug*	Ceritinib	Drug*
1.	RSK1	Staurosporine	2Z7R	-7.83	-10.30	1.83	0.02
2.	LCK	Dasatinib	1QPC	-7.49	-6.25	3.23	26.42
3.	TRKB	Entrectinib	4AT5	-7.43	-6.32	3.59	23.11
4.	AURKB	Tozasertib	4AF3	-7.18	-7.64	5.45	2.50

Table 1: Binding energy and inhibition constant values of polypharmacological-targets with Ceritinib and their reported therapeutic agents.

On docking of Aurora kinase B (PDB ID: 4AF3) with its marketed therapeutic agent Tozasertib (D number: D08279)[21], it was found that there was not much difference in their binding energies, although the inhibition constant was higher for Ceritinib. AURKB has been reported to be involved in various cancers such as breast cancer, hepatocellular carcinoma, lung adenocarcinoma, colorectal cancer models and acute lymphoblastic leukemia (ALL) which are currently being treated using Tozasertib[22,23].

On investigation of binding site residues of polypharmacological-targets of Ceritinib it was seen that all the proteins RSK1, LCK, TRKB and AURKB had similar binding site interacting residues as that of Ceritinib with its actual target ALK (PDB ID: 4KMC) tabulated in Table 2, Figure 1.

Analysis of the docking scores of all the four poypharmacological

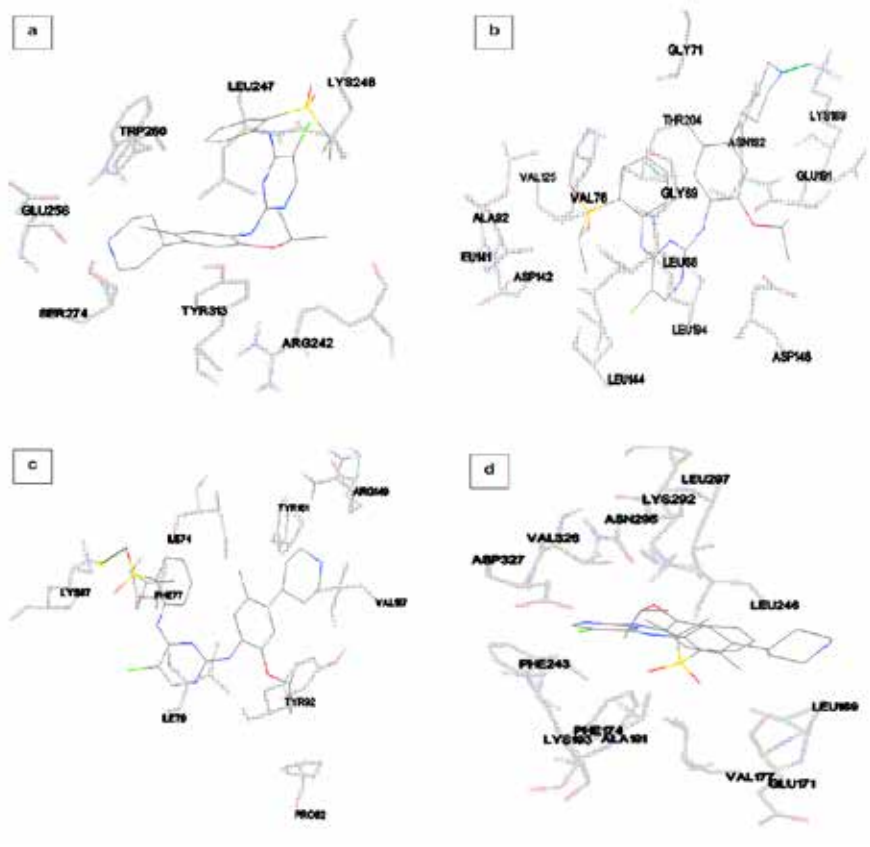

Figure 1: Interacting amino acid residues in the binding pockets of a) Ribosomal protein S6 Kinase alpha 1 (PDB ID: 2Z7R) b) LCK (PDB ID: 1QPC) c) TRKB/BDNF/NT-3 growth factors receptor (PDB ID: 4AT5) d) Aurora Kinase B (PDB ID: 4AF3) docked with Ceritinib visualized using AutoDock analysis tool.

S. No.	Protein	PDB ID	Interacting residues
1.	ALK	4KMC	LEU1122, VAL1130, LYS1150, GLU1167, ILE1171, PHE1174, ILE1179, MET1199, ASP1203, SER1206, GLU1210, LEU1256, GLY1269, ASP1270, PHE1271
2.	RSK1	2Z7R	LEU68, GLY69, GLY71, VAL76, ALA92, VAL125, LEU141, ASP142, LEU144, ASP148, LYS189, GLU191, ASN192, LEU194, THR204
3.	LCK	1QPC	ARG242, LYS246, LEU247, GLU258, TRP260, SER274, TYR313
4.	TRKB	4AT5	ALA564, PHE565, ASP600, GLU604, LEU607, PHE688, ARG691, ASP710, GLY712
5.	AURKB	4AF3	ILE74, PHE77, ILE79, PRO82, TYR92, LYS97, VAL107, ARG149, TYR151

Table 2: Binding site residues of actual target and polypharmacological-targets of Ceritinib.

targets namely Ribosomal protein S6 kinase alpha-1, LCK, Aurora kinase B and (Table 2) indicated that Ceritinib binds effectively to three proteins namely LCK, AURKB and TRKB as compared to their available marketed drugs.

Conclusion

Therefore, it may be concluded that three polypharmacological targets of Ceritinib i.e LCK, Aurora kinase B and Tropomyosin receptor kinase B, identified in the present study, bind to the

Ceritinib more effectively, as seen from their high binding energies, as compared to the drug's actual target ALK. This study paves new opportunities for Ceritinib in the treatment of various complex diseases such as cancer, central nervous disorders etc. associated with these proteins. In addition, experimental studies need to be carried out to further validate the results of this work.

Acknowledgement

The authors would like to thank their parent institute Panjab University, Chandigarh, India for providing the infrastructure for carrying out the research.

References

1. Kumar, N., Hendriks, B. S., Janes, K. A., de Graaf, D., & Lauffenburger, D. A. (2006). Applying computational modeling to drug discovery and development. Drug discovery today, 11(17-18), 806-811.

2. Rastelli, G., & Pinzi, L. (2015). Computational polypharmacology comes of age. Frontiers in pharmacology, 6, 157.

3. Boran, A. D., & Iyengar, R. (2010). Systems approaches to polypharmacology and drug discovery. Current opinion in drug discovery & development, 13(3), 297.

4. Ashburn, T. T., & Thor, K. B. (2004). Drug repositioning: identifying and developing new uses for existing drugs. Nature reviews Drug discovery, 3(8), 673.

5. Broder, S. (2010). The development of antiretroviral therapy and its impact on the HIV-1/AIDS pandemic. Antiviral research, 85(1), 1-18.

6. Anighoro, A., Bajorath, J., & Rastelli, G. (2014). Polypharmacology: challenges and opportunities in drug discovery: miniperspective. Journal of medicinal chemistry, 57(19), 7874-7887.

7. Peters, J. U. (2013). Polypharmacology–foe or friend?. Journal of medicinal chemistry, 56(22), 8955-8971.

8. DeBusk, R. F., Pepine, C. J., Glasser, D. B., Shpilsky, A., DeRiesthal, H., & Sweeney, M. (2004). Efficacy and safety of sildenafil citrate in men with erectile dysfunction and stable coronary artery disease. American Journal of Cardiology, 93(2), 147-153.

9. Chen, Z., Fillmore, C. M., Hammerman, P. S., Kim, C. F., & Wong, K. K. (2014). Non-small-cell lung cancers: a heterogeneous set of diseases. Nature Reviews Cancer, 14(8), 535.

10. Sahrawat, T. R., & Kaur, P. (2018). Investigation of Off-targets of NSCLC drug Ceritinib: A Structure Based Systems Biology Approach. International Journal of Advanced Scientific Research and Management (IJASRM), 3(12), 31-36.

11. Sussman, J. L., Lin, D., Jiang, J., Manning, N. O., Prilusky, J., Ritter, O., & Abola, E. E. (1998). Protein Data Bank (PDB): database of three-dimensional structural information of biological macromolecules. Acta Crystallographica Section D: Biological Crystallography, 54(6), 1078-1084.

12. Konc, J., & Janežič, D. (2012). ProBiS-2012: web server and web services for detection of structurally similar binding sites in proteins. Nucleic acids research, 40(W1), W214-W221.

13. Morris, G. M., Huey, R., Lindstrom, W., Sanner, M. F., Belew, R. K., Goodsell, D. S., & Olson, A. J. (2009). AutoDock4 and AutoDockTools4: Automated docking with selective receptor flexibility. Journal of computational chemistry, 30(16), 2785-2791.

14. Xue, L. Y., Chiu, S. M., & Oleinick, N. L. (2003). Staurosporine-induced death of MCF-7 human breast cancer cells: a distinction between caspase-3-dependent steps of apoptosis and the critical lethal lesions. Experimental cell research, 283(2), 135-145.

15. Stratford, A. L., Reipas, K., Hu, K., Fotovati, A., Brough, R., Frankum, J.,& Lasham, A. (2012). Targeting p90 ribosomal S6 kinase eliminates tumor initiating cells by inactivating Ybox binding protein 1 in triple negative breast cancers. Stem cells, 30(7), 1338-1348.

16. Kuenzi, B. M., Rix, L. L. R., Stewart, P. A., Fang, B., Kinose, F., Bryant, A. T., & Rix, U. (2017). Polypharmacology-based ceritinib repurposing using integrated functional proteomics. Nature chemical biology, 13(12), 1222.

17. De Keersmaecker, K., Porcu, M., Cox, L., Girardi, T., Vandepoel, R., de Beeck, J. O., & Hantschel, O. (2013). NUP214-ABL1 mediated cell proliferation in T-cell acute lymphoblastic leukemia is dependent on the LCK kinase and various interacting proteins. haematologica, haematol-2013.

18. Ottmann, O., Dombret, H., Martinelli, G., Simonsson, B., Guilhot, F., Larson, R. A., & Gollerkeri, A. (2007). Dasatinib induces rapid hematologic and cytogenetic responses in adult patients with Philadelphia chromosome–positive acute lymphoblastic leukemia with resistance or intolerance to imatinib: interim results of a phase 2 study. Blood, 110(7), 2309-2315.

19. Doebele, R. C., Davis, L. E., Vaishnavi, A., Le, A. T., Estrada-Bernal, A., Keysar, S., & Stephens, P. J. (2015). An oncogenic NTRK fusion in a patient with soft-tissue sarcoma with response to the tropomyosin-related kinase inhibitor LOXO-101. Cancer discovery, 5(10), 1049-1057.

20. Rolfo, C., Ruiz, R., Giovannetti, E., Gil-Bazo, I., Russo, A., Passiglia, F., & Raez, L. (2015). Entrectinib: a potent new TRK, ROS1, and ALK inhibitor. Expert opinion on investigational drugs, 24(11), 1493-1500.

21. Harrington, E. A., Bebbington, D., Moore, J., Rasmussen, R. K., Ajose-Adeogun, A. O., Nakayama, T., & Su, M. (2004). VX-680, a potent and selective small-molecule inhibitor of the Aurora kinases, suppresses tumor growth in vivo. Nature medicine, 10(3), 262.

22. Tang, A., Gao, K., Chu, L., Zhang, R., Yang, J., & Zheng, J. (2017). Aurora kinases: novel therapy targets in cancers. Oncotarget, 8(14), 23937.

23. Hartsink-Segers, S. A., Zwaan, C. M., Exalto, C., Luijendijk, M. W. J., Calvert, V. S., Petricoin, E. F.,& Hansen, B. R. (2013). Aurora kinases in childhood acute leukemia: the promise of aurora B as therapeutic target. Leukemia, 27(3), 560.

Received: 24 April 2019
Accepted. 10 May 2019

RESEARCHS / INVESTIGACIÓN

Study the effect of khazra iron nano chelate fertilizer foliar application on two rapeseed varieties

Hasan H. Mahdi[1], Lamiaa A. Mutlag[1] and Raghad S. Mouhamad[1*],

DOI. 10.21931/RB/2019.04.02.4

Abstract**: An experiment was conducted in Al-zafraniya station / Baghdad – Iraq, during the winter season 2017 - 2018 in order to study the effect of khazra iron nano chelate fertilizer foliar application on two rapeseed varieties for increasing yield and yield components. The experiment designed by randomized complete blocks design (RCBD) for three replicates. The first factor included two rapeseed varieties (Brassica napus var. oleifera and Brassica napus L. var. pactol) and second factor included khazra iron nano chelated in three levels 0, 5 (kg.ha-1) (0.5 kg nano iron fertilizers per 1000-liter water) and 10 (kg.ha-1) (1 kg nano iron fertilizers per 1000-liter water). Means of the treatments was compared with a significant difference in the use of the least significant difference (LSD) at the probability level (p ≤ 0.05). Results showed that effect of khazra iron nano chelate foliar application, rapeseed varieties and interaction of them had significant effects on yield, biological yield and total dry biomass, which were 1298.6 (kg.ha-1), 7900(kg.ha-1) and 7288 (kg.ha-1) respectively, at level (kg.ha-1) for rapeseed (Brassica napus var. oleifera). While rapeseed (Brassica napus L. var. pactol) only had biological yield and total dry biomass which were 4260 kg. ha-1 and 4460 (kg.ha-1) respectively. This is due to the genetic nature of each plant species. According to the results, rapeseed (Brassica napus var. oleifera) with 10 (kg.ha-1) khazra iron nano chelate fertilizer foliar application had the highest values at most of evaluated characters.**

Keywords: Nano khazra iron chelate fertilizer, yield, varieties, biological yield, rapeseed

Introduction

In the previous studies using khazra iron nano chelate zinc and manganese, supplements had the potential role in iron fertilizer [1]. In another study [2,] the influence of khazra iron nano chelate fertilizer on rice yield was examined and was shown that applied treatments have a significant effect on all characteristics except grain thousand weigh. Results show that wet weight and maximum leaf area index is influenced by the concentration of khazra iron nano chelate fertilizer and influence dry weight for both types of spinach. Using 4 kg. ha^{-1} khazra iron nano chelate fertilizer causes 58 and 47% increase in wet weight and maximum leaf surface index, respectively comparing to use of no fertilizer in wheat plant [3]. The investigating the effect of khazra iron nano chelate foliar application of amino acids and nanoparticles and chelated iron on photosynthetic pigments and yield of potato [4]. The interactive effect of amino acid and iron fertilizer indicated that application of amino acid, foliar application, and soil application of iron nano chelate had the best effects on chlorophyll a, total chlorophyll, and tuber yield. Other results indicated that both forms of khazra iron nano chelate fertilizer increased leaf chlorophyll concentration, compared to other spraying treatments and the control [5]. Application of nano-forms of fertilizers, compared to chemical forms of fertilizers, increased the phosphorus concentration, biomass, and crude protein and soluble carbohydrate concentration.

Winter rapeseed starts growing early in the spring. Therefore, after the snow falls, it is necessary to survey winter rapeseed crops in order to establish the preservation of plants. [6,7]. Apart from its role in direct feeding by humans and animals, it has expanded globally industrial use, including oil producing factories or as a source of biofuel in recent years [8]. Higher yield per unit area can be achieved by improving modern cultural practices with better macro and micronutrient management [9].

Recent research has shown that a small number of nutrients, especially Zn, Fe, and Mn applied by foliar spraying significantly increased the yield of crops [10,11]. Narimani and others reported that foliar application of microelements improved the effectiveness of macronutrients [12]. Effect of iron and zinc on micronutrient levels in wheat (Triticuma estivum L.) are defined substances that are significant crop growth; however, they are used in lower amounts as compared to macronutrients, such as N, P and K [13].

Materials and methods

The experiment carried out in Al-zafraniya station / Baghdad – Iraq, during the winter season (2017 - 2018). The factorial experiment that consists of two factors and with three replicates was designed by randomized complete blocks design (RCBD). The first factor consisted of two rapeseed varieties (Brassica napus var. oleifera and Brassica napus L. var. pactol) and second factor was three levels of khazra iron nano chelate fertilizer foliar application 0, 5 kg. ha^{-1} (0.5 kg khazra iron fertilizers per 1000-liter water) and 10 kg. ha^{-1} (1 kg khazra iron fertilizers per 1000-liter water). Rapeseed varieties were planted in a row with spacing 30 cm in plot (1 x 2) m^2; the plots were separated by 0.5 m in width from all sides to avoid the effect of fertilization. The iron nano chelate fertilizer sprayed after one month of agriculture on leaf and branch of studied cultivars. Triple superphosphate added as a phosphate resource at the sowing time and urea as a nitrogen resource at sowing and tillering stages, as recommended. Soil properties of the area under study showed in table 1.

Table 1: Soil properties of the area under study

pH	EC ds/m^{-1}	Soil texture	OM%	N%	P mg kg^{-1}	K mg kg^{-1}
7.1	6	silt clay loam	1.31	0.18	25.56	580

[1]Soil and Water Resources Center, Agricultural Research Directorate, Ministry of Sciences & Technology, Baghdad, Iraq
[*]Corresponding Author, e-mail: raghad1974@yahoo.com,

After physiological ripening biological yield were determined by draining of whole plants, which were harvested at 2 m^2 of the center of each plot at 75 ^{o}C for 48 h, an oven. For evaluation of grain yield after measurement of biological yield, spikes were removed from stems, and after winnow, net gain weight were determined. In order to determine of chemical and physical properties of farm soil samples were prepared from 0-30 cm depth. Samples were sieved and were analyzed at the laboratory.

The contents of the mineral elements for Ca, Na, Mg, Mn, K, Zn, Cu and Fe in soil determined using the DTPA method and analyzed by Atomic Absorption Spectroscopy (AAS). Electrical conductivity values were determined by EC meter in 1:1 soil-water mixture [14]. pH was determined by a glass electrode pH meter calibrated with a standard solution in a 1:1 soil-water mixture [15]. Available of the phosphorus (P) determined by the ascorbic acid method of 882 nm in a spectrophotometer [16]. N percentage determined by the Kjeldahl method. The Organic matter (OM) determined by Wakley - Black method [17]. The Soil texture determined by reading the hydrometer in water mixture for 40 seconds and 2 hours 18. The contents of the mineral elements for Ca, Na, Mg, Mn, K, Zn, Cu and Fe in the plant determined using the digestion method and analyzed by Atomic Absorption Spectroscopy (AAS). Khazra fertilizer analyzed by x-ray fluorescence (XRF) techniques; table 2 shows the XRF analysis of khazra fertilizer.

Data were subjected to analysis of variance using SAS and EXCEL software. The differences between the means were compared by the least significant difference test (LSD) ($p \leq 0.05$).

Results and discussion

Khazra iron nano chelate fertilizer: Khazra iron nano chelate had the strong and stable complex with 3<pH<11 range and make 9 % of solved iron in water available for the plant. Zinc and manganese supplements had a specific role in this fertilizer [19]. The results showed increases in micronutrient essentials elements such as Zinc, Iron, Manganese, Sodium, and Sulphur (table 2). Using khazra iron chelate enhances the process of photosynthesis as well as the speed of food preparation within plant leaves, and increases the number of sprouts and flowers, leading to the height of crop volume and speed of productivity in plants [20]. The presence of sulfur in khazra complex is one of its many advantages over similar fertilizers, as sulfur partially acidifies the unsuitable and alkaline soil and increases the absorption rate of microelements such as Iron, Manganese and Zinc [21].

Element	Symbol	Conc. mg kg^{-1}	Element	Symbol	Conc. mg kg^{-1}
Sodium	Na	3300	Selenium	Se	0.3
Magnesium	Mg	530	Bromine	Br	0.5
Aluminum	Al	130	Rubidium	Rb	0.3
Silicon	Si	60	Strontium	Sr	2.1
Phosphorus	P	158	Yttrium	Y	7
Sulfur	S	44370	Molybdenum	Mo	20
Chlorine	Cl	3.2	Silver	Ag	3.2
Potassium	K	27	Cadmium	Cd	3.6
Calcium	Ca	204	Tin	Sn	13.7
Titanium	Ti	8.5	Antimony	Sb	7.5
Vanadium	V	5.8	Tellurium	Te	5.8
Chromium	Cr	68	Iodine	I	28.4
Manganese	Mn	207.8	Barium	Ba	82.2
Iron	Fe	35300	Tungsten	W	3.9
Cobalt	Co	16.1	Mercury	Hg	1.1
Nickel	Ni	21.2	Thallium	Tl	1.3
Copper	Cu	11.5	Lead	Pb	3
Zinc	Zn	31.4	Bismuth	Bi	1
Gallium	Ga	0.8	Thorium	Th	1.2
Germanium	Ge	0.4	Uranium	U	1.3
Arsenic	As	0.9			

Table 2. Major elemental concentration in Khazra fertilizer analysis by X-ray fluorescence spectrometry

The results in table 3 show increasing significantly in the seed yield 1298.6 kg. ha^{-1} for rapeseed (Brassica napus var. oleifera) at a level of 10 kg. ha^{-1}. While, rapeseed (Brassica napus L. var. pactol) not has, seed yield. The status of seed yield is the most important field scale. The high seed yield for winter rapeseed (Brassica napus var. oleifera) may be due to increasing the number of capsules in the plant, the number of seeds in capsules and response to khazra iron nano chelate fertilizer and adaptation for climatic conditions. Rezaeei et al. [22] according to results, using of khazra iron nano chelated fertilizer foliar application at 2.5 % increased grain yield for wheat in drylands. Nazaran et al. [23] in order to study the effect of khazra iron nano chelated fertilizer application on quantitative and quality of wheat an experiment was arranged and results showed that khazra iron nano chelated fertilizer foliar application at shooting stage let to 99% increasing of grain yield. The rapeseed (Brassica napus L. var. pactol) not have seed yield can be explained by non-response to khazra iron nano chelate fertilizer and non-adaptation to climatic conditions.

As shown in table 3, the results of an increase in nano-Fe concentration increased biological yield. The rapeseed (Brassica napus var. oleifera) has 7900 kg. ha^{-1} at level of 10 kg. ha^{-1}. The rapeseed (Brassica napus L. var. pactol) had 4460 kg. ha^{-1} at the level of 10 kg. ha^{-1}. In experiments conducted earlier, biological yield loss due to Fe deficiency has been reported Mahmoudi et al. [24] [Ziaeian and Malakoti [25] compared the effect of Fe and manganese application in soil with the foliar application, and the combination of both, increased grain yield, biological yield, and protein content in wheat farms. The results are consistent with the findings of the research on the effect of micronutrient of iron on soybean seed [26].

Table 3 shows increasing significantly in the total dry biomass 7288 kg. ha^{-1} for rapeseed (Brassica napus var. oleifera), While the rapeseed (Brassica napus L. var. pactol) had total dry biomass 4260 kg. ha^{-1} at level of 10 kg. ha^{-1}. This may be due to increased growth rates of cells in number and volume, which lead to increased carbonation and dry matter production [27]. Dry matter in field crops is the result of the accumulation of net carbon representation during the growing season. Which is the result of the efficiency of vegetation in the interception of solar radiation as the dry weight of the plant generally increases slowly in the early stages of growth and continues to increase in the plant growing season and then decrease with time [28]. That is similar find in report peyvendi et al. [29], the highest mean dry and fresh weight of stems; roots and leaves were obtained in the nano-iron chelated treatment.

The nutrient content of leaves: in this study, adding khazra iron nano chelate fertilizer to winter rapeseed varieties significantly affected the contents nutrients in leaves (table 4). This is due to the genetic nature of each plant species, which in turn determines phenotypic properties, internal content, growth, and specific conditions [28].

The rapeseed (Brassica napus L. var. pactol) have the highest N 1.11%, P 0.56 mg kg^{-1}, S 1.6 mg kg^{-1}, Fe 259 mg kg^{-1} and Mn 36.1mg kg^{-1} at level of 10 kg. ha^{-1}. While the rapeseed (Brassica napus var. oleifera) has, N 1.09 %, P 0.44 mg kg^{-1}, S 1.38 mg kg^{-1}, Fe 246 mg kg^{-1} and Mn 30.6 mg kg^{-1} at level of 10 kg. ha^{-1}. The efficiency of using nano fertilizer from nitrogen and phosphorus is very high, rapid release and absorption by plants, which reduces the loss of unwanted nutrients in soil, water and air by direct absorption and avoids nutrient interaction with soil, microorganisms, water and air [29]

Parameter	Khazra fertilization					
	0 kg. ha^{-1}		5 kg. ha^{-1}		10 kg. ha^{-1}	
	rapeseed varieties					
	(Brassica napus var. oleifera)	(Brassica napus L. var. Pactol)	(Brassica napus var. oleifera)	(Brassica napus L. var. Pactol)	(Brassica napus var. oleifera)	(Brassica napus L. var. Pactol)
Yield (kg ha^{-1})	566.2^{a}	0	898.5^{b}	0	1298.6^{b}	0
Biological yield (kg ha^{-1})	3570^{a}	3120^{b}	6170^{c}	4440^{d}	7900^{e}	4460^{d}
Total dry biomass (kg ha^{-1})	4011^{a}	3004^{b}	5947^{c}	4177^{d}	7288^{e}	4260^{f}

Table 3: The effect of Khazra fertilization (0, 5 and 10 kg. ha^{-1}) on yield, biological yield and total dry biomass content of two rape varieties in Al-zafraniya station (2017-2018)

Parameter	Khazra fertilization					
	0 kg. ha^{-1}		5 kg. ha^{-1}		10 kg. ha^{-1}	
	rapeseed varieties					
	(Brassica napus var. oleifera)	(Brassica napus L. var. Pactol)	(Brassica napus var. oleifera)	(Brassica napus L. var. Pactol)	(Brassica napus var. oleifera)	(Brassica napus L. var. Pactol)
macro-micro nutrients of leaves (mg kg^{-1})						
N %	0.76^{a}	0.97^{b}	1.01^{c}	1.09^{d}	1.09^{d}	1.11^{e}
P	0.23^{a}	0.4^{b}	0.49^{c}	0.53^{d}	0.44^{b}	0.56^{d}
S	0.16^{a}	0.35^{b}	0.65^{c}	1.16^{d}	1.38^{e}	1.6^{f}
Fe	233^{a}	240^{b}	248^{c}	254^{d}	246^{c}	259^{d}
Mn	24.1^{a}	27.1^{b}	29.8^{c}	33.2^{d}	30.6^{c}	36.1^{e}

Table 4: The effect of Khazra fertilization (0, 5 and 10 kg. ha-1) on the nutrient content of leaves of two rape varieties in Al-zafraniya station (2017-2018) Values marked with the same letter do not differ significantly at $p \leq 0.05$

The nutrient content of roots: in table 5, adding khazra iron nano chelate fertilizer to rapeseed varieties significantly affected the content of nutrients in roots. The rapeseed (Brassica napus L. var. pactol) have the highest N 1.31%, P 0.46 mg kg^{-1}, S 1.06 mg kg^{-1}, Fe 253 mg kg^{-1} and Mn 38 mg kg^{-1} at level of 10 kg. ha^{-1}. While the rapeseed (Brassica napus var. oleifera) had, N 1.19%, P 0.34 mg kg^{-1}, S 0.88 mg kg^{-1}, Fe 243 mg kg^{-1} and Mn 31 mg kg^{-1} at level of 10 kg.ha^{-1}. Results show the nutrient content in roots of two rapeseeds varieties at different levels of nano fertilizer was directly proportional to the increase in the level of fertilizer.

Conclusion

The significant effect of khazra iron nano chelate fertilizerfoliar application at level 10 kg.ha-1 to rapeseed (Brassica napus var. oleifera) show increase in the majority of the studied traits; yield, biological yield and total dry biomass. Rapeseed (Brassica napus L. var. pactol) only has total dry biomassandbiological yield. The rapes(Brassica napus L. var. Pactol) was significantly outweighed the (Brassica napus var. oleifera) in the nutrient content of leafs and roots (N, P, S, Fe and Mn).

Para meter	Khazra fertilization					
	0 kg. ha^{-1}		5 kg. ha^{-1}		10 kg. ha^{-1}	
	rapeseed varieties					
	(Brassica napus var. oleifera)	(Brassica napus L. var. Pactol)	(Brassica napus var. oleifera)	(Brassica napus L. var. Pactol)	(Brassica napus var. oleifera)	(Brassica napus L. var. Pactol)
	macro-micro nutrients of roots (mg kg^{-1})					
N %	0.51^{a}	0.76^{b}	1.11^{c}	1.19^{d}	1.19^{d}	1.31^{e}
P	0.19^{a}	0.32^{b}	0.39^{c}	0.44^{d}	0.34^{b}	0.46^{d}
S	0.11^{a}	0.24^{b}	0.47^{c}	0.77^{d}	0.88^{e}	1.06^{f}
Fe	222^{a}	235^{b}	241^{c}	250^{d}	243^{c}	253^{d}
Mn	17^{a}	21.1^{b}	30.8^{c}	35^{d}	31^{c}	38^{e}

Table 5: The effect of Khazra fertilization (0, 5 and 10 kg. ha^{-1}) on the nutrient content of the root of two rape varieties in Al-zafraniya station (2017-2018). Values marked with the same letter do not differ significantly at $p \leq 0.05$

References

1 Khaje, Poor, M.R. Principles of Agriculture, Second Edition, published by Jahad Daneshgahi, Univ. Isfahan. 1998.

2. Baghaie, N., Keshavarz, N., Nazaran, M.H.1thNational Conference on new topics in agriculture,8-10 November,University of Saveh, Iran,-Saveh. 2011

3. Barrett, S.H. and Kohn, J.R., 1991. Genetic and evolutionary consequences of small population size in plants: implication for conservation. In: Falk D.A. and Holsinger, K.E. (eds), Genetics and Conservation of Rare Plants, Oxford University Press, New York, pp: 3-30.

4. Roozbahani, A., Ali, S. Evaluation Amino Acids and Iron Nano particles on Photosynthetic Pigments and Yield of Potato. J. Crop. Nut. Sci., 1(1):7-14.2015.

5. Mohammadi, K. and Rokhzadi, A. Effect of seed priming and foliar application with micronutrients on quality of forage corn (Zea mays). Environmental and Experimental Biology, 14, pp.151-156. 2016.

6. Malhi, S.S., and Gill K. S. "Interactive effects of N and S fertilizers on canola yield, seed quality, and uptake of S and N", Canadian Journal of Plant Science, Vol. (87), pp. 211-222. 2007.

7. Negawer, E. A. and Mahfouz S. A. "Response of canola (Brassica napus L.) to biofertilizers under Egyptian conditions in newly reclaimed soil", International Journal of Agricultural Science, Vol. (2), No. 1, pp. 12-17. 2010.

8. Kandil, A.A., Sharief, A.E. Abido, W.A.E. and Ibrahim, M.M.O. "Response of some canola cultivars (Brassica napus L.) To salinity stress and its effect on germination and seedling properties", Journal of Crop Science, Vol. (3), pp. 95-103. 2012.

9. Jan, M. T., and Khan, S. "Response of wheat yield components of N fertilizer their levels and application time", Pakistanian Journal of Biological Sciences, Vol. (3), pp. 1227-1230. 2000.

10. Sarkar, D. Mandal, B., and Kundu, M.C. "Increasing use efficiency of boron fertilizers by rescheduling the time and methods of application for crops in India", Plant and Soil, Vol. (301), pp. 77-85. 2007.

11. Wissuwa, M., Ismail, A.M. and Graham, R.D."Rice grain zinc concentrations as affected by genotype native soil-zinc availability, and zinc fertilization", Plant and Soil, Vol. (306), pp. 37-48. 2008.

12. Narimani, H., Rahimi, M.M., Ahmadikhah, A. and Vaezi, B."Study on the effects of foliar spray of micronutrient on yield and yield components of durum wheat". Archives of Applied Science Research, Vol. (2), pp. 168-176. 2010.

13. Ai-Qing, Z., Qiong-Li, B., Xiao-Hong, T., Xin-Chun, L., and Gale W. J. "Combined effect of iron and zinc on micronutrient levels in wheat (Triticumaestivum L.)," Journal of Environmental Biology, Vol. (32), pp. 235-239. 2011.

14. Page AL, Miller RH, Kenney DR. Method of Soil Analysis, 2nd (ed) Agron. 9, Publisher, Madiason, Wisconsin, 1982.

15. Mclean, E.O. Soil pH and Lime requirement. In: Methods of soil analysis Part2.Agronomy A.L. Page (ed) Am.Soc. Agron. Madison, 101. USA:199-234.1982.

16. Olsen, S. R., & Sommers, L. E. Phosphorus. In A. L. page et al., (ed) Methods of soil analisis, 2nd ed. Agronomy 9:403-430.1982.

17. Nelson, D.w. AND l.e. Sommers. Total x carbon, Organic carbon and organic Matter.
Methods of soil analysis. Part 2. Chemical and Microbiological properties. ASA, Madison.WI:359-580.1982.

18. Gee.G.W. and J.W. Bauder. Particle size analysis. In: Methods of Soil analysis.Part1. A.Klute (ed). Am.Soc. Agron. Madison 101. USA: 383-41.1986.

19. Khalaj H., Labaffi Hossein Abadi M.R. Nazaran M.H., Sheibani K. and Razazi A. 2008. Application of nano-organic fertilizer, foliar fertilizer and chelated iron on the apple and pear yield.

20. Sodour A.S.C. The technology owner and sole producer of chelated Nano fertilizers in the world. Unit 2, NO. 1, Iran. 2003.

21. Rezaeei, M., Daneshvar, M. and Shirani, A.H., 2014. Effect of iron nano chelated fertilizers foliar application on three wheat cultivars in

Khorramabad climatic conditions. Scientific Journal of Crop Science, 3(2), pp.9-16.
22. Nazaran, A., Pardakhti, M., Hokm Abadi, H., Ashtiani, M., 2005. The role of green space in reducing air pollution and the effect of iron chelate fertilizer Khazra' increase the efficiency of new plants. First Env. Eng. Conf.
23. Mahmoudi H, Ksouri R, Gharsalli M, Lachaâl M. 2005. Differences in responses to iron deficiency between two legumes: lentil (Lens culinaris) and chickpea (Cicer arietinum). Journal of plant physiology 162, 1237-1245.
24. Ziaeian A, Malakoti M.2001. Determination of critical level of Iron (Fe) in wheat farms and its effects on the yield and grain fortification in highly calcareous soils of Iran. IranianJournal of Soil and Water Sciences (Special issue: Agronomy) 12, 45-56.
25. Sheshbahr, M. and M. Movahedidehnoodi. 2012. The effect of foliar application of zinc and iron on soybean seed vigor grown under drought stress. J. Crop Prod. 5(1): 19–35.
26. Issa, A. T. Physiology of Crop Plants, Press of the Ministry of Higher Education and Scientific Research, University of Baghdad. Number of pages: 496. 1990.
27. Peyvendi M., Parande H., Mirza M. 2011. Comparison of the effects of nano-iron chelated with iron chelate on growth parameters and antioxidant enzyme activity of Ocimum basilicum. New Cell Mol. Biotech. Mag. 1: 89–98. 2011.
28. Barrett, S.H. and Kohn, J.R., 1991. Genetic and evolutionary consequences of small population size in plants: implication for conservation. In: Falk D.A. and Holsinger, K.E. (eds), Genetics and Conservation of Rare Plants, Oxford University Press, New York, pp: 3-30.
29. DeRosa, M.C.; Monreal, C.; Schnitzer, M.; Walsh, R. and Sultan, Y., 2010. Nanotechnology in fertilizers. Nat. Nanotechnol., 5(2): 91-93

Received: 8 April 2019
Accepted: 30 April 2019

RESEARCHS / INVESTIGACIÓN

The response of Faba bean (*Vicia faba L.*) varieties as evaluated by varied plant population densities in the highlands of Arsi Zone, Southeastern Ethiopia

Dereje Dobocha*[1], Wogayehu Worku [2], Debela Bekela[3], Zenebe Mulatu[4], Fasil Shimeles[5], and Almaz Admasu[6].

DOI. 10.21931/RB/2019.04.02.5

Abstract**: Field experiments were carried out in 2016 and 2017 cropping seasons under on-farm conditions in Lemuna Bilbilo District, Southeastern Ethiopia to evaluate the effects of three varieties Degaga, Gora, Moti, and six plant populations (10, 25 (control), 30,50, 70, and 90 plants m-2) on faba bean specific yield and yield components. The experiments were laid out in a randomized complete block design in split plot arrangement in which varieties were assigned to main plots and plant populations to subplots with three replications. The year combined analysis of data revealed that seed yield, total biomass yield and test weight of seed were significantly ($p<0.05$) affected by varieties and plant population densities m-2. The highest seed yield (4649, 4594 and 4162 kg ha-1) was obtained at 90,70 and 50 plant m-2 for Degaga, Moti and Gora varieties respectively but, no significant difference between control for Degaga and Moti varieties. The highest total biomass of 9 t ha-1 was recorded from the highest 90 plant population m-2 though not significantly different to the total biomass obtained from 70, 50 and 25 (control) plants m-2. Gora variety significantly recorded the highest test weight of seed (889.2g) than the rest Degaga and Moti varieties. In short, founded on studied agronomic parameters of faba bean, 25 plant population density m-2 was economically recommended for Degaga and Moti varieties whereas, 50 plant population density m-2 was for Gora variety.**

Key Words: Faba bean varieties, plant population density, seed yield, the test weight of seed

Introduction

Ethiopia is the second largest grower of faba bean in the world after the Peoples' Republic of China[1]. It is an important pulse crop grown in the highlands (1800-3000 masl) of Ethiopia, where the soil and weather are considered to be congenial for better growth and development of the crop [2]. It is a crop of high economic value [3] with its edible seed serving as an essential protein complement in the cereal-based Ethiopian diet, particularly for the poor who cannot afford animal protein [4]. Even though the crop plays a significant role for Ethiopian farmers as a source of food, feed, and cash crop, the yield generally is below the world average due to several factors: poor crop management practices, lack of high yielding cultivars, stress inflicted by harsh environmental conditions and poor soil fertility can be listed as some of the causes of low yield [5]. Central Statistics Agency in 2017 [7] reported that the annual national mean faba bean grain yield is 2.11 t ha^{-1} which is quite low when compared with the yield potential of some of the recently released improved varieties. Crop density significantly influences yield and yield components of faba bean due to competition for limited resources in the field especially, for light, water and nutrients [7].

Plant density defines the number of plants per square meter, which in turn determines the area available to each plant [8]. This determines the yield and productivity of a particular crop. Recently, Kulumsa Agricultural Research center has released a faba bean varieties Gora (large seed), Moti (medium seed) and Degaga (small seed) for the potential areas of the country with no specified plant populations per unit area and with seed rate of 200 kg ha^{-1} which is approximately 25 plants per meter square estimated from average test weight and seed rate of three varieties. Plant populations per meter squares vary with varieties in a given period. Since plant population m^{-2} has a direct effect on the cost of seed and final yield, information on this line is highly vital when a new variety is released, and growing environments are changed. Optimum plant density of a crop variety at one location may not apply at other locations because of variation in soil type and other environmental conditions; there is a need to develop site-specific recommendations. Therefore, the recommendation suggested at one time could be used for some time based on maturity groups and growth habit and other associated management factors. Hence, the objective of this study was to determine the optimum plant populations per unit area on yield and yield components of different faba bean varieties.

Materials and methods

Experimental Sites

The experiments were conducted at Lemuna Bilbilo District of Oromia Regional State, Southeastern Ethiopia under on-farm conditions (3 farmers' fields) during the 2016 and 2017 main cropping seasons. The experimental sites are located at 07º 31' 72'' to 07º 32' 79'' north latitude and 39º 13' 54'' to 39º 17' 31'' east longitude, altitude ranges of 2631-2817 meters above sea level. Nitosols dominated the soil of the area. Rainfall data recorded at experimental sites weather stations indicated that the rainfall was nearly normally distributed during the experimental years. The areas received an annual rainfall of 996 mm and 957 mm during the 2016 and 2017 cropping seasons, respectively (Figure 1). The mean maximum and minimum temperatures of the areas during the 2016 and 2017 growing seasons were ranges 20-20.3 ^{O}C and 3.7-4.2 ^{O}C, respectively. It was indicated that the highest mean maximum amount of rainfall was received in August and September respectively (Figure 1).

[1-5]Ethiopian Institute of Agricultural Research, Kulumsa Agricultural Research Center (EIAR/KARC), Department of Agronomy and Crop physiology, P.O.Box 489, Assela, Ethiopia. *Corresponding author E-mail: derejegoda@gmail.com

Experimental Design and Procedure

The experiments were conducted at Lemu Bilbilo Districts on three farmers' fields for two years (2016 and 2017) main cropping seasons. The experiments were laid out in a randomized complete block design in split plot arrangement consisting of 3 faba bean varieties (V1 = Gora, V2 = Moti and V3 = Degaga) as main plot and 6 seed rates (SR1=10 plants/m2, SR2=30 plants/m2, SR3=50 plants m^{-2}, SR4=70 plants m^{-2}, SR5= 90 plants m^{-2}, and recommended seed rate of 200 kg ha^{-1}(25 plants m^{-2}) as a control) as a subplot with 3 replications. Triple superphosphate (TSP), 100 kg ha^{-1}, was used at time of planting. Other cultural practices were applied as per the recommendations. The size of the subplot was 4 m x 2.6 m, and the distance between subplot and blocks (rep) were 1 m and 1.5 m, respectively. All the recommended packages for faba bean production; two times hand weeding at 25-30 and 40-45 days after an emergency, a single application of 100 kg ha^{-1} TSP fertilizer along with seeds was applied for each treatment. Seedbed preparation was conducted using oxen plow based on farmer's practices.

Data Collected

Agronomic parameters collected included, seed yield per hectare, biological yield per hectare (seed yield plus straw yield), thousand seed weight (TSW), harvest index (HI) which is calculated by the ratio of seed yield to biological yield. To estimate seed yield of faba bean, plot sizes of 2mx3m (6 m^{2}) were harvested from each plot in December. After threshing, the harvested materials, seeds were cleaned, weighed and adjusted to 10% moisture level. The total seed yields recorded on a plot basis were converted to kg ha^{-1} for statistical analysis.

Statistical Analysis

The crop data were subjected to analysis of variance using the General Linear Model Procedure of SAS computer software version 9.1 (SAS Institute, 2002). Data were not combined over the year due to heterogeneity. Whenever treatment effects were significant, the mean differences were separated using the least significant difference (LSD) test at 5% level of significance.

Results and discussion

Seed yield

Analysis of variance showed that seed yield was significantly affected by plant population m^{-2} and the interaction of varieties and plant population m^{-2} but, non-significantly affected by varieties (Table 3). The results showed that among the plant populations, ten plants m^{-2} (1998.4 kg ha^{-1}) and 30 plants m^{-2} (3105.7 kg ha^{-1}) gave significantly lower productivity than the control (3485.4 kg ha^{-1}) (Table 2 and Figure 3). Similarly, Al-Suhaibani et al. (2013) [8] stated that when the planting density is too low each plant may perform at its maximum capacity, but there may be insufficient total plants to reach the optimum yield. Upon the relationships between plant density and yield Mellendorf (2011) [9] explained two concepts. First, maximum crop yield can only be achieved if the crop community can produce sufficient leaf area to provide maximum light interception during reproductive growth. Second, equidistant plant spacing maximizes yield because it minimizes plant to plant competitions. Therefore, the reduction in yield caused by high plant density (90 plant m^{-2}) except for Degaga variety could be due to the competition between plants for this treatment begins during early vegetative growth. This new competition increases shading between leaves, leading to insufficient carbon fixation, increases respiration rate and increases intra-plant competition between vegetative and reproductive structures for assimilates. The result was in line with that of Al-Suhaibani et al. (2013) [8] who reported the seed yield per hectare was significantly increased with densities up to certain plant population m^{-2}. A significant interaction between varieties and plant populations' m^{-2} on seed yield showed that irrespective of varieties there was a reduction in grain yield $ha^{-1}$with reduced plant population m^{-2}. The variety Degaga has grown with a 90 plants m^{-2} produced significantly higher seed yield of 4649 kg ha^{-1} than the other plant populations' combinations except for 70 plants m^{-2} which exhibited the non-significance difference between two plant population m^{-2}. There was also a non-significance difference between 70 plants m^{-2} and 25 plants m^{-2} (control). In conformity with the results, Dahmardeh et al. (2010) [10] stated that the highest and lowest seed

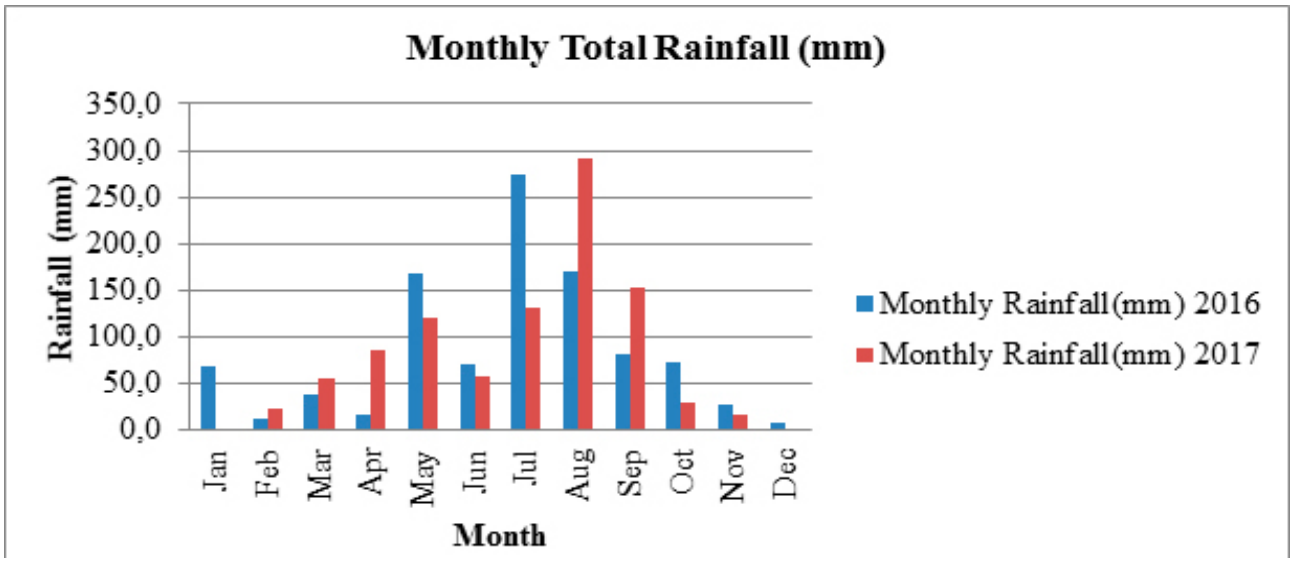

Figure. 1. Monthly Rainfall (mm) during the experimental years (2016-2017) at Lemu Bilbilo Districts

yields were obtained with the highest and lowest plant density, respectively. The next best seed yield (4594 and 4162 kg ha^{-1}) were obtained from Gora and Moti combined with 50 and 70 plants m^{-2}, respectively but, non-significant difference was observed between 70 and control (25) plants m^{-2} for Moti variety (Table 1 and figure 2). m^{-2}. The 50, 70 and 90 plants m^{-2} produced higher total biomass of 28.6 % and 14.3 % over the control, respectively. These results are confirmed by several faba bean investigators [10,11] who recorded the largest biological yield from the highest plant density due to an increased number of plants per unit area. These findings were

Plant populations m^{-2}						
Variety	**Control(25)**	**10**	**30**	**50**	**70**	**90**
Degaga	3549^{bcdef}	1876^{gh}	3206^{def}	3232^{def}	4455^{abc}	4649^{a}
Gora	3005^{ef}	1578^{h}	2677^{fg}	4594^{ab}	3099^{ef}	3494^{cdef}
Moti	3902^{abcde}	2541^{fgh}	3434^{cdef}	3740^{abcde}	4162^{abcd}	3798^{abcde}

Table 1. Mean number of seed yield (kg ha^{-1}) as affected by the interaction effect of varieties and plant populations

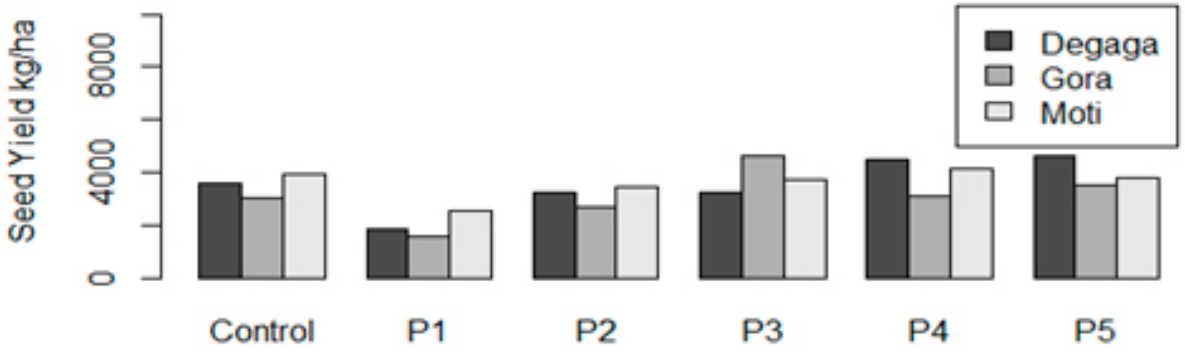

Figure 2. Interaction effect of plant populations and varieties on grain yield combined over sites and years.

Total biomass

The analysis of variance revealed that total biomass was significantly affected by plant population m^{-2}, but varieties and the interaction of varieties and plant population m^{-2} were not significant (Table 3). The highest total biomass of 9 t ha^{-1} was recorded in the treatment sown with 90 plant population m^{-2} though not significantly different to the total biomass obtained from 70,50 plants m^{-2} (8 t ha^{-1}) and control(7 t ha^{-1}) (Table 2 and Figure 3). The lowest total biomass of 4 t ha^{-1} was recorded in the treatment with 10 plants similar to that of Badawy (2011) [12] who stated biological, and seed yields were significantly increased with increasing plant density from 22 to 44 plant m^{-2}. Worku and Demisie (2012) [13] also reported that a large leaf area index at high plant density might attribute to improved light interception thus, ensuring high biomass and yield than at low plant density. Similarly, Dahmardeh et al. (2010) [14] reported higher biological yield in sandy loam soil in higher plant density due to an increase in the number of plants in the unit's area.

Treatments	Seed yield (kg ha^{-1})	Total biomass (t ha^{-1})	Harvest index (%)	1000-seed weight(gm)
Variety				
Degaga	3494.4	7.1	50.3	557.5^{b}
Gora	3074.6	6.9	44.4	889.2^{a}
Moti	3596.3	7.6	46.7	609.4^{b}
LSD(0.05)	NS	NS	NS	66.2
Plant population m^{-2}				
Control (25 plants m^{-2})	3485.4ab	7.0^{ab}	46.9	686.3
10 plants m^{-2}	1998.4c	4.0^{c}	45.6	670.0
30 plants m^{-2}	3105.7b	6.0^{b}	48.4	695.4
50 plants m^{-2}	3855.3a	8.0^{a}	46.3	681.1
70 plants m^{-2}	3905.4a	8.0^{a}	49.4	687.3
90 plants m^{-2}	3980.0a	9.0^{a}	46.2	692.1
LSD(0.05)	608.0	1.6	NS	NS

Table 2. Mean values of seed yield (kg ha-1), total biomass (t ha-1), harvest index (%), and thousand seed weight(gm), as affected by N and P combined over sitesand years.

Means followed by the same letter(s) within a column are not significantly different from each other at 5% level of significance, ns: Not significant

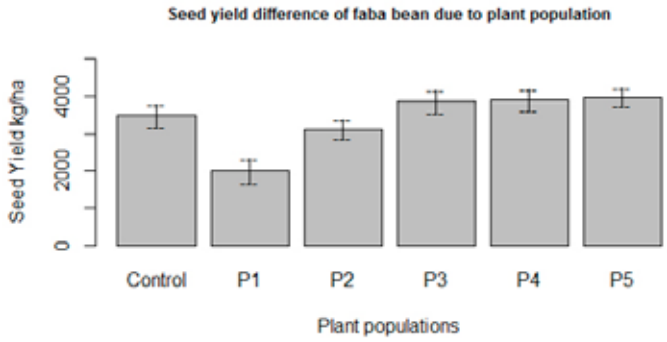

Figure 3. Effect of plant populations on seed yield of faba bean combined over sites and years

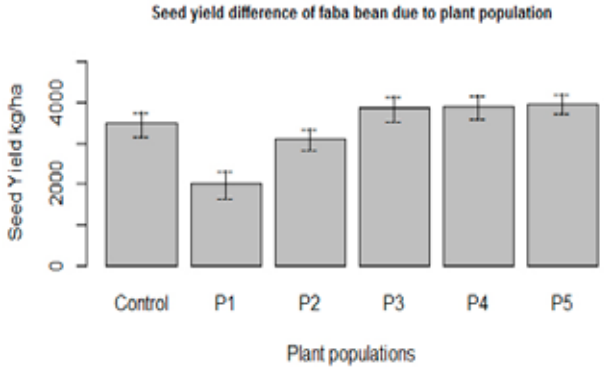

Figure 4. Effect of plant populations on total biomass of faba bean combined over sites and years

Mean Squares				
Sources of Variation	Grain yield (kg ha-1)	Total biomass (t ha-1)	Harvest index (%)	1000-seed weight (gm)
Replication	1310618ns	7ns	92ns	1003ns
Variety(V)	1376612ns	2ns	161ns	573040***
Error(a)	2562223	10	76	5115
Plant population(P)	5142505***	24***	20ns	731ns
(V*P)	888450*	4ns	22ns	1239ns
Error(b)	398840	3	72	900

Table 3. Mean squares of seed yield (kg ha^{-1}), total biomass (t ha^{-1}), harvest index (%) and thousand seed weight(gm), as affected by main and interaction effects of variety and plant populations combined over sites and years

Means followed by the same letter(s) within a column are not significantly different from each other at 5% level of significance, ns: Not significant

Harvest Index (HI %)

The harvest index reflects the ability of the genotypes to partition its dry matter into seed and straw, and the ability to maintain the right balance between seed and straw yield(Al-Rifaee et al.,2004). The result revealed that the harvest index did not show a significant difference among varieties, plant populations m^{-2}and their interactions (Table 3). Even though, statistically non-significance difference among varieties, the highest value of harvest index was recorded from the smaller seed size Degaga variety. This could be attributed to the rapid development of seed yield in smaller seeds, once the reproductive phase started so that the process of maturation proceeded quickly and led to a harvestable crop while weather conditions are right [15]. Plant population 70 plants m^{-2} has resulted in numerically higher harvest index (49.6) over the rest plant population m^{-2} even if they were statistically non-significant (Table 2). Similar results were obtained by Kubure et al. (2016) [2] who stated the genotypes, plant density, and their interaction did not differ in harvest index. The result is in line with Khamooshi et al. (2012) [16] who reported the non-significant effect of plant density on harvest index of faba bean.

Test weight of seed (g)

Test weight of seed significantly responded to variety but was not significantly affected by plant population m^{-2} and variety plant population m^{-2} interaction (Table 3). This agrees with Thangwana and Ogola (2012) [14] and Gezahegn et al. (2016) [8] who reported the non-significant effect of plant density on 100 seed weight of chickpea and faba bean, respectively. Highest test weight of seed was recorded from Gora variety which was statistically different from Degaga and Moti varieties, but no significant difference among Degaga and Moti varieties in test weight of seed (Table 2). That might be due to the seed size difference of varieties. In comfort with the results, Bakry et al. (2011) [4] reported a significant effect between among faba bean varieties concerning test weight of seed.

Conclusion

The results revealed that among agronomic parameters considered only seed yield was significantly affected by the interaction of varieties with plant population density m^{-2}. Total biomass was affected by plant population density m^{-2} whereas test weight of seed was affected by varieties. Variety Degaga has grown with a 90 plants m^{-2} produced significantly higher seed yield of 4649 kg ha^{-1} which exhibited the non-significance difference between 70 plants m^{-2}.Inturns no significance difference between70 plants m^{-2} and 25 plants m^{-2} (control). The highest seed yield of 4594 and 4162 kg ha^{-1} were obtained from Gora and Moti combined with 50 and 70 plants m^{-2}, respectively but, non-significant difference were observed between 70 and control (25) plants m^{-2} for Moti variety. The highest total biomass of 9 t ha^{-1} was recorded from the highest plant population m^{-2} though not significantly different to the total biomass obtained from 70, 50 and 25 (control) plants m^{-2} . The highest test weight of seed (889.2g) was recorded from Gora variety. In nutshell, based on seed yield and total biomass 25 plant population density m^{-2} was economically feasible for Degaga and Moti varieties whereas 50 plant population density m^{-2} was for Gora variety.

References

1. Temesgen, T., Keneni, G., Sefera, T., & Jarso, M. (2015). Yield stability and relationships among stability parameters in faba bean (Vicia faba L.) genotypes. The crop journal, 3(3), 258-268.

2. Kubure, T. E., Raghavaiah, C. V., & Hamza, I.

(2016). Production potential of faba bean (Vicia faba L.) genotypes in relation to plant densities and phosphorus nutrition on vertisols of central highlands of West Showa Zone, Ethiopia, east Africa. Advances in Crop Science and Technology, 1-9.3.

3. Tolessa, T. T., Keneni, G., & Mohammad, H. (2015). Genetic progresses from over three decades of faba bean ('Vicia faba'L.) breeding in Ethiopia. Australian Journal of Crop Science, 9(1), 41.

4. Bakry, B. A., Elewa, T. A., El Karamany, M. F., Zeidan, M. S., & Tawfik, M. M. (2011). Effect of row spacing on yield and its components of some faba bean varieties under newly reclaimed sandy soil condition.

5. Brink, M., Belay, G., & De Wet, J. M. J. (2006). Plant resources of tropical Africa 1: Cereals and pulses (pp. 54-57). Wageningen, The Netherlands: PROTA Foundation.

6. Tafere, M., Tadesse, D., & Yigzaw, D.(2012). Participatory varietal selection of faba bean (Vicia faba L.) for yield and yield components in Dabat district, Ethiopia, Wudpecker. Journal of Agricultural Research, 1, 270–274.

7. CSA (Central Statistics Agency) (2017). Report on Area and Production of Major Crops (Private Peasant Holdings, Meher Season): Agricultural Sample Survey. Central Statistics Agency, Addis Ababa, Ethiopia.

8. Kissi Wakweya, Reta Dargie, Tamiru Meleta (2016). Effect of Sowing Date and Seed Rate on Faba Bean (Vicia faba L.,) Growth, Yield and Components of Yield at Sinana, Highland Conditions of Bale, Southeastern Ethiopia. International Journal of Scientific Research in Agricultural Sciences, 3(1), pp. 025-034.

9. Gezahegn, A. M., Tesfaye, K., Sharma, J. J., & Belel, M. D. (2016). Determination of optimum plant density for faba bean (Vicia faba L.) on vertisols at Haramaya, Eastern Ethiopia. Cogent Food & Agriculture, 2(1), 1224485.

10. Al-Suhaibani, N., El-Hendawy, S., & Schmidhalter, U. (2013). Influence of varied plant density on growth, yield and economic return of drip irrigated Faba bean (Vicia faba L.). Turkish Journal of Field Crops, 18(2), 185-197.

11. Mellendorf, E.N. (2011). Soybean growth and yield response to interplant competition relief in various plant density environments. MSc Thesis, University of Illinois at Urbana- Champaign, USA.85 p.

12. Dahmardeh, M., Ramroodi, M., & Valizadeh, J. (2010). Effect of plant density and cultivars on growth, yield and yield components of faba bean (Vicia faba L.). African journal of Biotechnology, 9(50), 8643-8647.

13. Kubure, T. E., Raghavaiah, C. V., & Hamza, I. (2016). Production potential of faba bean (Vicia faba L.) genotypes in relation to plant densities and phosphorus nutrition on vertisols of central highlands of West Showa Zone, Ethiopia, east Africa. Advances in Crop Science and Technology, 1-9.3.

14. Badawy, R. A. W. (2011). Effect of planting date and plant density on growth and yield of some faba bean varieties. (2011) Published by Cairo Univ., Faculty of Agriculture, Egypt

15. Worku, W., & Demisie, W. (2012). Growth, light interception and radiation use efficiency response of pigeon pea (Cajanus cajan) to planting density in Southern Ethiopia. Journal of Agronomy, 11, 85–93. http://dx.doi.org/10.3923/ja.2012.85.93.

16. Thangwana, N. M., & Ogola, J. B. O. (2012). Yield and yield components of chickpea (Cicer arietinum): Response to genotype and planting density in summer and winter sowings. Journal of Food, Agriculture & Environment, 10, 710–715

17. Dahmardeh, M., Ramroodi, M., & Valizadeh, J. (2010). Effect of plant density and cultivars on growth, yield and yield components of faba bean (Vicia faba L.). African journal of Biotechnology, 9(50), 8643-8647.

18. Al-Rifaee, M. O. H. D., Turk, M. A., & Tawaha, A. R. M. (2004). Effect of seed size and plant population density on yield and yield components of local fababean (Vicia faba L. major). International Journal of Agriculture and Biology, 6(2), 294-299.

19. Khamooshi, H., Mohammadian, N., Saamdaliri, M., & Foroughi, Z. (2012). Study on effect of plant density and nitrogen on yield and yield components of Faba bean (Vicia faba L.). Journal of Ornamental and Horticultural Plants, 2, 161–167.

Received:3 April 2019

Aproved: 3 May 2019

RESEARCHS / INVESTIGACIÓN

Propiedades antioxidante y antiglicosilante de extractos de *Diplotaxis tenuifolia*

Antioxidant and antiglycation properties of extracts of *Diplotaxis tenuifolia*

Parada Romina B.[1], Vallejo Marisol[1], Marguet Emilio R[1].

DOI. 10.21931/RB/2019.04.02.6

Resumen: El objetivo de este trabajo fue investigar el contenido de fenoles y la actividad biológica en hojas de *Diplotaxis tenuifolia* recolectadas en la Patagonia (Argentina). La actividad de antiglicosilación se evaluó mediante los modelos de albúmina sérica bovina-glucosa (BSA-glu) y la reacción de Maillard. Solo en el extracto acuoso de materia seca, la reacción de Maillard se logró inhibir un 40 %. Los resultados restantes no permitieron realizar conclusiones. El extracto acuoso presentó mayor contenido de polifenoles que el metanólico (1074,25 y 647,5 mg equivalente de ácido gálico/100 g de materia seca, respectivamente). Por otro lado, el contenido de flavonoides fue comparable entre los extractos acuoso y metanólico (218,2 y 213,4 mg equivalente de quercetina/100 g de materia seca, respectivamente). En cuanto a las propiedades antioxidantes, CUPRAC (capacidad de antioxidante sobre el cobre) presentó valores de 655,6 mg equivalentes de Trolox /100 g de materia seca y 749,6 mg equivalentes de ácido ascórbico/100 g de materia seca para el extracto acuoso y 1045,2 mg equivalente de Trolox/100 g de materia seca y 1203,9 mg equivalente de ácido ascórbico/100 g de materia seca para el metanólico. El ensayo de reducción DPPH (2,2-difenil-1-picrilhidrazilo) exhibió valores de 203,3 mg equivalentes de Trolox/100 g de materia seca y 180,0 mg equivalentes de ácido ascórbico/100 g de materia seca para el extracto acuoso, y 97,7 mg equivalentes de Trolox/100 g de materia seca y 89,3 mg equivalentes a ácido ascórbico/100 g de materia seca para el metanólico. Los resultados obtenidos demuestran el potencial antioxidante de D. tenuifolia recolectada en las regiones extremas de la Patagonia. Esta planta comestible es una fuente rica de antioxidantes que debe considerarse como alimento funcional, su consumo es recomendable para prevenir el daño celular al eliminar los radicales libres nocivos. Palabras Clave: rúcula salvaje, polifenol, antioxidante.

Abstract: The goal of this study was to investigate phenolic contents and biological activities in leaves of *Diplotaxis tenuifolia* collected in Patagonia (Argentina). Anti-glycation activities were tested by bovine serum albumin-glucose (BSA-glu) and Maillard reaction models. Only in the case of water extract of dry matter, Maillard reaction could be 40 % inhibited. The remaining results do not allow make definitive conclusions. Water extracts exhibited higher polyphenol content than methanolic ones (1074.25 and 647.5 mg Gallic acid equivalent/100 g of dry matter, respectively). On the other hand, flavonoid content was comparable between the water and methanolic extracts (218.2 and 213.4 mg quercetin equivalent/100 g of dry matter, respectively). Regarding antioxidant properties, CUPRAC (Cupric reducing antioxidant capacity) showed values of 655.6 mg Trolox equivalent/100 g of dry matter and 749.6 mg ascorbic acid equivalent/100 g of dry matter for water extracts and 1045,2 mg Trolox equivalent/100 g of dry matter and 1203,9 mg ascorbic acid equivalent/100 g of dry matter for methanolic ones. DPPH (2,2-diphenyl-1-picrylhydrazyl) radical scavenging assay displayed values of 203,3 mg Trolox equivalent/100 g of dry matter and 180.0 mg ascorbic acid equivalent/100 g of dry matter for water extracts, and 97.7 mg Trolox equivalent/100 g of dry matter and 89,3 mg ascorbic acid equivalent/100 g of dry matter for methanolic ones. The results obtained highlight the antioxidative potential of D. tenuifolia collected in extreme regions like Patagonia. This edible plant is an antioxidant-rich source that should be considered as functional food, its consumption is recommendable to prevent cell damage by scavenging deleterious free radicals.

Keywords: wild rocket, polyphenol, antioxidant

Introducción

La familia Brassicaceae (Cruciferae) presenta 350 géneros y alrededor de 3.500 especies. Incluye algunas especies de relevancia en la economía mundial, tanto hortícolas, como ornamentales, oleaginosos, forrajeros y una gran variedad de condimentos [1]. *Diplotaxis tenuifolia* (L.) DC. es una de las especies pertenecientes a la familia Brassicaceae, conocida vulgarmente como "rúcula salvaje" [1] o "flor amarilla" [2]. Esta planta perenne, originaria de Europa y Asia occidental, se introdujo en el año 1920 en Argentina como planta melífera pero se ha difundido convirtiéndose en una de las especies invasoras más abundantes [3].

Las brasicáceas son importantes fuentes de compuestos bioactivos con propiedades farmacológicas debido a la presencia de glucosilonatos, flavonoides, folatos, fibras y carotenoides [4]. La flor amarilla se caracteriza por presentar elevados niveles de hierro, calcio y potasio; contiene algunas vitaminas, particularmente vitamina A y ácido ascórbico. Con excepción de las raíces, todos los tejidos de *D. tenuifolia* contienen flavonoides y polifenoles que, en forma conjunta con el ácido ascórbico, le confieren propiedades antioxidantes por lo que su inclusión en la dieta resulta recomendable [5].

[1]Laboratorio de Biotecnología Bacteriana, Facultad de Ciencias Naturales y Ciencias de la Salud (Sede Trelew), Universidad Nacional de la Patagonia San Juan Bosco – Argentina. Email parada.ro91@gmail.com

Los antioxidantes son compuestos capaces de retrasar o inhibir los procesos de oxidación que se producen bajo la influencia del oxígeno o especies reactivas de oxígeno. Recientemente, los antioxidantes han atraído considerable atención en relación con los radicales y el estrés oxidativo como preventivos de enfermedades degenerativas, cáncer y envejecimiento celular [6].

En nuestro país se han realizado numerosos estudios sobre *D. tenuifolia* como especie invasora, pero existen escasas investigaciones vinculadas con sus propiedades nutricionales y/o farmacológicas. Este trabajo tiene como objetivo determinar el contenido de polifenoles, flavonoides, la actividad antioxidante y antiglicosilante presentes en extractos acuosos y metanólicos de hojas de *D. tenuifolia.*

Materiales y Métodos

Recolección del material de estudio

Se recolectaron plantas de *D. tenuifola* silvestre en enero de 2017 del Valle Inferior del Río Chubut (VIRCh), Argentina. Las hojas de *D. tenuifolia* se sometieron a desecación en estufa a 37 °C durante 2 días. El material se conservó en un lugar fresco y seco hasta su posterior estudio.

Preparación de extractos, acuoso y metanólico

El extracto acuoso se obtuvo a partir de 1 g del material seco suspendido en 10 ml de agua destilada y luego tratado en autoclave a 120 °C durante 15 min. El extracto metanólico se obtuvo de 1 g de material seco suspendido en 10 ml de metanol y en agitación durante 3 h a 37 °C. En ambos casos los extractos se centrifugaron a 3.000 rpm y los sobrenadantes obtenidos se conservaron a -20 °C hasta el momento de su procesamiento.

Propiedades antiglicosilación de los extractos

Reacción de Maillard (Lys-Glu)

Los efectos de los extractos en la reacción de Lys-Glu Maillard se determinaron mediante protocolos descritos anteriormente [7]. Se realizó una mezcla de glucosa y lisina (1 mol/l, 0,5 ml) con 0,5 ml de los extractos y 0,5 ml de buffer fosfato de sodio (0,25 ml/l) en tubos de ensayo con tapa a rosca y se sometieron a 50 °C en baño termostático durante 3 h. Se midió la absorbancia a 465 nm y el porcentaje de inhibición de la reacción de Maillard se calculó según la fórmula[8]

Inhibición de la reacción de Maillard (%) =

$$\left(1-\frac{(\text{Abs 3 h de la muestra - Abs 0 h de la muestra})}{(\text{Abs 3 h del blanco - Abs 0 h del blanco})}\right)\times 100$$

Modelo de glicosilación BSA-Glu

El ensayo de antiglicosilación se realizó según el modelo albúmina sérica bovina-glucosa (BSA-Glu) [9]. La glucosa (1,5 ml/l, 0,5 ml) se agregó a 0,5 ml del buffer de fosfato de sodio (50 mmol, pH 7,4) y 0,5 ml de los extractos, se incubó por 2 h a 37 °C. Luego del agregado de albúmina de suero bovino (30 mg ml^{-1}, 0.5 ml) se incubó a 37 °C durante 5 días. Se centrifugaron las mezclas y se tomó 100 µl del sobrenadante de cada reacción y se adicionó 1 ml de NBT (cloruro de nitroblue tetrazolium), se dejó incubar durante 10 min y se midió la absorbancia a 500 nm. El porcentaje de la capacidad de antiglicosilación se obtuvo mediante la siguiente fórmula [8]

Capacidad de antiglicosilación (%) =

$$\left(1-\frac{(\text{Abs 5 días de la muestra - Abs 0 días de la muestra})}{(\text{Abs 5 días del blanco - Abs 0 días del blanco})}\right)\times$$

Capacidad antioxidante de los extractos

Capacidad antioxidante según el método de reducción DPPH

La capacidad antioxidante se evaluó según el método de reducción de DPPH [10]. Se realizaron curvas estándares con Trolox y ácido ascórbico como agentes reductores (10-200 µg/ml) y los resultados fueron expresados como mg equivalentes (Eq) de Trolox o ácido ascórbico por 100 g de materia seca.

Capacidad antioxidante sobre el cobre (CUPRAC)

La capacidad reductora de los extractos se determinó mediante el poder antioxidante reductor del cobre siguiendo la metodología previamente descrita [11]. Se utilizó como estándares Trolox y ácido ascórbico como agentes reductores (10-200 µg/ml) y los resultados fueron expresados como mg Eq de Trolox o ácido ascórbico por 100 g de materia seca.

Contenido fenólico total

El contenido fenólico total de los extractos se determinó por el método de Folin-Ciocalteu siguiendo las recomendaciones detalladas previamente [12]. Se realizó una curva de calibración utilizando ácido gálico como estándar, los resultados se expresaron como mg Eq de ácido gálico por 100 g de materia seca.

Contenido total de flavonoides

El contenido total de flavonoides en los extractos se determinó según la técnica descrita previamente [13]. Se realizó una curva de calibración utilizando quercetina como estándar y el resultado de la concentración de flavonoides se expresó como mg Eq de quercetina por 100 g de materia seca.

Resultados y Discusión

En este trabajo se utilizaron dos técnicas para determinar la capacidad antiglicosilante de los extractos de *D. tenuifolia*: la reacción de Maillard y el modelo de glicosilación glucosa-albúmina sérica humana. En la primera se determina la capacidad de los extractos de inhibir la reacción no enzimática entre los grupos amino de un aminoácido con un azúcar reductor. En el modelo restante se determina la capacidad de interferir la reacción de Maillard entre los grupos amino libre de las 59 lisinas que posee la albúmina y la glucosa a través de su grupo carbonilo libre. Los resultados nos permiten decir que solo en el caso de los extractos acuosos se logró inhibir parcialmente la reacción de Maillard (≥40 %). En el modelo de glicosilación glucosa-albúmina los datos no permiten llegar a conclusiones definitivas poniendo en duda la utilidad de la técnica con estos tipos de extractos. Este método está basado en la formación de las bases de Schiff y se utiliza principalmente para controlar el nivel de proteínas glicosiladas en sangre en los diabéticos [14] sin embargo, la técnica muestra interferencia cuando se trabaja con extractos de absorbancia elevada como los obtenidos con *D. tenuifolia*. En la actualidad se utilizan métodos basados en fluorescencias de los productos de glicosilación avanzada (AGEs) [8], siendo un modelo más eficiente que evita este tipo de interferencia.

El extracto acuoso de *D. tenuifolia* presentó un 60 % más de concentración de fenoles con respecto al extracto metanólico, mien-

tras que las concentraciones de flavonoides resultaron semejantes para ambos métodos de extracción (Tabla 1). Estudios previos han determinado que la cuantificación de fenoles varía según la especie de *Diplotaxis*, los órganos vegetales, como también depende de los factores ambientales y de crecimiento [13]. Los resultados de este trabajo concuerdan con los obtenidos en estudios anteriores, donde se implementó la metodología basada en la reducción de molibdeno del reactivo Folin-Ciocalteu. En ensayos realizados con extractos metanólicos de *D. harra*, se registraron una concentración de fenoles y flavonoides de 547 mg Eq de ácido gálico/100 g de materia seca y 383 mg Eq de quercetina/100 g materia seca, respectivamente [15]. Mientras que en estudios con extractos acuosos de *D. harra*, se determinaron concentraciones de 1017 mg de ácido cafeico/100g materia seca y 383,7 mg de Rutin/100 g de materia seca, para fenoles y flavonoides, respectivamente [13]. Los resultados obtenidos permiten afirmar que resultan comparables

Conclusiones

Los resultados obtenidos en este trabajo indicarían el potencial de *D. tenuifolia* como alimento o como suplemento dietario debido a sus propiedades fitoquímicas. Su contenido en polifenoles, flavonoides y actividad antioxidante se vincularía con la capacidad de disminuir o eliminar efectos del estrés oxidativo y en consecuencia favorecer la salud de los consumidores. Investigaciones posteriores deberán estar dirigidas a determinar las variaciones de los parámetros estudiados en función de diferentes especies, regiones geográficas, variación estacional y también la aceptación del consumidor sobre la base de su palatabilidad.

Extractos (*D. tenuifolia*)	Fenoles [a]	Flavonoides [b]	DPPH [c, d]		CUPRAC [c, d]	
Acuoso	1074,25 ± 55	218,2 ± 22,4	203,3 ± 41,2	180,0 ±18,1	655,6 ± 42,2	749,6 ± 29,9
Metanólico	647,5 ± 43	213,4 ± 36,5	97,0 ± 22,1	89,3 ±5,7	1045,2 ± 80,4	1203,9 ± 217,0

Tabla 1: Actividades biológicas de los extractos de Diplotaxis tenuifolia: fenoles, flavonoides, DPPH, CUPRAC (media ± desvío estándar).

[a] Resultados expresados como mg equivalente de ácido gálico/100 g de materia seca; [b] resultados expresados como mg equivalentes de quercetina/100 g de materia seca; [c] resultados expresados como mg equivalentes de Trolox/100 g de materia seca; [d] resultados expresados como mg equivalentes de ácido ascórbico/100 g de materia seca.

las concentraciones de polifenoles y flavonoides entre las especies D. tenuifolia y D. harra. Si bien se muestran pequeñas variaciones en la cuantificación de fenoles, estas pueden estar asociadas a diferentes factores como la especie evaluada, el lugar de cosecha del material vegetal, las condiciones climáticas y las etapas de desarrollo de la planta [13].

Debido a la falta de un método estandarizado que determine con precisión la capacidad antioxidante de extractos vegetales, resulta recomendable usar más de un ensayo analítico. En este trabajo se utilizaron los métodos DPPH y CUPRAC basados en la transferencia simple de electrones [16]. La capacidad antioxidante de los extractos acuoso y metanólico exhibieron valores más altos por el método CUPRAC que los determinados por el método de reducción de DPPH. La técnica de CUPRAC permite determinar antioxidantes hidrofílicos y lipofílicos en simultáneo, mientras que el análisis DPPH interfiere en la detección de antioxidantes hidrofílicos, debido al solvente utilizado, alcanzando valores menores. Los resultados obtenidos en general concuerdan con trabajos previos donde evalúan diferentes especies de la familia Brassicaceae [6,17]. Resultaría conveniente estandarizar los métodos de extracción y los métodos de detección con el propósito de establecer comparaciones entre géneros/especies y las influencias ejercidas por factores externos, como clima, región geográfica, estadio del cultivo etc. cultivo etc.

Referencias

1. Pratap A, Gupta S. Biology and Ecology of Wild crucifers. In: Gupta Kumar S (ed). Biology and Breeding of Crucifers. CSR Press, 2009, pp 37–68.

2. Fernández A. Evaluación de la calidad de la flor amarilla (Diplotaxis tenuifolia) y sus efectos en la producción de la carne. 2009.

3. Mitidieri A. Diplotaxis tenuifolia, Senecio madagascariensis poiret, and Senecio grisebachii baker , three perennial weeds now spreading in Argentina. In: Food and Agriculture Organization of the United Nations (ed). Ecology and Control of Perennial Weeds in Latin America. Chile, 1986, pp 185–203.

4. Jin J, Koroleva OA, Gibson T, Swanston J, Maganj J, Zhang Y et al. Analysis of phytochemical composition and chemoprotective capacity of rocket (Eruca sativa and Diplotaxis tenuifolia) leafy salad following cultivation in different environments. J Agric Food Chem 2009; 57: 5227–5234.

5. Nicoletti R, Raimo F, Miccio G. Diplotaxis tenuifolia : biology , production and properties. Eur J Plant Sci Biotechnol 2007; 1: 36–43.

6. Pisoschi AM, Negulescu GP. Methods for Total Antioxidant Activity Determination : A Review. Biochem Anal Biochem 2011; 1: 1–10.

7. Kuda T, Yano T. Changes of radical-scavenging capacity and ferrous reducing power in club mackerel Scomber japonicus and Pacific saury Cololabis saira during 4 oC storage and retorting. LWT-Food Sci Technol 2009; 42: 1070–1075.

8. Kuda T, Eda M, Kataoka M, Takahashi H, Kimura B. Anti-glycation properties of the aqueous extract solutions of dried algae products harvested and made in the Miura Peninsula, Japan, and effect of lactic acid fermentation on the properties. J Food Chem 2016; 28: 1109–1115.

9. Wang W, Yagiz Y., Buran TJ, Nunes CN, Gu L. Phytochemicals from berries and grapes inhibited the formation of advanced glycation end-products by scavenging reactive carbonyls. Food Res Int 2011; 44: 2666–2673.

10. Chen YC, Sugiyama Y, Abe N, Kuruto-Nima R, Nozawa R, Hirota A. DPPH radical scavenging compounds from Dou-Chi, a soybean fermented food. Biosci Biotechnol Biochem 2005; 69: 999–1006.

11. Apak R, Güçlü K, Demirata B, Özyürek M, Çelik SE, Bektasog˘lu B et al. Comparative evaluation of various total antioxidant capacity assays applied to phenolic compounds with the CUPRAC assay. Molecules 2007; 12: 1496–1547.

12. Agbor G, Vinson J, Donnelly P. Folin-Ciocalteau Reagent for Polyphenolic Assay. Int J Foos Sci Nutr Diet 2014; 3: 147–156.

13. Bahloul N, Bellili S, Aazza S, Chérif A, Faleiro M, Antunes M et al. Aqueous Extracts from Tunisian Diplotaxis: Phenol Content, Antioxidant and Anti-Acetylcholinesterase Activities, and Impact of Exposure to Simulated Gastrointestinal Fluids. Antioxidants 2016; 5: 12.

14. Rosenthal M, Olenick L. Evaluation of a Single-Color-Reading Method for Determining Fructosamine. Clin Chem 1988; 34: 360–363.

15. Falleh H, Msilini N, Oueslati S, Ksouri R, Magne C, Lachaâl M et al. Diplotaxis harra and Diplotaxis simplex organs: Assessment of phenolics and biological activities before and after fractionation. Ind Crops Prod 2013; 45: 141–147.

16. Shahidi F, Zhong Y. Measurement of antioxidant activity. J Funct Foods 2015; 18: 757–781.

17. Halvorsen BL, Holte K, Myhrstad MCW, Barikmo I, Hvattum E, Remberg SF et al. Nutrient Requirements A Systematic Screening of Total Antioxidants in Dietary Plants. J Nutr 2001; 132: 461–471.

Recibido: 8 marzo 2019

Aprobado: 4 mayo 2019

RESEARCHS / INVESTIGACIÓN

Effectiveness of chitosan as natural coagulant in treating turbid waters

Marey AM

DOI. 10.21931/RB/2019.04.02.7

Abstract: Aluminum, Lime and iron coagulants are commonly used in most industries for many decades to coagulate particles in surface water also removing turbidity from the water prior to flocculation, sedimentation or filtration. Although effective, inorganic coagulants have several disadvantages, there has been a concern about the relation between aluminum residuals in treated water and Alzheimer disease and toxic effects of metallic coagulants on the aquatic environment. Hence nowadays, there has been great attention in the improvement of natural coagulants in treated water such as chitosan; chitosan is a natural linear cellulose-like copolymer of glucosamine and N-acetyl-glucosamine widely distributed in nature. The present study was aimed to investigate the effects of chitosan on the removal of suspended solids (bentonite clay) from water. A series of batch flocculation tests with chitosan under different conditions was conducted. The results indicate that chitosan is a potent coagulant for bentonite suspension. Coagulation of chitosan showed efficiency of 96.9%. The coagulant performed well at concentration of 1g chitosan/100 ml water at PH=6.

Key words: Chitosan, coagulation, flocculation, bentonite, turbidity, water

Introduction

Water is a key substance in all natural and human activities, the production of potable water from rawest water sources usually use coagulation-flocculation techniques for removing turbidity in the form of suspended and colloidal materials.[1]. Coagulants are used that added to the water to withdraw the forces that stabilize the colloidal particles and causing the particles to suspend in the water [2]. Once the coagulant is introduced in the water the individual colloids must aggregate and grow bigger so that the impurities can be settled down at the bottom of the beaker and separated from the water suspension (as shown in table 1).

Some inorganic coagulants like Aluminum and iron are used in most industries, when aluminum is used as coagulant in water treatment, it can have caused several bad effect on human health such as intestinal constipation, loss of memory, convulsions, abdominal colic's, loss of energy and learning difficulties. In recent years, chitosan and moringa oleifera have been applied as coagulant in water treatment [4]. Chitosan is a derivative of chitin which naturally occurs in shells of crustaceans, fungi and insects. Chitosan is obtained from partial deacetylation of chitin which is removal of acetyl groups (-CH3CO) on N-acetyl glucosamine (GlcNAc) units of chitin polymer to reveal amino groups (-NH2) (as shown in Figure 1).

Coagulant Applications	Effective Characteristics	Natural Water Properties
Coagulants Extraction	Settling time	Alkalinity
Coagulants Solubility	Turbulence	Availability of Bacterias
Coagulants Dosage	Rapid Mixing	Presence of Elements (Cl, Na, Mn, Si, Fl, NH3, Fe)
Charge on Particles	Slow Mixing	Total dissolved solids
Basicity of a coagulant	Coagulant adds quantity	Suspended Solids
	Particles type	Temperature Turbidity Dissolved Oxygen

Table 1. Factors Affecting Coagulation

Various types of coagulants show potential application in treating water and wastewater. It ranges from chemical to non-chemical coagulant. The coagulant also could be synthetic material or natural coagulant with the properties of coagulant having +ve charge, these positive charge proteins would bind to the -ve charged particles in the solution that cause turbidity [3]. Coagulants normally in form of natural (as shown is Table 2) & inorganic (as in Table 3). Both coagulants aim to remove pollutant in form of physical (solids & turbidity) or chemical (BOD & COD).

Natural Coagulants	Turbidity
Cicer Aretinum	81.20%
Moringa Oleifera	82.02%
Cactus	78.54%

Table 2. Natural coagulants Efficiency

Department of Basic Science, Valley Higher Institute for Engineering and Technology, Cairo, Egypt.

Corresponding author: amera_muhammad@hotmail.com

Name	Advantages	Disadvantages
Aluminiumsulphate (Alum) Al2 (SO4)3. 18H2O	Easy to handle and apply; most commonly used; produces less sludge than lime; most effective between pH 6.5 and 7.5	Adds dissolved solids (salts) to waster; effective over a limited PH range.
Sodium Aluminate Na2Al2O4	Effective in hard waters; small dosage usually needed	Often used with alum; high cost; ineffective in soft waters
Polyaluminium Chloride (PAC) Al13(OH)20(SO)4.Cl15	In some applications, Floc, formed is more dense and faster settling than alum	Not commonly used; little full scale data compared to other aluminum derivatives
Ferric Sulfate Fe2(SO4)	Effective between pH 4-6 and 8.8-9.2	Ads dissolved solids(salts) to water; usually need to add alkalinity
Ferric Chloride FeCl3.6H2O	Effective between pH 4 and 11	Adds dissolved solids (salts) to water; consumes twice as much alkalinity as alum
Ferrous Sulfate (Copperas) FeSO4 .7H2O	Not as pH sensitive as lime	Ads dissolved solids(salts) to water; usually need to add alkalinity
Lime Ca(OH)2	Commonly used; very effective; may not add salts to effluent	pH dependent; produces large quantities of sludge; overdose can result in poor effluent quality

Table 3. Inorganic Coagulants: Advantages and Disadvantages

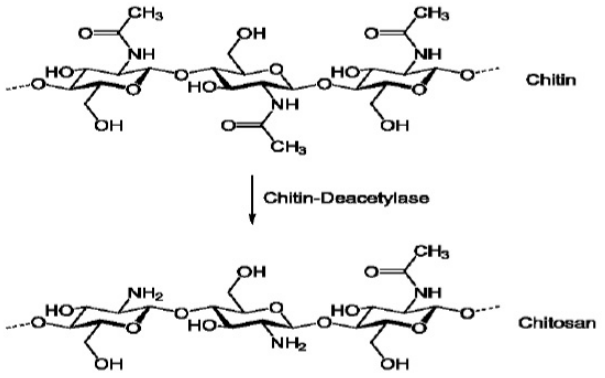

Figure 1: De-acetylation of chitin to obtain chitosan, acetyl group (-CH3CO) on acetyl glucosamine monomer on chitin chain is removed to reveal amino group (-NH2) becoming glucosamine monomer making chitosan.

It is a long chain carbohydrate that is non-soluble in water but dissolves in most acids, and contains positively charged moieties. Possessing properties such as non-toxicity, biocompatibility, and biodegradability, chitosan has been studied for its application in many sectors such as industrial wastewater treatment, pharmaceuticals, cosmetics, agriculture, and biomedical use. Chitosan is a weak base and is insoluble in water and in organic solvent. However, it is soluble in dilute aqueous acidic solutions (PH<6.5), which can convert glucosamine units into soluble form R-NH3. Chitosan is inexpensive, and nontoxic for mammals [5]. Chitosan molecule has the ability to interact with bacterial surface and is adsorbed on the surface of the cells and stack on the microbial cell surface and forming impervious layer around the cell, leading to the block of the channels [5], in addition chitosan has been studied for use as a coagulant or flocculants in river water and in wastewater. In laboratory studies chitosan has been reported to perform well as a coagulant for removing Chlorella sp. In algal turbid water [6], removing turbidity from sea water [7], and for microalgae harvesting [8]. It has several industrial and commercial uses, can be recycled, and is an excellent chelating agent for many metals such as arsenic, molybdenum, cadmium, chromium, lead, and cobalt [9]. The effective coagulation for turbidity removal was achieved in tap water when using lower doses of chitosan required for complete charge neutralization of the bentonite [10].

The infrared (IR) absorption spectra of chitosan and chitin are presented in (figure 2). It can be observed that three types of absorption bands exist: the amide (I) bands of chitosan characterized by absorption at approximately 1655-1630 cm^{-1}, the amide (II) bands of chitin at approximately 1560 cm-1 and the absorption bands for -OH groups at 3450 cm^{-1} [11] and the presence of very reactive amino (-NH_2) and hydroxyl (-OH) groups in its backbone, which makes chitosan to be used as an effective adsorbent material for the removal of water pollutants. Anionic particles of bentonite are electrostatically attracted by the protonated amino groups of chitosan [12]. This reaction facilitates the neutralization of the anionic charges which can bind together and settle rapidly by the effect of gravity. The practical application of chitosan in terms of chitosan dose, PH, stirring and time effect. As water treatment coagulant is examined in the study presented here.

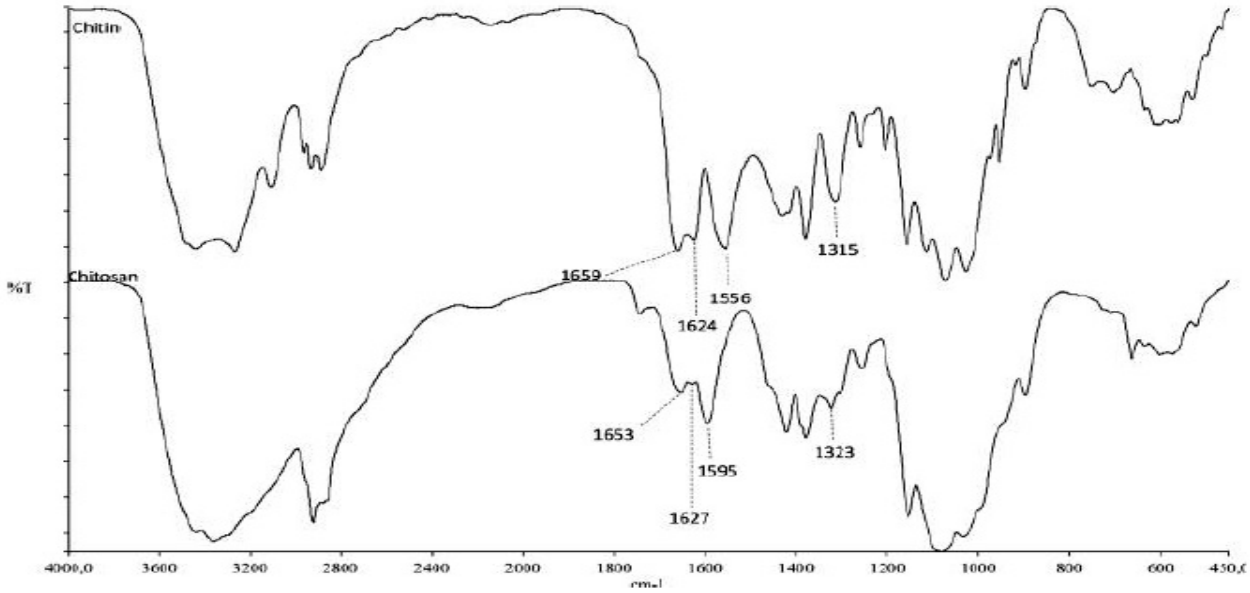

Figure 2: Infrared spectra of chitin (A) and chitosan (B) (12)

Materials and methods

Preparation of synthetic water

10 gm. of kaolinite was added to 1L of tap water. The suspension was stirred slowly at 20 rpm for 1hr for uniform dispersion of kaolinite particle. The suspension was then stand for 24hr. this suspension was used as the stock solution for the preparation of turbid water samples of varying turbidities. Original PH=7 and Temperature 30^{0}C. The PH was controlled by adding either strong acid (H_2SO_4) or strong base (NaOH). Turbidity of raw water was 1 NTU.

Preparation of chitosan solution

Chitosan (Deactylated chitin: poly-[1-4]-B-glucosamine). (C6H-11NO4) n with minimum 85% deactyl prepared from crab shells was obtained from ACROS ORGANICS Company. It was in the form of a pale brown powder soluble in dilute acetic acid hydrochloric acids. With molecular weight 100.000-300.000. Chitosan powder (5 mg) was weighed into a glass beaker, mixed with10mL of 0.1 M HCl solution, and kept for about one hour to dissolve. It was then diluted to 500 ml distilled water solution stirred at 100 rpm with a magnetic stirrer until the solution was completely dissolved. It was observed that chitosan solution in acid undergo some changes in properties over period; the solutions were prepared freshly before each set of experiments [13], Stock solution was stored at room temperature (25^{o}C).

Test water

In this study, the test water (six beakers) was filled with 500ml synthetic water. Then kaolinite and chitosan were added (Coagulant was added with rapid mixing for 2 minutes at 100 rpm, slow mixing for 30 minutes at 30 rpm. The mixer is turned off and flocs are allowed to settle for 30 minute [14]. The samples were taken from the top 4 in of the suspension. Turbidity was measured on the settled water filtered through Whatman 40 (8um) filter paper of each beaker and then measured by Nephelometer, Turbidity becomes 5 NTU, and Hardness measurements were conducted by EDTA titrimetric Method. Six chemical water quality parameters

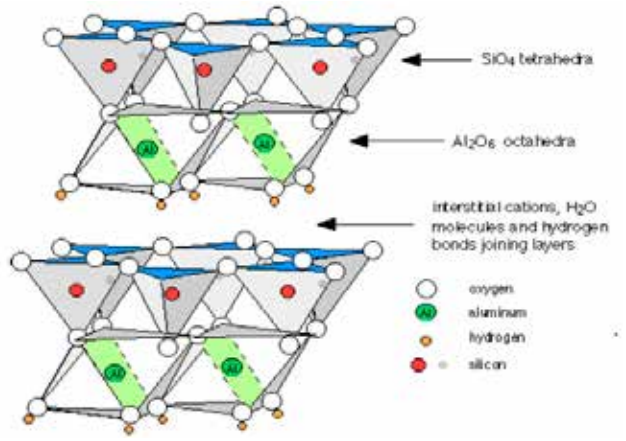

Figure 3: Kaolinite structure

were tested: PH, turbidity, Temperature, time, stirring, chemical dosage of chitosan. Water at PH 6 and PH 9 was compared with the standard test water control at neutral PH of 7.0. The PH was adjusted using 1M hydrochloric acid (HCl) and 1M sodium hydroxide (NaOH). For effects of turbidity level on chitosan coagulation, turbidity was set at 5 and 10,15,20,25 NTU compared to control water turbidity of 1 NTU and kaolinite was used as the turbidity source. Doses of chitosan were: 1,3,10 and 30 mg/L,

Results and discussion

Optimal dosage of chitosan

We all agree about that The lowest turbidity in the suspension is the optimal dosage condition so at chitosan dose 1,3mg/L, kaolinite removals were high 96%, at chitosan dose above than 3mg/L, there was decrease (or) no removal of kaolinite turbidity by chitosan. Overall, kaolinite reductions were significantly lower as chitosan dose become higher.

Chitosan dose	Turbidity reduction %
1	96.9
3	96
10	60
30	43

Table 4. Relation between chitosan dose and turbidity reduction%

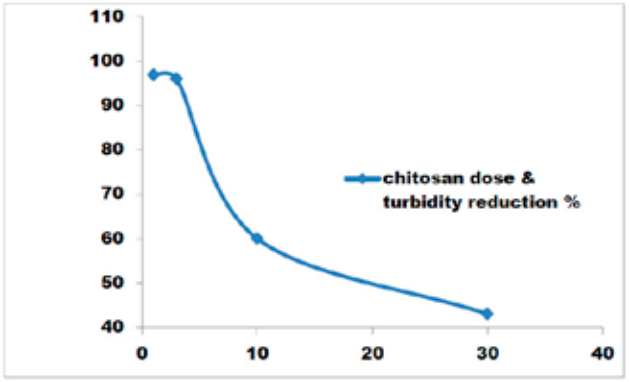

Figure 4. Relation between chitosan dose and turbidity reduction%

Effects of water PH on turbidity removal.

Effects of water PH on removal of kaolinite turbidity.

Kaolinite turbidity was (5, 5 NTU), temperature of the turbid water was (35° C), chitosan dosage (1g/L), stirring (300 rpm). As the PH was increased, chitosan was less effective as a coagulant on settled water turbidity [15]. The PH selected for optimum selected water turbidity removal was 5, 6,7,8,9. In the PH range of 5 to 7, the residual turbidities of supernatant can be reduced to less than 1 NTU. But at PH 6 lowest turbidity achieved 0.65 NTU. These results also indicate that the residual turbidities are increased at PH 8, 9.

Residual turbidity(NTU)	PH VALUE
0.95	5
0.65	6
0.85	7
1.5	8
4	9

Table 5. Relation between Turbidity and PH value

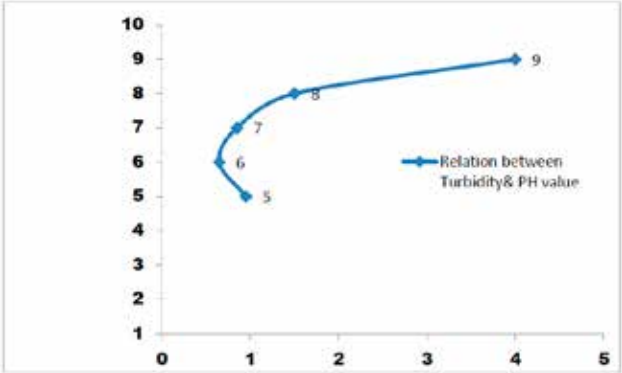

Figure 5. Relation between Turbidity and PH value

Effect of contact tine on turbidity removal.

Kaolinite turbidity was (5, 5 NTU), chitosan dosage (1g/L), stirring (300 rpm), PH= (6). Temperature (25°C). Time was the only factor that decreases turbidity gradually.

Turbidity removal (NTU)	Contact time(min)
7	5
2.5	10
2	15
1.8	20
1.3	25
1.3	30

Table 6. Relation between turbidity Removal and contact time (min)

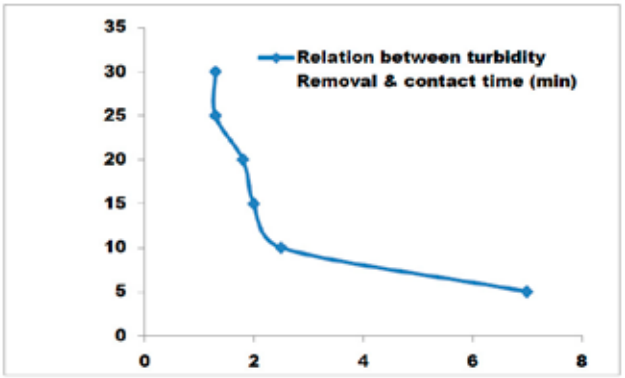

Figure 6. Relation between turbidity removal and contact time (min)

Effect of Temperature on turbidity removal.

Kaolinite turbidity was (5, 5 NTU), different temperature of the turbid water from (25 to 43° C) chitosan dosage (1g/L), stirring (300 rpm), PH= (6), time of the turbid water was (30 min). the influence of temperature on the rate of turbidity was rising at increasing temperature.

Turbidity removal %	Temperature(°C)
96.9	25
96.3	30
95.8	35
95.4	40

Table 7. Relation between turbidity removal (%) and Temperature (°C)

Conclusion

Overall, the results of this study provide evidence that Chitosan had significant effects on the efficiency of kaolinite turbidity reduction from test water; chitosan dose had significant effects on kaolinite turbidity reduction from test water. Only lower doses were needed for effective removal of kaolinite turbidity from water, with chitosan doses for 96.9% turbidity removal is 1gm/L. Higher chitosan dose was less effective and provided poor kaolinite turbidity removal than did lower doses which overdosing of chitosan can result in destabilization of a dispersion. The optimal conditions were determined on the basis of turbidity removal. In addition, the principal factors affecting coagulation were determined throughout the study, including optimal coagulant dosage, Time, PH and Temperature. The optimum PH found for coagulation to remove settled water turbidity was 6.0, sedimentation and paper filtration lowered treated water turbidity 96.9% for chitosan.

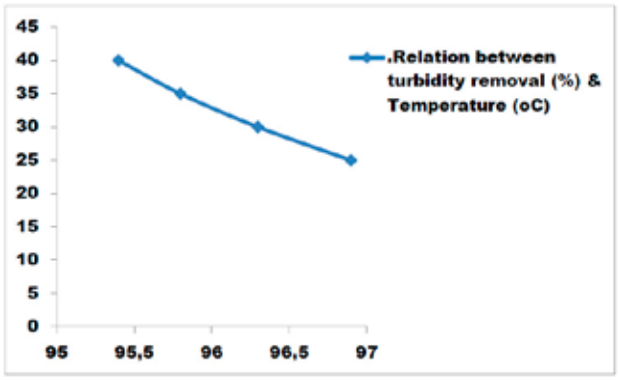

Figure 7. Relation between turbidity removal (%) and Temperature (°C)

References

1. A.I. Cissouma, F.Tounkara, M. Nikoo, N. Yang, and X.Xu. Physico-Chemical Properties and Antioxidant Activity of Roselle Seeds Extracts, Advance J. of Food Science and Technology, 5(11), 1483-1489(2013)
2. A.L.Ahmad, N.H May Yasin, J.C.Derek, and J.K.Lim."Optimization of Microalgae Coagulation Processes Using Chitosan." Chemical Engineering Journal, vol.173, 2011, pp.879-882.
3. Divakaran, R., Pillai, V.N., (2002). Flocculation of river silt using chitosan. Water. Res., 36:2414-2418.
4. Folkard, G.K., Sutherland, J., Shaw, R., (2000). Water clarification using Moringa oleifera seed coagulant. On Electronic products: http: // www.lboro.ac.uk/well/resources/technical-briefs/60.
5. Ganjidoust H, Tatsumi K, Wada S, Kawase M: Role of peroxidase and chitosan in removing chlorophenols from aqueous solution. Water Sci.Technol.1996; 34(10): 151-159.
6. H. Altaher." The use of chitosan as a coagulant in the pre-treatment of turbid sea water." Journal of Hazardous Materials, vol.233-234, 2012, pp. 97-102.
7. L. Rizzo, A. Di Gennaro, M. Gallo, and V.Belgiorno "Coagulation/ chlorination of surface water: a comparison between chitosan and metal salts. "Separation and Purification Technology, vol.62, 2008, 79-85.
8. M.A.Abu Hassan and M.H.Puteh. "Pretreatment of palm oil effluent (POME): a comparison study using chitosan and alun." MJCE, vol.19, 2007, 128-141.
9. Mackenzie, L.D., Cornwell, D.A., (1991). Introduction to Environmental Engineering.2nd Ed. McGraw Hill, New York, 157-163.
10. Pan, J.R., Chih P., Huang, S.C., Chen, Ying C.Evaluation of modified chitosan biopolymer for coagulation of colloidal particles.Colloids and Surfaces A: Physicochemical and Engineering Aspects 1999; 147: 359-364.
11. Qin,C., Li,H., Xiao, Q., Liu, Y., Zhu, J., Du, Y.,(2006). Water-solubility of chitosan and its antimicrobial activity. Carbohydrate Polymers. 63:367-374.
12. Roussy,J., Van Vooren, M.,Dempsey, B., Guibal, E.,(2005). Influence of chitosan characteristics on the coagulation and the flocculation of bentonite suspensions. Water.Res. 39: 3247-3258.
13. R.Rajendran, M. Abirami, P. Prbhavathi, P. Premasudha, B. Kanimozhi, A.Manikandan, Biological treatment of drinking water by chitosan based nanocomposites. African J.of Biotechnology, 14(11), 930-936(2015).
14. S.A.Fast, B.Kokabian and V.G.Gude. "Chitosan enhanced coagulation of algal turbid waters-Comparison between rapid mix and ultrasound coagulation methods "Chemical Engineering Journal, vol.244, 2014, pp. 403-410.
15. Shellshear, M.S. Urban storm water treatment using chitosan. B. Eng. In civil Engineering Thesis, Faculty of Engineering and Surveying, University of Southern Queensland, 2008.

Received: 10 April 2019
Approved: 10 May 2019

RESEARCHS / INVESTIGACIÓN

Evaluación de la descomposición de imágenes digitales, para la estimación indirecta de la turbidez en muestras de agua de cuerpos naturales

Evaluation of the decomposition of digital images, for indirect estimation of turbidity in water samples

*Juan Manuel Agudelo Luna[1]; Carlos Augusto Benjumea Hoyos[2]

DOI. 10.21931/RB/2019.04.02.8

Resumen: Las cámaras digitales ofrecen la posibilidad de captura y análisis de datos de manera sencilla y asequible, lo que permite realizar tomas rápidas y en algunos casos in situ del objeto de estudio. En esta investigación se utilizó una DSLR (Digital Single Lens Reflex por sus siglas en ingles) y una CCD (Charged Coupled Device por sus siglas en ingles) para capturar imágenes digitales analizadas bajo dos metodologías mediante un script en MATLAB, de muestras agua obtenidas de dos zonas de Antioquia y tres cuerpos de agua: rio San Carlos y quebrada San Antonio en San Carlos además de la quebrada La Marinilla. Adicional a lo anterior, se construyeron dos entornos para realizar la captura de las imágenes digitales y dos ensayos en orden de establecer una ecuación de correlación entre los datos obtenidos y la turbidez (NTU). Encontrando que existe una correlación entre la turbidez y la intensidad de luz extraída de las imágenes digitales con $R^2 = 0.97428$ para el primer ensayo, ajustes superiores a 0.9 para el canal G en el espacio de color RGB
Palabras clave: Imágenes digitales; turbidez; muestras de agua; estimación.

Abstract: Digital cameras offer the possibility to capture and analyze data in a simple and affordable way, allowing quick and in some cases on-site shots of the study object. This research use a DSLR (Digital Single Lens Reflex for its acronym in English) and a CCD (Charged coupled device for its acronym in English) to capture digital images analyzed under two methodologies using a MATLAB script, water samples Obtained from two areas of Antioquia Colombia, and three water bodies: rio San Carlos and brook San Antonio in San Carlos (Ant), in addition to brook La Marinilla in Marinilla (Ant). In addition to the foregoing, two capture environments were built to capture digital images and two trials in order to establish a correlation equation between the data obtained in light intensity and turbidity (NTU). Finding that there is a correlation between turbidity and the intensity of light extracted from digital images with $R^2 = 0.97428$ for the first trial, and above 0.9 for the G-channel in the RGB color space.
Keywords: Digital Images, turbidity, water sample, estimation.

Introducción

La turbidez es un parámetro clave en el monitoreo de la calidad de agua. La organización mundial de la salud establece que su nivel para agua destinada a consumo humano no debe superar las 5 unidades nefelometricas de turbidez o NTU por sus siglas en ingles recomendando valores de 1 NTU[1] y, la legislación colombiana[2] adopta un valor máximo aceptable de 2 NTU para la misma. El aumento o disminución de este parámetro esta relaciona con el riesgo por contaminación microbiológica de agua para consumo humano[3] además de aportar información valiosa para el diseño de operaciones y procesos que permitan mejorar su calidad.

El análisis imágenes digitales ha sido utilizado en muchos campos de la ciencia debido al gran número de aplicaciones que posee. Algunas de estas como el mapeo satelital de terreno en diferentes longitudes de onda, reconstrucción de geometrías tridimensionales, en medicina para la detección de tumores y medición de áreas de neuronas. Más concretamente, el análisis de color en las imágenes digitales ha sido aplicado a la clasificación de frutas[4], el análisis de color en insectos y plantas[5], el análisis de muestras de alimentos como carne[6].

Las imágenes digitales en entorno controlado se han utilizado como método alternativo para la determinación de concentraciones de sustancias[7, 8, 9, 10,11]. Algunos de estos métodos emplean el sistema de coordenadas de color RGB (Red, Green, Blue por sus siglas en ingles) donde cada componente es medido en intensidad de gris (IG) que va de 0-255, siendo 0 negro absoluto y 255 blanco absoluto. Este tipo de datos puede extraerse de cámaras digitales convencionales como cámaras web y teléfonos inteligentes, que utilizan sensores CCD's (Dispositivos de carca acoplada) y CMOS (Semiconductor complementario de Metal – Oxido).

Otros estudios como el llevado a cabo por Goddijn & White, M. (2006)[11] utilizaron los datos de las intensidades en el modelo de color RGB obtenidos de una cámara digital convencional para la medición de calidad de agua en la bahía de Galway en Irlanda. Encontrando que existía una correlación marcada (R2 = 0,81) entre el cociente Rojo/Azul entregado por la cámara y el material orgánico disuelto (denominado sustancia amarilla) presente en la bahía.

Kohl, S.K., Landmark, J.D., & Stickle, D.F., (2006)[12], mediante un experimento sencillo que buscaba demostrar la absorbancia utilizando el análisis de imágenes digitales a color, logró demostrar como con la coloración de una muestra de agua mediante colorante amarillo se podían extraer datos suficientes a diferentes concentraciones relativas (100%, 75%, 50%, 25% y 0%), para obtener un comportamiento exponencial en el canal azul medido de 0-255 intensidad de gris (IG) contra las concentraciones relativas del colorante mencionado.

1 Ingeniero Ambiental Universidad Católica de Oriente. Autor de correspondencia: manuel9519@hotmail.com
2 Magister en Ingeniería, Docente Asistente Universidad Católica de Oriente, Grupo Limnología y Recursos Hídricos. Rionegro - Colombia

Otros espacios de color han sido utilizados en la determinación de concentraciones, Cantrell, K., Erenas, M., Orbe-Payá, I., & Vallvey, C. (2010)[13] evaluaron el espacio de color HSV (Hue, Saturation, Value por sus siglas en inglés) como un parámetro de análisis cuantitativo y lo comparó con el espacio RGB, encontrando que la principal ventaja del HSV respecto al RGB yacía en la representación completa de color en un único valor que variaba de 0 a 1. Haciendo este último de especial interés para su uso en sensores ópticos de membrana y otras aplicaciones, donde la falta de homogeneidad derivada de reacciones entre sustancias, afectara la captura de datos. También resaltó la ventaja de los dispositivos de captura de imágenes convencionales como cámaras digitales, escáneres y cámaras web al ser baratos y fáciles de utilizar para el tipo de aplicaciones que trataban en su investigación.

El monitoreo remoto utilizando cámaras digitales no es un concepto desconocido Dean, C., Warner, A., & McGraw, J.B. (2000)[14] evaluaron la conveniencia de una cámara digital comercial (DCS460c) para el monitoreo remoto cuantitativo aplicado al análisis de vegetación. Siguiendo una línea similar, Dymond, J.R., & Trotter C.M. (1997)[15] utilizaron una cámara digital comercial con un lente de gran ángulo para obtener distribuciones de reflectancia direccional de dos cubiertas vegetales, pasto (lolium spp) y bosque de pinos (Pinnus radiata).

En Colombia, el Área Metropolitana del Valle de Aburra en conjunto con otras entidades y universidades, llevaron a cabo una investigación conjunta en torno al parámetro color. Una de estas investigaciones, realizada por Silva W., y Villegas N., (2015)[16] implementaron el análisis de imágenes digitales capturadas mediante una cámara comercial, para establecer el color base del río Medellín realizando un recorte del área de interés en la imagen y procesando los datos en el espacio de color RGB comparados contra muestras de colorantes comerciales. Llegando a la conclusión de que es posible establecer con cierto margen de confianza el color del rio en el espacio mencionado y su potencial alejamiento en caso de contaminación con colorantes.

El incremento o disminución de los sólidos en sistemas acuáticos que indirectamente se representa con la turbidez medida en NTU (Nefelometric Turbidity Units), puede incrementar el potencial erosivo de un caudal[17] afectar el intercambio de oxígeno en peces y degradar hábitats de especies acuáticas por sedimentación[18, 19]. También su aumento afecta directamente el ingreso de radiación solar, una de las principales fuentes de energía para los ecosistemas acuáticos[20]. La turbidez en sistemas acuáticos está directamente influenciada por la cantidad de sólidos que esta carga en un momento determinado ya sean disueltos o suspendidos. Estos constituyentes provienen de diversos orígenes, como la degradación de material vegetal en ácidos húmicos o fúlvicos, erosión de los suelos aledaños en el caso de sistemas acuáticos loticos y sales disueltas (Bilottaa, G., & Braziera, R. 2008)[21]. En mayor o menor medida la luz que interacciona con los cuerpos de agua se ve afectada por su contenido de sales, sólidos y materia orgánica disuelta, esta última como resultado de los muchos procesos de degradación llevados a cabo por organismos presentes en el agua[22].

El cambio de la turbidez en sistemas acuáticos es perceptible a simple vista, este cambio es debido al aumento de concentraciones en los componentes añadidos del agua, las cámaras digitales convencionales al estar diseñadas para captar la luz en el espectro visible también pueden captar estas diferencias, que son convertidas en señales digitales y representadas en un espacio de color determinado. En esta investigación se realiza una aproximación que busca explorar la posibilidad que existe en el uso de cámaras digitales convencionales, para mostrar el comportamiento de la turbidez presentada en muestras de agua de cuerpos naturales analizadas bajo condiciones de laboratorio y, minimizando algunas de las variables que se presentan al capturar imágenes digitales in situ, como lo son la hora del día, nubosidad, ángulo e intensidad de la luz.

Materials and methods

Esquema experimental

Se construyeron dos entornos de captura para la adquisición de las imágenes digitales. Para el primero de ellos se construyó una caja de luz blanca (CLB), compuesta de plástico blanco en el interior y el exterior, con el propósito de bloquear la luz externa. La iluminación fue posicionada encima de la muestra, constaba de una lámpara LED con difusor incorporado, de 600 lúmenes, una temperatura de color de 6000k y un cri >80 (Color Rendering Index).

Arreglos experimentales similares al realizado fueron llevados a cabo por Mullins et al. (2018)[23], Zhang, X. (2017)[24], Belfort, B., Weill, S. y Lehmann F. (2017)[25], Ohi, Inoue, S., y Ezaki, T. (1999)[26] y Kohl, S.K., Landmark, J.D., & Stickle, D.F., (2006)[12].

Se utilizó un contenedor de vidrio con un volumen de 10 ml utilizado en espectrofotometría. Para este montaje se utilizó una cámara DSLR Nikon D5100 (Sensor CMOS, 23.6 x 15.6 mm, 16.2 MP, resolución de imagen de 4928 x 3264 píxeles y 40mm de longitud focal) ubicada a través de una abertura circular y a 10 cm de la muestra. La captura fue realizada con los ajustes automáticos por parte de la DSLR arrojando datos en bruto (RAW) para evitar la interpretación errónea del color de la escena capturada.

El segundo entorno de captura se construyó mediante una base plástica de acrílico blanco (BAB), donde la muestra era posicionada en la superficie de acrílico y la fuente de luz de iguales características (LED, 600 lúmenes y 6000k) provenía de la parte baja.

Las imágenes fueron capturadas en cuarto oscuro donde la única fuente de iluminación provenía de la BAB. En este montaje fueron utilizadas dos cámaras, ubicadas a 15 cm de la muestra: DSLR Nikon D5100 con ajustes fijos [f 3.0, 1/350 s, iso 100] junto con una cámara CCD industrial fabricada por The Imaging Source DMK41BU02.H [sensor CCD, 12.7 x 12.7mm, 1.2MP y una resolución de imagen de 1280 x 960 píxeles] y ajustes [Exp -6, ganancia 278, f 3.0, 1/250 s]. El objetivo principal de la construcción de los dos entornos de captura radica en la eliminación de influencias de luz externas que pudieran afectar la captura de las imágenes digitales, p.ej variación diurna de la intensidad de iluminación y las interacciones no deseadas de la luz con algunos materiales.

Figura 1. Entorno de captura Caja de Luz Blanca (CLB). Fuente autor

Procesado de imágenes
Se utilizó el software MATLAB® para el procesado de imágenes. Este procesado incluye la región de interés que abarcaba un máximo de datos utilizables de 600 x 1100 pixeles para la imagen entregada por la DSLR en ambos entornos de captura (CLB y BAB), y una zona de 200 x 280 pixeles para la CCD en el entorno de captura BAB; en ambos casos evitando la estructura que contenía la muestra. De las imágenes capturas se extrajo la intensidad de gris en el campo de color RGB para cada canal en el caso de la DSLR y la intensidad total para la CCD.

Figura 2. Entorno de captura Base de Acrílico Blanco (BAB). Fuente autor

Dos métodos de análisis se tomaron en cuenta para el tratamiento de los datos, el método utilizado por Sumriddetchkajorn (2013, 2014)[27, 28] que corresponde a la metodología uno (M1) en el que propone la razón de color (1) para la relación de las intensidades del nivel de gris en cada canal del campo RGB:

$$CR = \frac{Rm/Rr + Gm/Gr + Bm/Br}{3} \quad (1)$$

Donde R_m, G_m y B_m corresponden a la intensidad de gris promedio calculada como el promedio de los valores de cada pixel en la región de interés (IGP) en cada canal de color en la muestra. Mientras que R_r, G_r y B_r al plano de referencia (fondo), y se calcula como la IGP de dos regiones a lado y lado de la muestra.

Figura 3. Regiones de interés para metodología uno (M1).

Además, se propuso la segmentación de las imágenes digitales en cuatro sectores como segunda metodología (M2), ubicados dentro de las regiones definidas anteriormente, dispuestos horizontalmente hacia abajo (S1, S2, S3, S4). De cada sector se extraerá la IGP para cada canal en el campo de color RGB en la DSLR y la IGP total para la CCD. Este método con el propósito de establecer si existen diferencias entre las IGP de regiones en las imágenes, además si uno u otro canal en el campo RGB se ajusta mejor a los datos, para la comparación entre las diferencias de los sectores de la imagen se llevó a cabo un análisis de varianza multi-factor con varias muestras por grupo en orden de establecer si existían diferencias entre sectores y entre los canales de color (RGB) de las imágenes capturadas.

Turbidez
Para la determinación de la turbiedad se utilizó un turbidímetro Hach® 2100Q en todas las muestras, corresponde al método de referencia establecido que cumple con los criterios de diseño del método 180.1 USEPA[29].

Área de estudio
Se realizó toma de muestras en tres cuerpos de agua. Las muestras fueron tomadas en el centro del cuerpo de agua, sub-superficiales utilizando un recipiente de polipropileno atado a una cuerda al que se le realizaba su respectiva lavado y purga al momento de ser utilizado, las muestras se almacenaron en un recipiente plástico; analizadas 30 min después de ser tomadas, cuando no fue posible analizarlas en el momento se almacenaron refrigeradas a 4ºC para prevenir la degradación orgánica de los sólidos presentes en la misma y analizadas en las 8h subsiguientes.

Cinco muestras en la quebrada San Antonio ubicada en San Carlos (Ant), Colombia con coordenadas 6.187376 N, -75.000571 E y cinco muestras en el rio San Carlos en San Carlos (Ant), Colombia y con coordenadas 6.185392 N, -74.996961 E, en el mes de diciembre de 2016. Por último, se tomaron cinco muestras de agua de la quebrada La Marinilla en Marinilla (Ant) en los meses de julio y agosto de 2017 con coordenadas 6°10’14.4”N 75°20’02.6”W (Fig. 4 y 5).

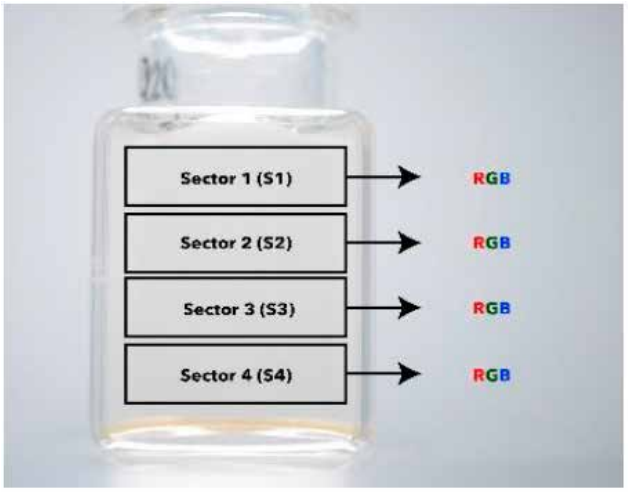

Figura 4. Regiones de interés por sector para metodología dos (M2).

Ensayos de laboratorio
Adicional a la toma de muestras realizadas y con el fin de establecer una correlación entre los valores en NTU entregados por el turbidímetro y la IGP, fueron llevados a cabo dos ensayos de laboratorio (E1, E2). El primer ensayo (E1) fue realizado en el entorno de captura CLB y consistió en la generación de turbidez artificial utilizando arcilla de color rojizo tomada de un sector adyacente a la Quebrada la Marinilla, con coordenadas 6°10’15.0”N 75°20’02.1”W; correspondiente a suelos andisoles de la llanura aluvial de la quebrada [30]. Se realizaron ocho diluciones sucesivas desde 0,039 g/l hasta 5 g/l midiendo en cada una el valor de turbidez (NTU), posteriormente capturando la imagen digital utilizando la celda espectrofotométrica de 10ml, comenzando desde 925 NTU hasta 103 NTU.

Figura 5. Zonas de muestreo en (a) San Carlos y (b) Marinilla Antioquia, Colombia.

Para el segundo ensayo (E2) y siguiendo el mismo desarrollo, se utilizaron las muestras de calibración y verificación estándar que contenía el turbidímetro de fábrica, con valores que van desde 800 hasta 10 NTU (10, 20, 100, 800 NTU) y la posterior captura en el mismo recipiente.

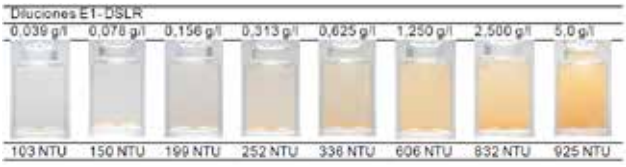

Figura 6. Diluciones sucesivas para el ensayo uno capturadas con la DSLR en CLB

Resultados and Discusión

Los valores superiores a uno pueden explicarse desde la configuración misma del entorno de captura CLB, donde la posición de la muestra respecto a la fuente de iluminación y el fondo causaban que la muestra recibiera un poco más de iluminación que el plano de referencia o entorno circundante. Sumado a lo anterior, los valores de NTU presentados por las muestras del rio San Carlos y la quebrada San Antonio fueron bajos, estando relacionados directamente con los sólidos presentes, hacían que la dispersión de la luz fuera menor, presentando valores de CR 1.0033 (Figura 9).

Así mismo, la metodología uno utilizada bajo el entorno de captura BAB en las muestras de la quebrada La Marinilla capturadas con la DSLR, arrojaban valores de CR muy por encima de 1 y en algunos casos llegando a valores de 2596.04 para un NTU de 24 (Figura 11). Es de esperarse estos resultados debido a que la IGP del plano de referencia en ninguna de las imágenes capturadas con la DSLR y la CCD (Figura 11 y 13) superaba el valor de 1.

Los valores de CR presentados por las imágenes capturadas por la DSLR y la CCD de la quebrada La Marinilla en el entorno BAB se mostraron directamente proporcionales a los de NTU, cuando se producía un incremento en los valores de NTU aumentaba la CR. El aumento en la cantidad de partículas en las muestras reflejados en NTU, y teniendo en cuenta la configuración del entorno de captura BAB, hacían que mucha más luz fuera dispersada a medida que la turbidez aumentaba, elevando

Metodología uno y dos

La razón de color (CR) propuesta por Sumriddetchkajorn (2013, 2014)[27, 28] como una medida conjunta que agrupa el espacio de color RGB, presentó algunos inconvenientes al momento de ser utilizada en los diferentes entornos de captura utilizados en esta investigación.

Para el entorno de captura CLB se obtuvieron valores de intensidad de gris promedio (IGP) en la región de interés de la muestra superiores a aquellos del plano de referencia, esto se puede ver en los datos obtenidos de las muestras del rio San Carlos (Figura 7) y la quebrada San Antonio (Figura 9). Los valores de IGP para el plano de la muestra, datos similares fueron encontrados por Mizutani, N., Saito, K., Numata, Y. (1988)[31] donde la relación R*B/G*G en el espacio de color RGB aumentaba a medida que la turbidez medida en ppm aumentaba también.

Se presentó una variación elevada entre los valores de IGP para valores de NTU similares en las muestras del rio San Carlos y la quebrada San Antonio analizadas bajo la metodología dos (Figura 8 y 10) en los cuatro sectores de la región de interés. El responsable de este comportamiento puede ser la función de balance de blancos por parte de la DSLR, debido a que, aunque las condiciones de captura se mantuvieron constantes en cada una de las capturas, la cámara interpretaba el blanco de manera diferente en cada una de las oportunidades, situación similar fue reportada por L.M Goddijn & M. White (2006)[11] en su estudio donde recomiendan investigaciones adicionales para establecer los efectos de las diferentes condiciones de iluminación sobre esta función.

Esta misma situación se presentó en los valores de IGP para imágenes digitales capturadas de las muestras de la quebrada La Marinilla con la DSLR, donde valores de NTU de 14.8 arrojaban valores de IGP de 44.3, 47.9 y 55 para RGB respectivamente y, posteriormente valores de NTU de 13.2 arrojaban valores de 53.9, 60.6, 69.5 para RGB en S1 (Figura 12).

Esto hace muy difícil correlacionar un aumento de la IGP cuando se presenta un aumento en los valores de NTU, en el caso del entorno de captura CLB donde la iluminación se encontraba en la parte superior, cada sector analizado en las imágenes digitales en el siguiente orden S1>S2>S3>S4 presentaba valores más bajos de IGP para cada espacio de color (RGB) mostrando un gradiente de dispersión longitudinal de luz alejándose de la fuente de iluminación. Este gradiente también se presentó en el entorno BAB de manera contraria donde los valores más altos de IGP iban de S4>S3>S2>S1 y la fuente de iluminación en la parte baja.

Entornos de captura

La principal diferencia entre los dos entornos de captura utilizados fue el color de fondo y la posición de la iluminación. En el primero de ellos (CLB), un fondo blanco aislado de la iluminación externa mediante una caja de luz blanca, la intensidad de gris promedio base para el plano de referencia utilizado en M1-E1-DSLR fue de 210.33 IGP para el canal rojo, 212.82 IGP para el canal verde y 216.76 IGP en el canal azul. Estos valores son cercanos al límite de intensidad de 255 correspondiente a una saturación con blanco

del 100% por esto, un cambio que sea detectado por la cámara debe reflejar valores por debajo de los tomados en el plano de referencia, de lo contrario el margen de toma de datos utilizables en las regiones de interés se reduce.

La configuración del entorno de captura CLB evitaba influencias de fuentes de luz externas, pero, debido a la posición de la fuente de luz respecto a la cámara se aumentaba la cantidad de iluminación que llegaba a esta, reduciendo un poco el rango dinámico de la misma. La configuración de la iluminación respecto a la muestra y a las paredes contiguas del entorno, generaban algunas zonas cercanas a los extremos de las imágenes digitales capturadas, donde la luz no llegaba de manera uniforme. Esta zona de iluminación no uniforme también es producto del viñeteado derivado del lente, aunque no alcanzaban a ser cubiertas por las regiones de interés tomadas para el análisis, es preciso en nuevos ensayos tratar de minimizarlas.

El entorno de captura BAB, donde la fuente de iluminación se encontraba en la parte inferior respecto a la muestra evitaba que parte de la luz interaccionara con otros elementos a diferencia del entorno CLB, produciendo zonas con menos pixeles sobre expuestos que pudieran ser utilizados en el análisis de las regiones de interés. Mullins et al. (2018)[23] también utilizó un cuarto oscuro para la captura de imágenes, pero a diferencia del entorno BAB, posicionó la fuente de iluminación en un lateral a 90º respecto a la cámara, pruebas realizadas previamente con los recipientes de verificación estándar del turbidímetro en forma de cilindro dieron como resultado la aparición de zonas sobre saturadas con datos inutilizables que disminuía la región de interés para el análisis de datos

Ensayo uno
Se logró establecer una ecuación de correlación mediante un ajuste polinómico entre los datos obtenidos de las muestras de dilución en el entorno CLB con un $R^2 = 0.97428$ y para una ecuación de tercer orden, presentando una relación inversamente proporcional entre la CR, el contenido de sólidos y los valores de NTU. Los datos cercanos a los valores de NTU más bajos (103 y 105) presentaron un CR de 1.011 y 1.004 (Figura 15) respectivamente debido tal vez a los efectos del entorno de captura mencionados. Se logra evidenciar que la dispersión de la luz causada por el incremento de sólidos en las muestras preparadas, causo una disminución de la intensidad de luz captada por la DSL en el entorno CLB. Resultados similares fueron reportados por Sumriddetchkajorn (2013, 2014)[27, 28] con el contenido de cloro medido en ppm, Mizutani, N., Saito, K. y Noumata, Y. (1988)[30] con la turbidez medida en ppm y las relaciones de color establecidas, Kohl, S.K., Landmark, J.D., & Stickle, D.F., (2006)[12] entre la intensidad de luz en azul y la concentración relativa de colorante.

Para el canal azul (B) en la metodología dos y el sector dos (S2) mostró mejor ajuste con un $R^2 = 0.97645$ para una ecuación de tercer orden, mostrando un comportamiento similar a los datos obtenidos para CR con una disminución de la IGP con un aumento en los valores de NTU. Contrario al canal azul, el canal rojo (R) mostró tendencia a aumentar los valores de IGP con el incremento de NTU y un mejor ajuste en el sector uno (S1) con un $R^2 = 0.96342$ para tercer orden (Figura 16). Debido a que la interpretación del color por parte de la DSRL es una coordenada tridimensional compuesta por los datos individuales en RGB, el color presentado por las muestras utilizadas influye de manera directa en cuál de los canales de color se presenta un mejor ajuste.

Ensayo dos
Los datos obtenidos para la DSLR presentaron un aumento directamente proporcional de IGP en los valores de 10, 20 y 100 NTU respectivamente (Figura 17), mientras que el valor de IGP para 800 NTU disminuyo. Un comportamiento similar fue observado en los datos entregados por la CCD (Figura 19) donde los primeros tres datos aumentaban y el ultimo disminuia. Esta disminución repentina después de un aumento directamente proporcional, puede relacionarse a la dispersión de la luz sobre las regiones de interés tomadas para el análisis, causando un ligero aumento en la IGP que precipito el valor en el cálculo de la CR.

Utilizando la segunda metodología, todos los sectores analizados mostraron un incremento directamente proporcional de la IGP con el aumento en NTU de las muestras de calibración, con un $R^2 > 0.9$ para todos canales (R, G y B) en cada sector (S1, S2, S3 y S4) (Figura 18), sin embargo, el canal verde (G) mostró un ajuste ligeramente mayor en todos los sectores analizados. El aumento de los sólidos presentes en las muestras, y por ende de la turbidez, se ve reflejado en la intensidad de luz captada por las cámaras para cada una de las muestras, contrario a lo evidenciado en el ensayo uno donde el aumento causaba una disminución en la intensidad de luz.

En el caso de la CCD para el segundo ensayo, el sector uno (S1) presento mejor ajuste con un $R^2 = 0.94148$ seguido del sector dos (S2) con un $R^2 = 0.92266$ (Figura 20). El comportamiento fue igual al descrito para el ensayo uno en la segunda metodología utilizando la DSLR.

Ecuaciones de correlación
La precisión de las ecuaciones de correlación encontradas entre la razón de color y los valores de NTU para el ensayo uno, depende en gran medida de la estabilización de los valores medidos en las muestras de agua del rio San Carlos y la quebrada San Antonio. Debido a que estos presentaban una gran variación, solo en unos pocos casos se logró porcentajes de alejamiento con respecto al valor, del orden del 16.61 % por debajo del valor real, para una muestra de la quebrada San Antonio con un NTU de 1.253 y un valor determinado por la ecuación de 1.0447 respectivamente.

Resultados y Discusión

Los resultados están organizados por zona de muestreo y metodología, comenzando por el rio San Carlos, quebrada San Antonio y quebrada La Marinilla de igual modo, para esta última, se hace la distinción de las cámaras utilizadas. Seguidamente, se presentan los resultados de los ensayos realizados separados por cámara digital utilizada.

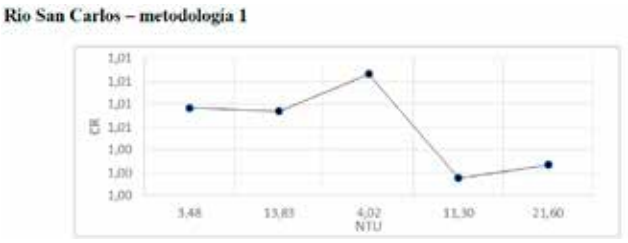

Figura 7. Razón de color contra NTU en las muestras del Rio San Carlos con la DSLR para la metodología 1 en CLB.

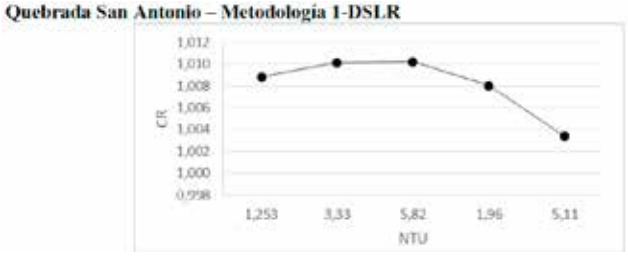

Figura 9. Razón de color contra NTU en las muestras de la quebrada San Antonio utilizando la DSLR para la metodología uno

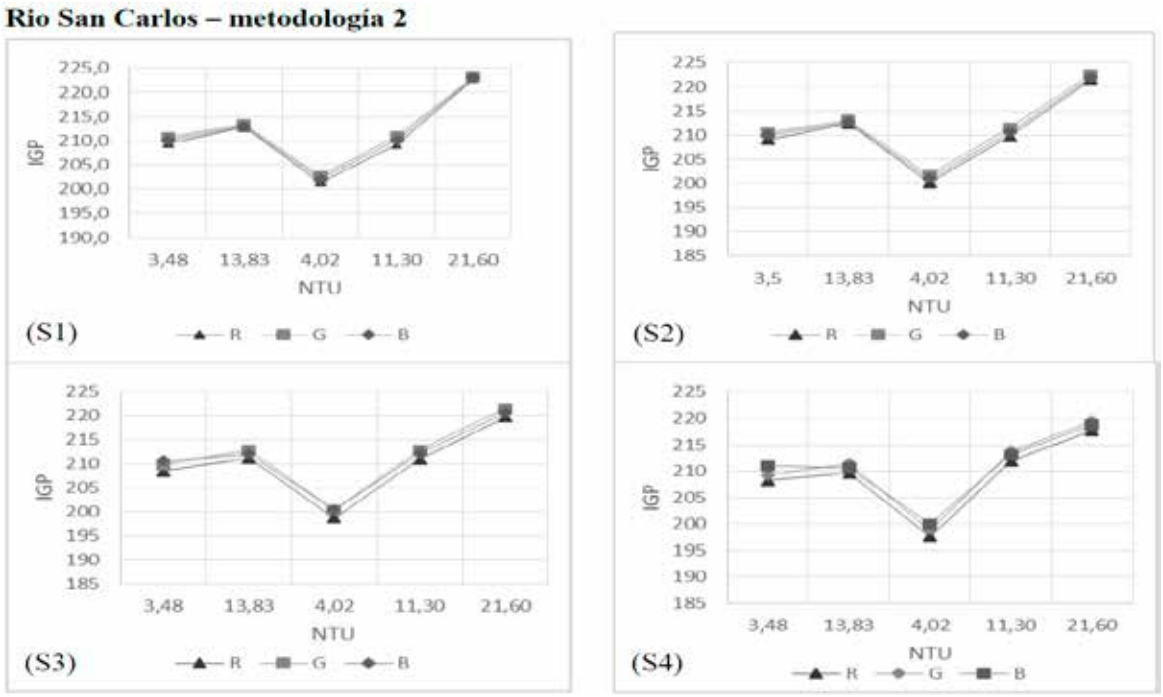

Figura 8. Intensidad de gris promedio (IGP) contra NTU utilizando la metodología dos en la DSLR y en CLB.

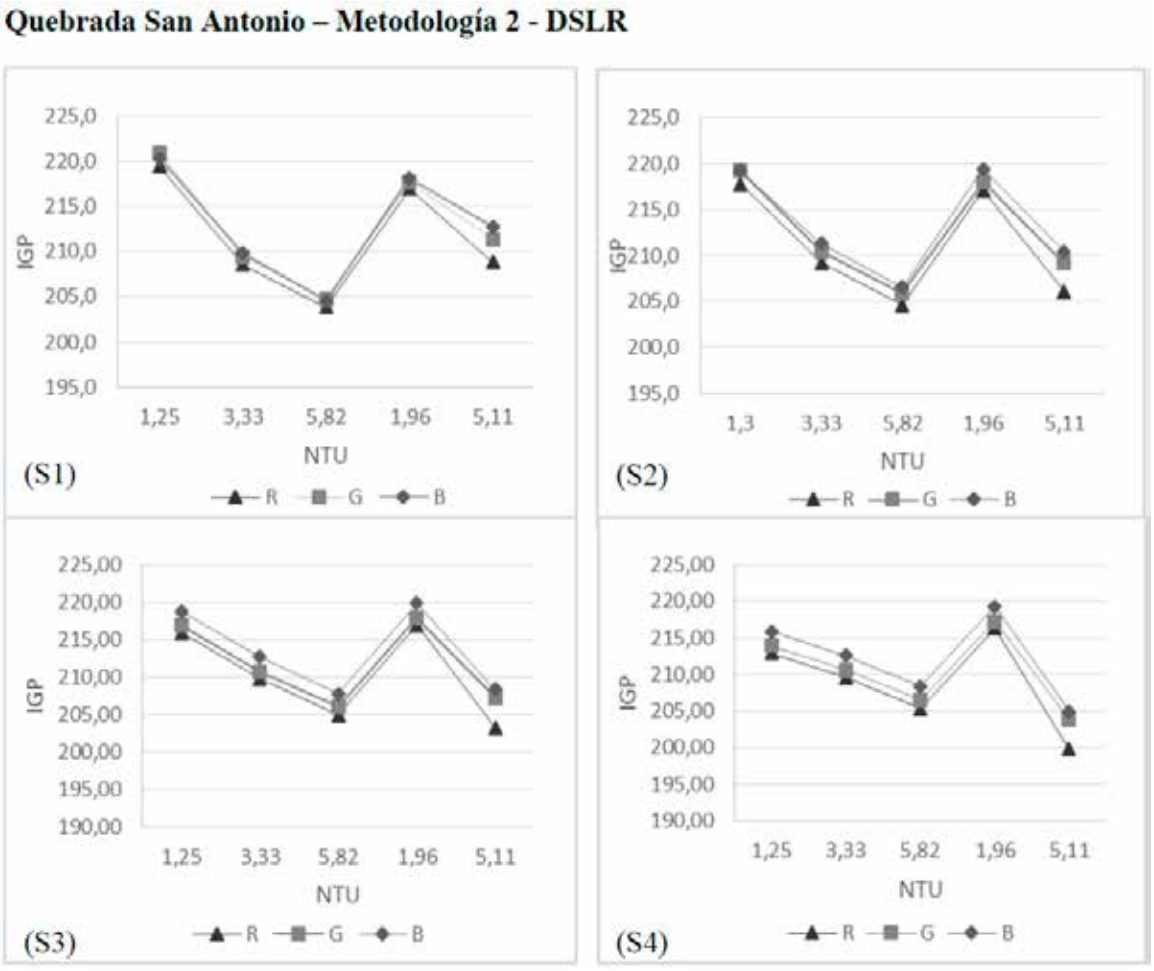

Figura 10. Intensidad de gris promedio contra NTU para todos los sectores utilizando la DSLR para la metodología dos

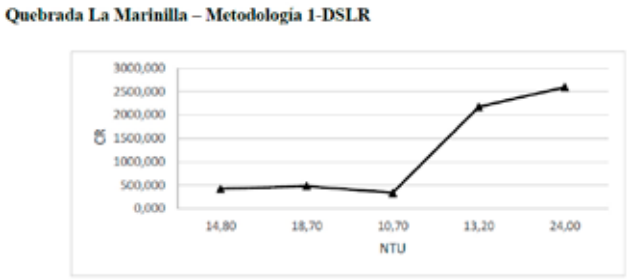

Figura 11. Razón de color contra NTU en las muestras de la quebrada la marinilla utilizando la DSLR para la metodología uno en BAB

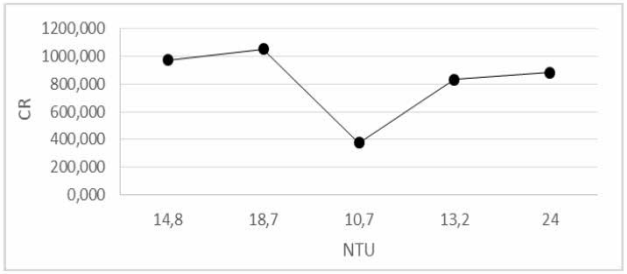

Figura 13. Razón de color contra NTU en las muestras de la Quebrada La Marinilla utilizando la CCD para la metodología uno en BAB.

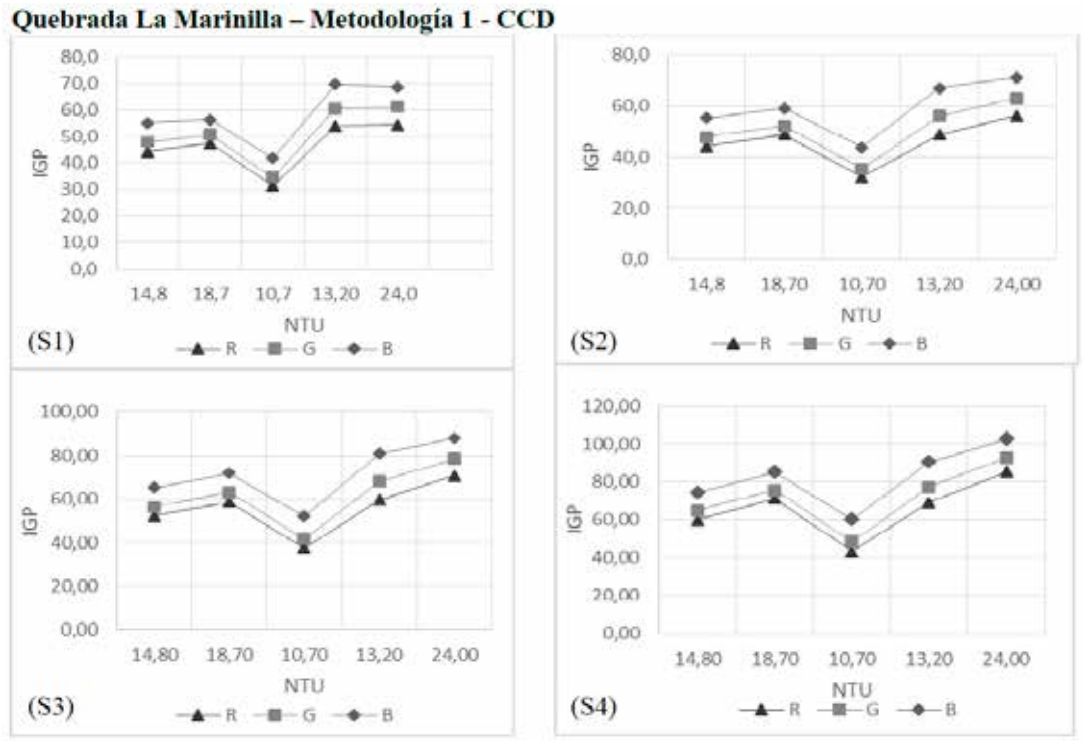

Figura 12. Intensidad de gris promedio contra NTU para todos los sectores utilizando la DSLR utilizando la metodología dos, en BAB.

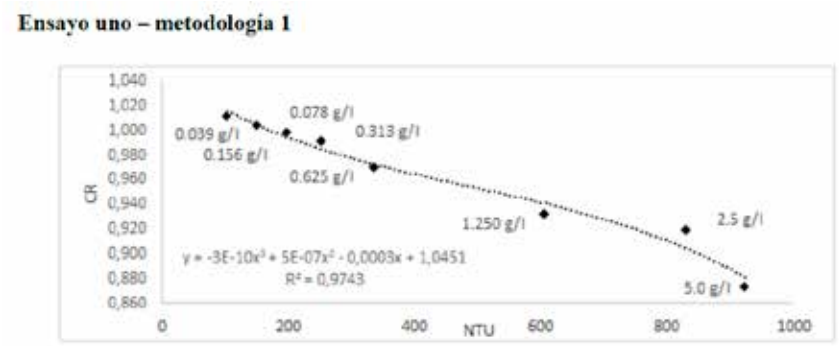

Figura 15. Razón de color contra NTU para el ensayo uno, utilizando la DSLR en el entorno CLB para la metodología uno.

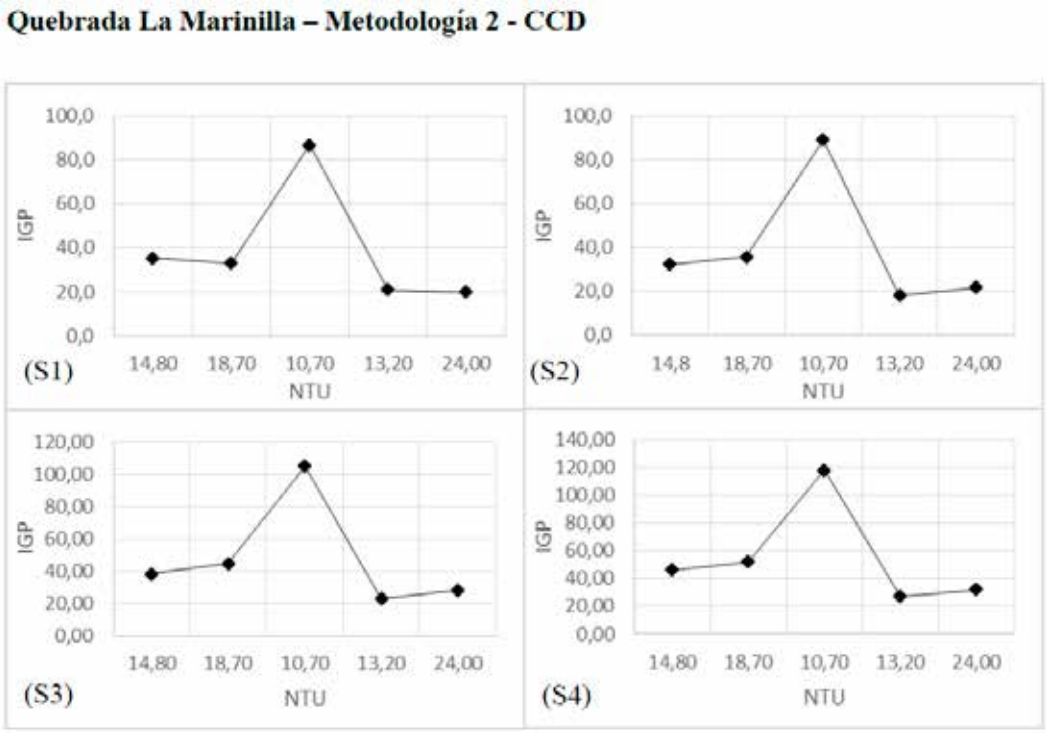

Figura 14. Intensidad de gris promedio contra NTU para todos los sectores utilizando la CCD en la metodología dos, entorno BAB

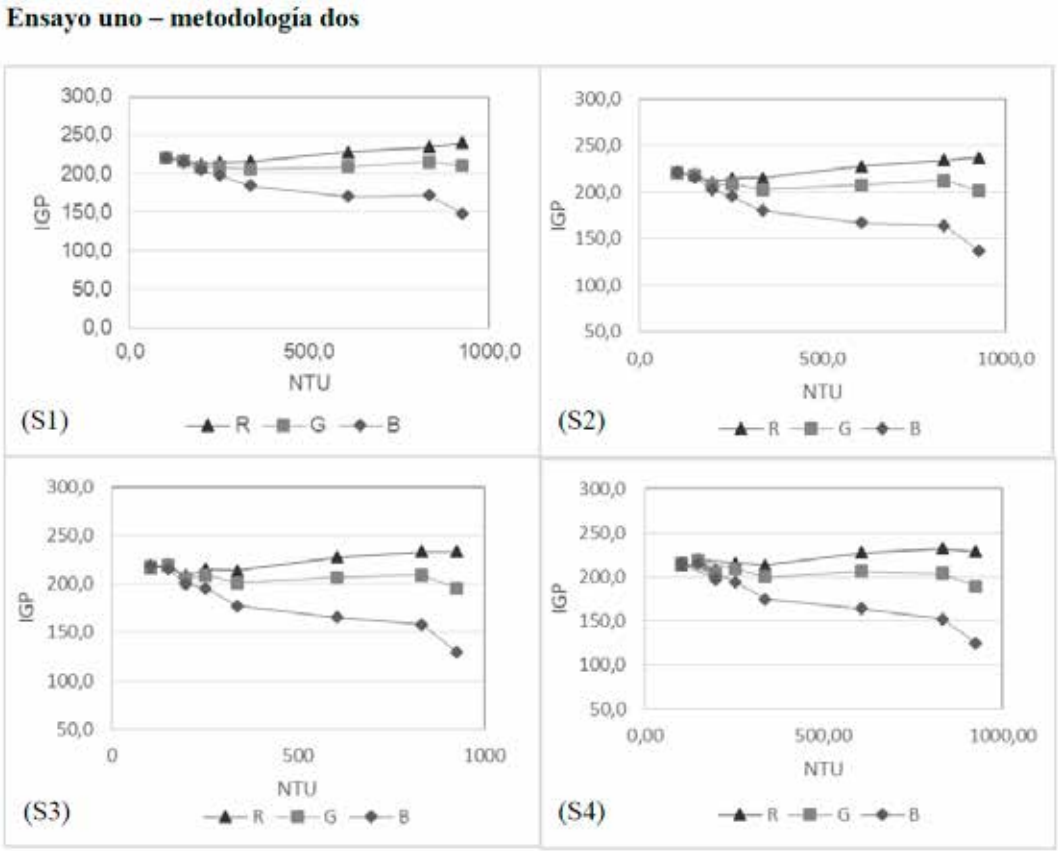

Figura 16. Intensidad de gris promedio contra NTU para todos los sectores utilizando la DSLR para la metodología dos, en CLB.

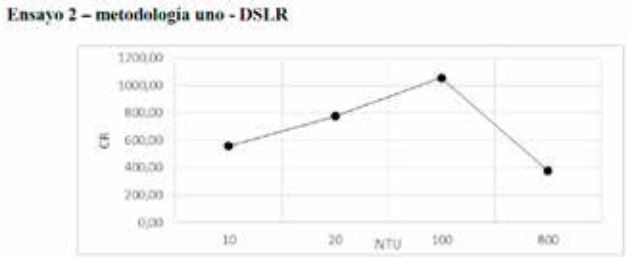

Figura 17. Razón de color contra NTU para el ensayo 2 con DSLR utilizando la metodología uno, en BAB.

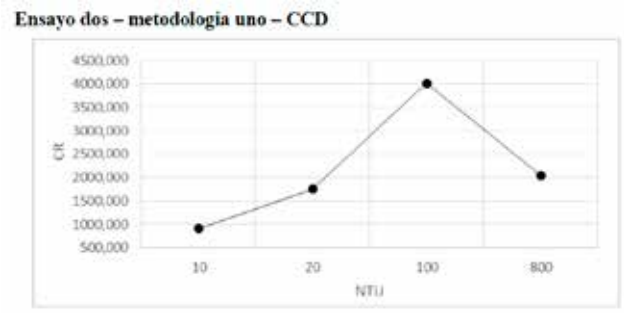

Figura 19. Razón de color (CR) contra NTU, ensayo dos utilizando la metodología uno en BAB para la CCD.

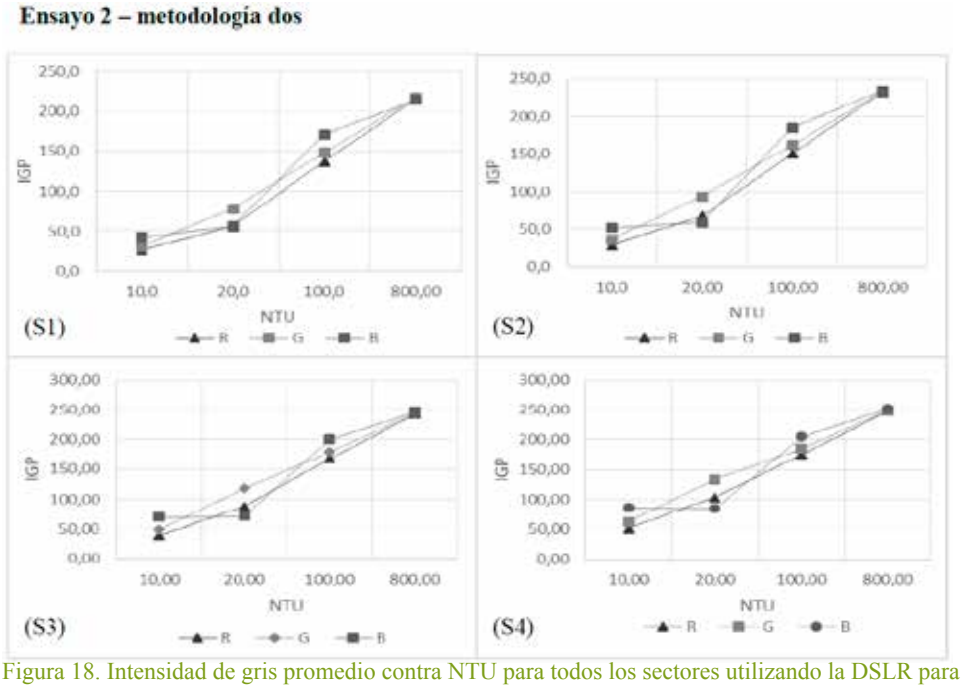

Figura 18. Intensidad de gris promedio contra NTU para todos los sectores utilizando la DSLR para la metodología dos en BAB.

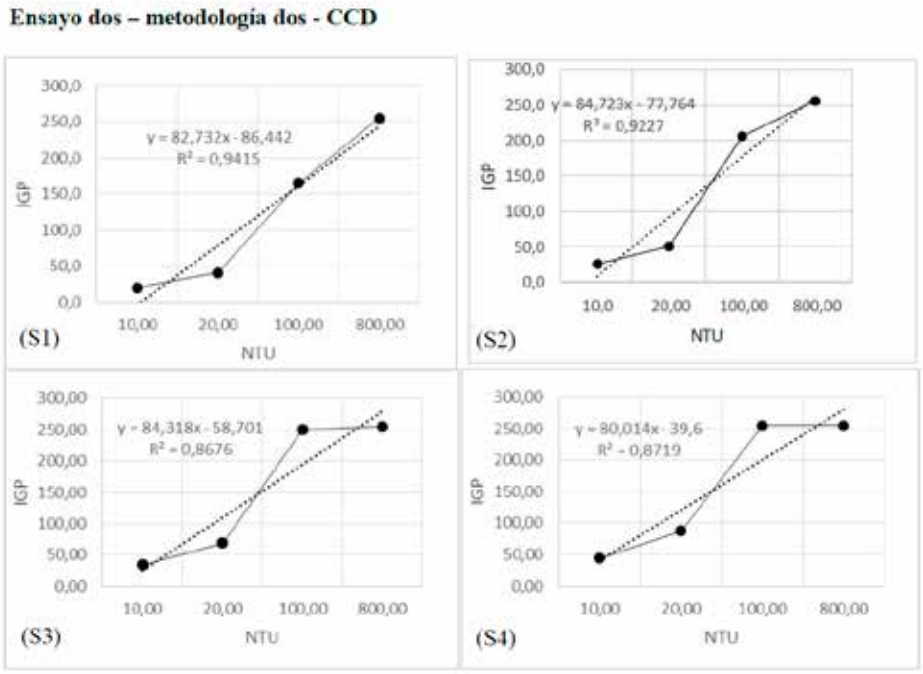

Figura 20. Intensidad de gris promedio contra NTU para todos los sectores utilizando la CCD para la metodología dos en BAB.

Conclusiones

Se evaluó la descomposición de imágenes digitales para la estimación indirecta de la turbidez en tres cuerpos de agua naturales. Se encontró una relación inversa para el caso del ensayo uno donde el aumento de turbidez reflejaba una disminución de la IGP con la DSLR utilizando la metodología uno y dos con diferencias en los canales de color evaluados. El color aparente otorgado por la turbidez de las muestras en el caso del ensayo uno, afecta de manera significativa cuál de los canales de color se ajusta mejor al momento de realizar las correlaciones. Se debe llevar a cabo más ensayos para determinar una metodología que permita disminuir la varianza presentada entre las diferentes capturas, que incluya la utilización de sólidos similares a los presentados por cuerpos de agua naturales al igual que la utilización de diferentes intensidades y tipos de iluminación.

El tipo de fondo en los entornos de captura CLB y BAB afecta la precisión de los datos extraídos de las imágenes digitales, siendo menos sensible a los cambios de NTU el fondo blanco de CLB que el negro en BAB.

Existe una correlación inversa entre la cantidad de sólidos presentes en una muestra de agua y la intensidad de luz captada por la DSLR en el ensayo uno. Para el ensayo dos la correlación era directamente proporcional al aumento de la turbidez en las muestras utilizadas.

No fue posible realizar una estimación indirecta precisa por medio de las ecuaciones de correlación obtenidas en ambos ensayos mediante los ajustes polinómicos y lineales, debido a la alta variación de la IGP en las muestras de agua naturales, derivadas de los sólidos presentes en las mismas y algunas variaciones atribuidas a las cámaras digitales utilizadas.

Agradecimientos

Los autores agradecen al Grupo de investigación Limnología y Recursos Hídricos de la Universidad Católica de Oriente, al programa de ingeniería ambiental de la misma institución por su apoyo durante todo el proceso y al docente Daniel Gómez por la ayuda brindada en las fases iniciales de la investigación.

Referencias Bibliográficas

1. World Health Organization. (2017). Guidelines for drinking-water quality, 4th edition, incorporating the 1st addendum. [online] Disponible en: http://www.who.int/water_sanitation_health/publications/drinking-water-quality-guidelines-4-including-1st-addendum/en/

2. Resolución 2115. Diario oficial de la república de Colombia, Bogotá, junio 22 de 2007

3. Allen, M.J., Brecher, R.W., Copes, R., Hrudey, S.E., Payment, P. (2008). Turbidity and Microbial Risk in Drinking Water. Prepared for The Minister of Health Province of British Columbia. http://www.wsabc.ca/wp-content/uploads/2011/04/TAC-Turbidity-Report.pdf

4. Zawbaa, H., Abbass, M., Hazman, M. and Hassenian, A. (2014). Automatic Fruit Image Recognition System Based on Shape and Color Features. Communications in Computer and Information Science, pp.278-290.

5. Byers, J. (2006). Analysis of Insect and Plant Colors in Digital Images Using Java Software on the Internet. Annals of the Entomological Society of America, 99(5), pp.865-874.https://doi.org/10.1603/0013-8746(2006)99[865:AOIAPC]2.0.CO;2

6. Sun, X., Gong, H., Zhang, F. and Chen, K. (2009). A Digital Image Method for Measuring and Analyzing Color Characteristics of Various Color Scores of Beef. 2009 2nd International Congress on Image and Signal Processing.doi: 10.1109/CISP.2009.5302150

7. Choodum, A., Boonsamran, P., NicDaeid, N. and Wongniramaikul, W. (2015). On-site semi-quantitative analysis for ammonium nitrate detection using digital image colourimetry. Science & Justice, 55(6), pp.437-445. http://dx.doi.org/10.1016/j.scijus.2015.05.001

8. Firdaus, M., Alwi, W., Trinoveldi, F., Rahayu, I., Rahmidar, L. and Warsito, K. (2014). Determination of Chromium and Iron Using Digital Image-based Colorimetry. Procedia Environmental Sciences, 20, pp.298-304.doi: 10.1016/j.proenv.2014.03.037

9. Lopez-Molinero, A., Liñan, D., Sipiera, D. and Falcon, R. (2010). Chemometric interpretation of digital image colorimetry. Application for titanium determination in plastics. Microchemical Journal, 96(2), pp.380-385.doi: 10.1016/j.microc.2010.06.013

10. Lopez-Molinero, A., Tejedor Cubero, V., Domingo Irigoyen, R. and Sipiera Piazuelo, D. (2013). Feasibility of digital image colorimetry—Application for water calcium hardness determination. Talanta, 103, pp.236-244.http://dx.doi.org/10.1016/j.talanta.2012.10.038

11. Goddijn, L. and White, M. (2006). Using a digital camera for water quality measurements in Galway Bay. Estuarine, Coastal and Shelf Science, 66(3-4), pp.429-436. DOI: 10.1016/j.ecss.2005.10.002

12. Kohl, S., Landmark, J. and Stickle, D. (2006). Demonstration of Absorbance Using Digital Color Image Analysis and Colored Solutions. Journal of Chemical Education, 83(4), p.644.

13. Cantrell K., Erenas, M., de Orbe-Payá, I. and Capitán-Vallvey, L. (2010). Use of the Hue Parameter of the Hue, Saturation, Value Color Space As a Quantitative Analytical Parameter for Bitonal Optical Sensors. Analytical Chemistry, 82(2), pp.531-542.doi:10.1021/ac901753c

14. Dean, C., Warner, A., & McGraw J.B. (2000). Suitability of the DSC460c colour digital camera for quantitative remote sensing analysis of vegetation. ISPRS J. Photogram. 55, 105-108

15. 16 Dymond, J. and Trotter, C. (1997). Directional reflectance of vegetation measured by a calibrated digital camera. Applied Optics, 36(18), p.4314.https://doi.org/10.1364/AO.36.004314

16. Silva, W., Villegas, N. (2015). Implementación de la metodología de análisis De descomposición de Imágenes digitales para la determinación de contaminación por color en un cuerpo de agua. Investigación Básica Y

Aplicada Sobre El Parámetro Color En Los Vertimientos De Aguas Residuales Generados En El Sector Industrial Y De Servicios, Ubicado En La Jurisdicción Del Área Metropolitano Del Valle De Aburra. Tomado de http://www.metropol.gov.co/recursohidrico/Color/Informes/INVESTIGACION%20PARAMETRO%20COLOR%20EN%20VERTIMIENTOS.pdf

17. Brea, D. and Balocchi, F. (2010). Procesos de erosión – sedimentación en cauces y cuencas. [online] Unesdoc.unesco.org. Available at: http://unesdoc.unesco.org/images/0021/002163/216338s.pdf

18. Berkman, H. and Rabeni, C. (1987). Effect of siltation on stream fish communities. Environmental Biology of Fishes, 18(4), pp.285-294.

19. WOOD, P. and ARMITAGE, P. (1997). Biological Effects of Fine Sediment in the Lotic Environment. Environmental Management, 21(2), pp.203-217.

20. Kirk, J. (2011). Light and Photosynthesis in Aquatic Ecosystems. (3rd ed., p. 404). New York: Cambridge University Press.

21. Bilotta, G. and Brazier, R. (2008). Understanding the influence of suspended solids on water quality and aquatic biota. Water Research, 42(12), pp.2849-2861. https://doi.org/10.1016/j.watres.2008.03.018

22. Jonasz, M. and Fournier, G. (2011). Light Scattering by Particles in Water: Theoretical and Experimental Foundations. 1st ed. Elsevier Science. ISBN: 9780080548678

23. Mullins, D., Coburn, D., Hannon, L., Jones, E., Clifford, E. and Glavin, M. (2018). A novel image processing-based system for turbidity measurement in domestic and industrial wastewater. Water Science and Technology, 77(5), pp.1469-1482. doi: 10.2166/wst.2018.030

24. Zhang, X. (2017). Water Quality Turbidity Detection Based on Image Recognition System Design and Implementation. Advances In Intelligent Systems And Computing, 613, 63-70. doi: 10.1007/978-3-319-60744-3_7.

25. Belfort, B., Weill, S., & Lehmann, F. (2017). Image analysis method for the measurement of water saturation in a two-dimensional experimental flow tank. Journal Of Hydrology, 550, 343-354. doi: 10.1016/j.jhydrol.2017.05.007

26. Oh, J., Inoue, S., & Ezaki, T. (1999). The Potential Use of Digital Image in Turbidity Measurement. Journal Of Rainwater Catchment Systems, 4(2), 27-30. doi: 10.7132/jrcsa.kj00003257807

27. Sumriddetchkajorn, S., Chaitavon, K., & Intaravanne, Y. (2013). Mobile device-based self-referencing colorimeter for monitoring chlorine concentration in water. Sensors And Actuators B: Chemical, 182, 592-597. doi: 10.1016/j.snb.2013.03.080

28. Sumriddetchkajorn, S., Chaitavon, K., & Intaravanne, Y. (2014). Mobile-platform based colorimeter for monitoring chlorine concentration in water. Sensors And Actuators B: Chemical, 191, 561-566. doi: 10.1016/j.snb.2013.10.024

29. EPA (1993). METHOD 180.1 DETERMINATION OF TURBIDITY BY NEPHELOMETRY. Environmental Monitoring Systems Laboratory Office of Research and Development U.S. Environmental Protection Agency Cincinnati, Ohio 45268

30. Jaramillo, D.F. (1995). Andisoles del Oriente Antioqueño: caracterización química y fertilidad. Instituto Ciencias Naturales y Ecología-ICNE. Universidad Nacional de Colombia. Medellín. 35p

31. Mizutani, N., Saito, K., Numata, Y. (1988). Real-time monitoring of turbid water by using video camera, personal computer and image processing, in Asia Air Survey Co., Ltd. 13-16 Tamura-cho, Atsugi-shi, Kanagawa- Ken, 243, Japan.

Recibido: 10 abril 2019
Aprobado: 5 mayo 2019

RESEARCHS / INVESTIGACIÓN

Hábitos alimentarios y estado nutricional de los trabajadores de una empresa láctea del norte de Ecuador.

Food habits and nutritional status of workers in a dairy company in northern Ecuador.

Espín Capelo Concepción Magdalena[1], González Pardo Secundino[2], Folleco Guerrero Juan Carlos[3], Quintanilla Bedón Rosa Ana[4], Silvia Marcela Baquero Cárdena[5], Chamorro Pinchao Jaqueline[6]

DOI. 10.21931/RB/2019.04.02.9

Resumen: El objetivo del presente estudio fue determinar los hábitos alimentarios y estado nutricional de los trabajadores de una empresa láctea del norte de Ecuador. Investigación observacional, descriptiva y transversal, que utilizó la encuesta a través de un cuestionario con variables sociodemográficas y antropométricas para determinar el estado nutricional; y, la frecuencia de consumo para identificar hábitos alimentarios. Los resultados reportan preponderancia del sexo masculino y etnia mestiza entre los trabajadores, con rango de edad entre los 30 a 60 años. Respecto al estado nutricional, según el Índice de Masa Corporal el 56.0% de los trabajadores presentan sobrepeso, 8.2% Obesidad nivel I, y 0.5% Obesidad nivel II. En la Circunferencia de Cintura según sexo, se encontró que en mujeres (82-88 cm) existe riesgo elevado en el 32,7 %; riesgo muy elevado (> 88 cm) y 26,5 %; en hombres el 13.5% riesgo elevado (95-102 cm) y el 5.3% riesgo muy elevado (> 102 cm). En cuanto a hábitos alimentarios, según encuesta de frecuencia de consumo el 78.0% consume de 3 a 4 tiempos comida; siendo los refrigerios los menos consumidos, los alimentos que más ingieren son arroz, papa, pan, azúcar, huevos y lácteos con frecuencia de consumo diaria y los menos consumidos son frutas, verduras y leguminosas con frecuencia de consumo de 1 vez semana. Se concluye que índice de masa corporal y circunferencia de cintura aumentan en relación con el avance de la edad y los hábitos alimentarios por exceso y desbalance nutricional.

Palabras claves: estado nutricional, hábitos alimentarios, riesgo cardiovascular, perímetro de circunferencia de cintura.

Abstract: The aim of the present study was to determine the dietary habits and nutritional status of workers in a dairy company in northern Ecuador. Observational, descriptive and transversal research, which used the survey through a questionnaire with sociodemographic and anthropometric variables to determine the nutritional status; and, the frequency of consumption to identify eating habits. The results report a preponderance of the masculine sex and mestizo ethnicity among the workers, with an age range between 30 and 60 years. Regarding the nutritional status, according to the Body Mass Index, 56.0% of workers are overweight, 8.2% Obesity level I, and 0.5% Obesity level II. In the Waist Circumference according to sex, it was found that in women (82-88 cm) there is a high risk in 32.7%; very high risk (> 88 cm) and 26.5%; in men 13.5% high risk (95-102 cm) and 5.3% very high risk (> 102 cm). In terms of eating habits, according to the frequency of consumption survey, 78.0% consume 3 to 4 meal times; being the less consumed refreshments, the foods that ingest the most are rice, potatoes, bread, sugar, eggs and dairy with frequent daily consumption and the less consumed are fruits, vegetables and legumes with a frequency of 1 week consumption. It is concluded that body mass index and waist circumference increase in relation to the advance of age and eating habits due to excess and nutritional imbalance.

Key words: nutritional status, dietary habits, cardiovascular risk, waist circumference perimeter.

Introducción

El sobrepeso y la obesidad, se han convertido en una epidemia que afecta a todos los grupos de edad a nivel mundial, se estima que 1 de cada 2 adultos presentan sobrepesos. Según la Organización mundial de la salud OMS, el sobrepeso y la obesidad es un problema de salud pública y está vinculada a la mayoría de las causas de muertes en todas las regiones excepto en África subsahariana y Asia [1-2].

El Índice de masa corporal IMC según la OMS es el indicador de obesidad y sobrepeso en los adultos , relacionando la altura y el peso , siendo obesidad grado I valores entre 30-34.9 Kg/m2, obesidad grado II entre 35-39.9Kg/m2, y obesidad III o mórbida, mayor a 40 Kg/m2 [3] , un estudio concluyó que aquellos trabajadores que presentaban obesidad severa y mórbida se asocian a patologías secundarias, y tienen un efecto significativo en el aumento de los costos en salud y en el ausentismo laboral [4].

En Ecuador las principales causas de mortalidad en adultos son las enfermedades crónicas no transmisibles ECNT, que están muy relacionadas con los malos hábitos alimentarios, según La Agencia de noticias públicas de Ecuador y Sudamérica ANDES señala que en Ecuador 6 de cada 10 personas mueren por las ECNT [5-6]; asimismo el Instituto Nacional de Estadísticas y Censos INEC señala que las principales causas de muerte en el sexo masculino y femenino son la diabetes mellitus, seguida de la hipertensión arterial. Investigaciones afirman que llevar una vida saludable podría disminuir en un 5% la mortalidad global, de igual manera concluyen que la mayoría de problemas de morbimortalidad en la actualidad están asociados directamente con la alimentación [7-8].

Tanto la obesidad como la inactividad física afectan el rendimiento laboral de un trabajador y su salud. Un estudio encontró que las personas con exceso de peso tienen dificultades para moverse

1.Magister en docencia universitaria e investigación educativa. Facultad Ciencias Salud. Carrera de Nutrición. UTN. cmespin@utn.edu.ec
2.Especialista en Anestesiología y Reanimación. Magíster en Educación superior. Facultad de Ciencias de la Salud, Carrera de Nutrición. sgonzalez@utn.edu.ec.
3.Magister en desarrollo local. Facultad Ciencias Salud. Carrera de Nutrición. UTN. jcfolleco@utn.edu.ec.
4.Doctora en nutrición y dietética. Facultad Ciencias Salud. Carrera de Nutrición. raquintanilla@utn.edu.ec
5.Magister en gerencia de salud para el desarrollo local. Facultad Ciencias Salud. Carrera de Terapia Física Médica.smbaquero@utn.edu.ec
6.Licenciada en Nutrición y salud comunitaria. jacquelinechamorro@live.com

y están restringidas a realizar sus actividades de trabajo, además sufren de constantes dolores de rodillas, espalda, pies, malestares que provocan ausentismos laborales, que disminuyen la productividad de las empresas. En respuesta la OMS considera reducir dietas mal sanas y la inactividad física [2-9].

Existen publicaciones en las que concluyen que la implementación de educación nutricional a mediano y largo plazo ayudan a corregir los malos hábitos alimentarios, y tratamientos individualizados en aquellas personas que requieran mayor grado de intervención y monitoreo, aumentando la productividad de los empleados, mejora de la imagen institucional y moderación de los costos de asistencia médica. Por lo que se considera que el ambiente laboral se vuelve un lugar idóneo para trabajar en el mejoramiento de los hábitos alimentarios y prevenir el desarrollo de ECNT [10 -11-12].

Considerando que estas personas pasan la mayoría de su tiempo en sus trabajos y los alimentos son consumidos fuera de casa, existe mayor riesgo de desarrollar enfermedades derivadas de los malos hábitos alimentarios. Por lo tanto, la situación de salud y nutrición en los trabajadores es preocupante, porque no sólo afecta su calidad de vida y la de sus familias, sino porque aumenta costos en salud y reduce su productividad, comprometiendo el desarrollo del país [13-14-15].

El objetivo del presente estudio fue determinar los hábitos alimentarios y estado nutricional de los trabajadores de una empresa láctea del norte de Ecuador. A través de los resultados se podrán establecer acciones correctivas sobre posibles problemas y/o factores de riesgo nutricionales que pudieran incidir en el estado de salud general y por ende en la calidad de vida delos trabajadores de la empresa; y, ejecutar programas de educación nutricional enfocados en cambiar algunos de los hábitos nutricionales.

Materiales y Métodos

Fue un estudio descriptivo, observacional, transversal. Donde se incluyó a todos los trabajadores de ambos sexos que desde julio del 2018 fueron reportados por la Oficina de Talento Humano de la Empresa "ALPINA", Provincia del Carchi- Ecuador, productora de alimentos lácteos.

Se excluyeron a quienes no asistieron a la toma de datos por motivo de vacaciones, maternidad, permisos y trabajadores que no firmaron el consentimiento informado para participar en la investigación, quedando una población de estudio de 182 personas. Para determinar los hábitos alimentarios se utilizó un cuestionario con base al Manual de instrumentos de evaluación dietética del 2006 considerado como el de mayor uso en muchas investigaciones por su facilidad de respuesta por parte del encuestado. Este instrumento se basa en una lista de alimentos que permite evaluar la ingesta de un alimento hasta un periodo de un año, con hábitos y frecuencia de consumo de alimentos aplicado individualmente a cada servidor de la Empresa [16-17].

El estado nutricional se evaluó mediante medidas antropométricas: peso y talla, se interpretó mediante el IMC según los criterios establecidos por la OMS. El Riesgo de Enfermedades Cardiovasculares se evaluó a través de la circunferencia de cintura, tomando como puntos de corte los establecidos por la American Diabetes Association (ADA) y según el sexo [(18)]. La tabulación y análisis de datos se realizó en SPSS versión 20.

Resultados y Discusión

De los 182 trabajadores, el 73.1% son de sexo masculino el restante 26.9% femenino, grupo predominante es el rango de 30 a 60 años de edad 54,9%, mientras que el 45.1% restante está en el rango de 18 a 29 años de edad.

Al relacionar el IMC con el sexo, se observó que el 56.0% de los trabajadores presentaron estado nutricional catalogado como sobrepeso, mientras que obesidad I el 6.6% y obesidad II el 0.5%, el sexo masculino presenta los valores más altos de exceso de peso, (tabla 1). Por el contario en relación a la circunferencia de cintura y sexo, el mayor riesgo de desarrollar enfermedades cardiovasculares se encuentra en el sexo femenino (tablas 2). (Tablas 3-4) se muestra la relación entre el IMC y edad, circunferencia de cintura y edad, destacando que los valores más altos de peso y el riego elevado de tener enfermedades cardiovasculares están entre los 30 – 60 años de edad.

GÉNERO						
IMC	Masculino		Femenino		Total	
	N°	%	N°	%	N°	%
Obesidad II	1	0.5	0	0	1	0.5
Obesidad I	12	6.6	3	1.6	15	8.2
Sobrepeso	75	41.2	27	14.8	102	56.0
Normal	45	24.7	19	10.4	64	35.2
Total	133	73.1	49	26.9	182	100.0

Tabla 1. Índice de Masa Corporal, en relación al género de los trabajadores de una empresa láctea, norte de Ecuador.

ÍNDICE DE CINTURA EN MUJERES Y HOMBRES	N°	%
Mujer < 82 Normal	20	40.8
Mujer 82 - 88 Elevado	16	32.6
Mujer ≥ 88 Muy elevado	13	26.5
Total	49	100.0
Hombre < 95 Normal	108	81.2
Hombre 95 - 102 Elevado	16	12.0
Hombre > 102 Muy Elevado	9	6.7
Total	133	100.0

Tabla 2. Índice de cintura en mujeres y hombres, de los trabajadores de una empresa láctea, norte de Ecuador.

EDAD						
IMC	18 a 29		30 a 60		Total	
	N°	%	N°	%	N°	%
Obesidad II	0	0.0	1	0.5	1	0.5
Obesidad I	5	2.7	10	5.5	15	8.2
Sobrepeso	36	19.8	66	36.3	102	56.0
Normal	41	22.5	23	12.6	64	35.2
Total	82	45.1	100	54.9	182	100.0

Tabla 3. Índice de Masa Corporal, en relación a la edad de los trabajadores de una empresa láctea, norte de Ecuador.

En cuanto a los hábitos alimentarios, en la relación del IMC y los tiempos de comida consumidos la mayoría de los trabajadores con exceso de peso tienes de 3 a 4 tiempos de comida (tabla 5).

En la frecuencia de consumo de alimentos, se destacó el mayor consumo son arroz, papa, pan, azúcar, huevos y lácteos con frecuencia de consumo diaria y los menos consumidos son frutas, verduras y leguminosas con frecuencia de consumo de 1 vez semana.

En los trabajadores evaluados predominan mayoritariamente los hombres, más de la mitad de los trabajadores se encuentran entre los 30 a 60 años de edad. Para Kenny W en su libro Physiology of Sport and Exercise, Fifth Edition menciona que en la edad adulta se presentan cambios fisiológicos como el aumento de peso desde los 25 a 45 años de edad, que trae como consecuencia sobrepeso y obesidad, así mismo una acumulación de masa grasa desde los 20 años en cantidad pequeñas, los grandes cambios se hacen notorios a partir de los 35 años de edad, así como también la reducción del metabolismo basal desde los 40 años y una disminución en la masa ósea a partir de los 35 años16, lo cual constituye un mayor riesgo de salud, porque a mayor edad aumentan los factores de riesgo y las posibilidades de enfermar [13].

CIRCUNFRENCIA DE CINTURA	EDAD					
	18 a 29		30 a 60		Total	
	N°	%	N°	%	N°	%
Mujer < 82 Normal	13	26.5	7	14.3	20	40.8
Mujer 82 - 88 Elevado	8	16.3	8	16.3	16	32.7
Mujer > 88 muy elevado	2	4.1	11	22.4	13	26.5
Total	23	47	26	53	49	100.0
Hombre < 95 Normal	54	40.6	54	40.6	108	81.2
Hombre 95 - 102 Elevado	4	8.2	14	28.6	18	13.5
Hombre > 102 Muy Elevado	1	2.0	6	12.2	7	5.3
Total	59	50.8	74	81.4	133	100.0

Tabla 4. Circunferencia de cintura en mujeres y hombres por edad de los trabajadores de una empresa láctea, norte de Ecuador.

consumir un tiempo de comida, cuando los intervalos de tiempo entre comidas son mayores da como consecuencia un exceso de apetito en la siguiente comida, en una dieta basada en 2000 calorías se comen 52 calorías extras. Un exceso de 100 -150 calorías podrían provocar sobrepeso y obesidad [22].

Los alimentos de mayor consumo son arroz, papa, pan, azúcar, huevos y lácteos con frecuencia de consumo diaria, semejantes al de la población ecuatoriana según la Encuesta de salud y nutrición ENSANUT- ECU [23]. Según una investigación realizada en trabajadores, el sobrepeso representa el porcentaje más alto de malnutrición los mismos que consumen a diario papas panes blancos, arroz con una frecuencia de 1 vez por semana [17].

Mientras que los menos consumidos son frutas, verduras y leguminosas con frecuencia de consumo de 1 vez semana datos similares al de la población ecuatoriana según la Encuesta de salud y nutrición ENASANUT- ECU [23]. La recomendación es consumir 400 gr/ día incluyendo frutas, verduras, que equivale a consumir 3 porciones de frutas y dos de verduras para cubrir con los requerimientos de fibra y micronutrientes, que necesita el organismo para prevenir ECNT y deficiencias de micronutrientes según FAO/ OMS[24].

IMC	TIEMPOS DE COMIDA									
	2		3 a 4		5 a 6		más de 6		Total	
	N°	%	N°	%	N°	%	N°	%	N°	%
Obesidad II	0	0	0	0	0	0	1	0.5	1	0.5
Obesidad I	1	0.5	12	6.6	1	0.5	1	0.5	15	8.2
Sobrepeso	6	3.3	79	43.4	16	8.8	1	0.5	102	56
Normal	3	1.6	51	28	8	4.4	2	1.1	64	35.2
Total	10	5.5	142	78	25	13.7	5	2.7	182	100

Tabla 5. IMC, en relación a los tiempos de comida consumidos por los de los trabajadores de una empresa láctea, norte de Ecuador.

En el grupo se observó un alto porcentaje de sobrepeso y obesidad, similar a estudios realizados en trabajadores ecuatorianos [13-17].En cuanto al riego cardiovascular, evaluado a través del perímetro de cinturas, fueron considerados los criterios de la ADA la cual considera que el perímetro de cintura es tal vez la herramienta más práctica y segura que dispone en la actualidad el ser humano, para conocer si está en riesgo de tener enfermedades cardiovasculares, para lo cual siguiere los siguientes puntos de corte para latinoamericanos, en mujeres <82 normal, 82-88 riesgo elevado y > 88 riesgo muy elevado, en hombres son <95 normal, 95-102 riesgo elevado y > 102 riesgo muy elevado [18].En el estudio se mostró el más de la mitad del sexo femenino presenta riesgo elevado y muy elevado, porcentaje mayor a una investigación sobre Riesgo cardiovascular en trabajadoras [19], en referencia al sexo masculino en su mayoría no presentar riego cardiovascular.

En cuanto a los hábitos alimentarios el 78.0% consume de 3 a 4 tiempos comida; siendo los refrigerios los menos consumidos; al relacionar IMC y tiempos de comida se observó que el mayor porcentaje de trabajadores que tiene un exceso de peso consumen 3 a 4 tiempos de comida, datos similares a un estudio sobre Hábitos alimentarios y actitudes hacia el cambio en trabajadores [20]. La ingesta calórica a lo largo del día, debe ser de 5 tiempos de comida, lo que hace que el perfil del hambre sea más estable y menos intenso según un estudio realizado en trabajadores [21]. Se asume que los trabajadores omiten los refrigerios y prefieren consumir los 3 platos principales por motivo de falta de tiempo. Según la FAO una alimentación adecuada, debe incluye el consumo de 2 refrigerios o colaciones durante el día, es así que, cada 4 horas se debe

Conclusiones

La mayoría de la población son de género masculino 73.1% de nacionalidad ecuatoriana 98.4%; mestizos en el 98.9%; solo el 0.5% es de etnia afro- ecuatoriana. Respecto a los hábitos alimentarios más de la mitad de población tiene sus tiempos de comida en el comedor de la fábrica, el 78.0% consumen de 3 a 4 comidas en el día. Los alimentos que se consumen con menor frecuencia son verduras, frutas, semillas, leguminosas, pescado, mientras que los alimentos de mayor consumo son arroz de castilla, pan, papa, azúcar blanca, huevos, leche entera, pollo y jugo de frutas naturales con azúcar. En el estado nutricional, según el indicador Índice de Masa Corporal el 56.0% de los trabajadores evaluados presentó sobrepeso, mientras que el 35.2% presentó un peso normal, representando a obesidad nivel I el 8.2% y Obesidad nivel II el 0.5%. En el perímetro de circunferencia de cintura en mujeres, el 40.8% se encuentran en un rango normal, el 59.2 restante presento riesgo de desarrollar enfermedades cardiovasculares, teniendo que el riesgo elevado 32.7% y riesgo muy elevado 26.5%, mientras que en los hombres el 81.2% se encuentra en el rango normal, el 13.5% riesgo elevado y el 5.3% muy elevado.

Referencias

1. OPS/OMS. (2014). Ecuador para la prevención de la obesidad y las enfermedades crónicas no transmisibles. [En línea]. Citado 30 04 2018.

2. OMS. (2017). Obesidad y Sobrepeso. [En línea]. Citado 30 04 2018. Disponible en: http://www.who.int/es/news-room/fact-sheets/detail/obesity-and-overweight

3. OMS. (2017). Obesidad y Sobrepeso. [En línea]. Citado 02 11 2017. Disponible en: http://www.who.int/mediacentre/factsheets/fs311/es/

4. Zarate A. Influencia de la obesidad en los costos en salud y en el ausentismo laboral de causa médica en una cohorte de trabajadores. Revista Médica Chilena. [En línea].2009 [citado May 08]; 20(2). Disponible en: http://www.revistamedicadechile.cl/ojs/index.php/rmedica/article/view/277/9.

5. Diabetes e hipertensión, dos males silenciosos que afectan la salud. El universo [en línea], 21 ene 2014 [citado 30 abr. 2018]. Disponible en: https://www.paho.org/ecu/index.php?option=com_content&view=article&id=1115:enero-21-2014&Itemid=972

6. Agencia de Noticias Públicas de Ecuador y Sudamérica. Las enfermedades no transmisibles son la principal causa de muerte en Ecuador. Ecuador: ANDES, [en línea], 07 jul 2013 [citado 30 abr. 2018].Disponible en: https://www.andes.info.ec/es/noticias/sociedad/1/enfermedades-no-transmisibles-son-principal-causa-muerte-ecuador

7. Instituto Nacional de Estadísticas y Censos. Anuario de estadísticas vitales nacimientos y defunciones 2014.Ecuador: INEC,2013, Disponible en: http://www.ecuadorencifras.gob.ec/documentos/web-inec/Poblacion_y_Demografia/Nacimientos_Defunciones/Publicaciones/Anuario_Nacimientos_y_Defunciones_2014.pdf

8. Alexis LL. Promoción de hábitos saludables en el trabajo para el bienestar de la población trabajador. Rev. Colomb Cardiol. [En línea]. 2014; 21 (4): 57-66. Disponible en: http://www.elsevier.es/es-revista-revista-colombiana-cardiologia-203-articulo-promocion-habitos-saludables-el-trabajo-S0120563314000229.

9. Carol V, Juan P, Ray T. Relación entre el estado nutricional y los grados de ausentismo laboral en trabajadores de dos empresas peruanas. Acta Med Perú. [En línea]. 2017; 34 (1): 6-17. Disponible en: http://www.scielo.org.pe/pdf/amp/v34n1/a02v34n1.pdf

10. José G. Sobrepeso, Obesidad y Riesgos Laborales. Preventionworld. [en línea]. 2014 Disponible en: https://prevention-world.com/actualidad/articulos/sobrepeso-obesidad-y-riesgos-laborales/

11. Alexis LL. Promoción de hábitos saludables en el trabajo para el bienestar de la población trabajador. Rev. Colomb Cardiol. [en línea]. 2014; 21 (4): 57-66. Disponible en: http://www.elsevier.es/es-revista-revista-colombiana-cardiologia-203-articulo-promocion-habitos-saludables-el-trabajo-S0120563314000229.

12. Natalie R, Margarita S, Fabiana P, Fernando V. E Efecto de una intervención educativa nutricional en un entorno laboral. ALAN [en línea]. 2017; 67 (2) [citado 07 05 2018].

13. Judith S, Lydia L, Carmen G, Elisa V, Fernando V. Estilos de vida, alimentación y estado nutricional en trabajadores de la construcción de la Región Metropolitana de Chile. Rev. Cubana Salud Pública [en línea]. 2014; 142 (7) [citado 07 mayo 2018]. Disponible en: http://www.scielo.cl/scielo.php?script=sci_arttext&pid=S0034-98872014000700003

14. Tamayo JA, Rodríguez K, Escobar K, Mejía AM. Estilos de vida de estudiantes de odontología. Hacia promoc. Salud. [en línea].2015; 20(2). [Citado 08 mayo 2018]. Disponible en: http://dx.doi.org/10.17151/hpsal.2015.20.2.10.

15. Serra L, Aranceta J, Rivas L, Ortega R, Salvador G, Álvarez E, et al. Nutrición Comunitaria. Rev. Med Univ. Navarra. [en línea] .2006; 50 (4) [citado 07 mayo 2018]. Disponible en: http://www.bvsde.ops-oms.org/texcom/nutricion/6-NUTRICIONc.pdf.

16. Kenney, W. Larry, Wilmore, Jack, Costill, David. Physiology of Sport and Exercise [en líneas].5 ed. Human Kinetics, 2014; [citado en 29 mayo 2018]. Disponible en: https://books.google.co.in/books?id=Ho8uBgAAQBAJ&dq=cambios+en+la+masa+grasa+y+osea+a+partir+de+los+40+a%C3%B1os&source=gbs_navlinks_s.

17. Jácome J. Influencia de los hábitos alimentarios y la actividad física en la malnutrición de los trabajadores de la "aseguradora del sur", en el periodo febrero – julio 2012. [Tesis previas a la obtención de la licenciatura en línea].Quito: Pontificia Universidad Católica Del Ecuador, Facultad de Enfermería; 2012 [citado 29 mayo 2018]. Disponible en: epositorio.puce.edu.ec/handle/22000/3491.

18. American Diabetes Association (ADA 2008). Perímetro de la cintura medida para conocer el riesgo cardiovascular y Alzheimer. [En línea]. Citado 29 mayo 2018. Disponible en: https://www.ciclobr.com/cintura.html.

19. Roma RR, José NZ, Tania TD, Isela PR, Oscar ZG, Iris GG. Detección de riesgo cardiovascular en trabajadores del sector salud con base en los criterios OMS/ JNC 7/ATP III. Rev. Med [en línea]. 2017 [citado 29 mayo 2018]; 55 (3). Disponible en: http://www.medigraphic.com/pdfs/imss/im-2017/im173e.pdf.

20. Itziar Z, María M , Ana ST , Ana RM , Juan-José B, Susana S, Alejandro FM, Hábitos alimentarios y actitudes hacia el cambio en alumnos y trabajadores universitarios españoles.Nutr. Hosp [en línea]. 2013 [citado 29 mayo 2018]; 28 (5). Disponible en: http://www.nutricionhospitalaria.com/pdf/6553.pdf.

21. Adriana M. "Conocimientos, actitudes y prácticas acerca de refrigerios durante las horas de trabajo entre los trabajadores administrativos y los trabajadores de call center y su relación con el género y las horas de trabajo en la corporación nacional de telecomunicaciones de la ciudad de Guayaquil. [Tesis previas a la obtención de la licenciatura en nutrición [en línea]. Guayaquil: Universidad Católica Pontífice del Ecuador, Facultad de Ciencias de la Salud; 2014 [Citado 29 mayo 2018]. Disponible en: http://repositorio.puce.edu.ec/bitstream/handle/22000/7522/8.29.001747.pdf?sequence=4&isAllowed=y.

22. Judith S, Lydia L, Carmen G, Elisa V , Fernando V. Estilos de vida, alimentación y estado nutricional en trabajadores de la construcción de la Región Metropolitana de Chile. Rev. Cubana Salud Pública [en línea]. 2014 [citado 29 mayo 2018]; 142 (7). Disponible en: http://www.scielo.cl/scielo.php?script=sci_arttext&pid=S0034-98872014000700003

23. Encuesta Nacional de Salud y Nutrición. Estado nutricional a partir de indicadores antropométricos. Ecuador. ENASANUT 2014. Disponible en: http://www.ecuadorencifras.gob.ec/documentos/web-inec/Estadisticas_Sociales/ENSANUT/MSP_ENSANUT-ECU_06-10-2014.pdf.

24. Organización Mundial de la Salud OMS (2018). Aumentar el consumo de frutas y verduras para reducir el riesgo de enfermedades no transmisibles. [En línea]. Citado 29 mayo 2018. Disponible en: http://www.who.int/elena/titles/fruit_vegetables_ncds/es/.

Recibido: 31 enero 2019
Aprobado: 25 abril 2019

CASE REPORTS / REPORTE DE CASO

Ocronosis exógena secundario al uso de hidroquinona. A propósito de un caso.

Exogenous ochronosis secondary to the use of hydroquinone. About a case.

Adrian Isacc Nieto Jiménez

DOI. 10.21931/RB/2019.04.02.10

Resumen: Se presenta el caso de una paciente ecuatoriana de 56 años valorada en el hospital Provincial Docente Arnaldo Miliàn Castro, Santa Clara por presentar manchas en la cara predominantemente en mejillas y frente de varios años de evolución. Tratada durante largo tiempo con hidroquinona 2% por diagnóstico de cloasma facial. Se plantearon varios diagnósticos diferenciales como la hemocromatosis y la ocronosis exógena como complicación del uso prolongado con hidroquinona. Se realiza biopsia cutánea y se concluye como ocronosis a descartar etiología. Esta entidad constituye un síndrome causado por la acumulación de ácido homogentìsico en los tejidos conectivos, puede ser endógena o exógena siendo esta última muy poco frecuente. La condición está frecuentemente asociada a alcaptonuria pero puede también ocurrir con la administración exógena de complejos fenólicos, tales como la hidroquinona. . La presentación de este caso es importante porque en la actualidad existe un gran número de cremas despigmentantes que contienen este fármaco en su fórmula y que se venden al público, por lo cual su uso y abuso es común y puede conducir al desarrollo de ocronosis.

Palabras claves: ocronosis, hidroquinona.

Abstract: We present the case of an Cuban patient of 56 years evaluated in the provincial hospital of Ibarra, Imbabura for having spots on the face predominantly on cheeks and front of several years of evolution. Treated for a long time with hydroquinone for diagnosis of facial chloasma. Several differential diagnoses, such as hemochromatosis and exogenous ochronosis, were proposed as complications of prolonged hydroquinone use. Skin biopsy is performed and it is concluded as ochronosis to rule out etiology. This entity constitutes a syndrome caused by the accumulation of homogenous acid in the connective tissues, it may be endogenous or exogenous, the latter being very rare. The condition is frequently associated with alkaptonuria but may also occur with the exogenous administration of phenolic complexes, such as hydroquinone. The presentation of this case is important because at present there is a large number of depigmenting creams that contain this drug in its formula, are sold to the public, so its use and abuse is common, and can lead to the development of ochronosis.

Key words: ochronosis, hydroquinone

Introducción

Derivado del griego ochro (amarillo) y osis (estado), ocronosis es un trastorno que se manifiesta con lesiones hiperpigmentadas, reticuladas y asimétricas, decoloración negruzca, negro-azulada o parda o negruzca de la piel, localizadas casi siempre en las regiones malar, mejillas y cuello. Suelen ser permanentes y pueden desarrollarse con el uso prolongado de fármacos y cosméticos que contengan hidroquinona y compuestos fenólicos.[1, 2,3]. Se ha postulado que el trastorno se debe a un defecto en la degradación del ácido homogentísico, y probablemente de fenilalanina y tirosina.[4]

La Ocronosis puede ser de origen endógeno –secundario a una alteración del enzima ácido homogentísico oxidasa (ahgo), variedad que se acompaña de manifestaciones renales y/o del sistema nervioso central– o bien, de origen exógeno (desarrollándose en áreas expuestas a tratamientos tópicos, lo que deriva en la formación del pigmento ocronótico característico).[5, 6]

Dogliotti ha descrito tres estadios de la enfermedad: I-eritema y pigmentación leve; II-eritema, pigmentación, milia y atrofia leve; y el III datos de Estadio II más elementos pápulonodulares eruptivos.

En años recientes, los casos documentados de ocronosis han sido secundarios a hidroquinona, sustancia presente en altas concentraciones en gran número de cremas blanqueadoras y artículos de belleza.[7, 8] Aunque en Estados Unidos y Europa se han realizado esfuerzos para suspender su comercialización y retirarlos del mercado, los productos que contienen hidroquinona no tienen restricciones de venta.[9,10,11] La formulación de numerosas cremas blanqueadoras puede incluir algún derivado de la hidroquinona, como 1,4-benzenodiol, quinol, benceno-1,4-diol, p-difenol, p-dihidroxibenceno, p-hidroxifenol, hidroquinolytequinol.[9]

La Ocronosis se observa sobre todo en mujeres negras, en la tercera o cuarta década de la vida. En la población latinoamericana, el padecimiento ha sido documentado sobre todo en fenotipos oscuros (III-V), con antecedentes de abuso en la cantidad y/o tiempo de administración de hidroquinona.[9]

Objetivo General: Considerar la Ocronosis exogena como diagnóstico y complicación del uso indiscriminado de la hidroquinona.

Caso Clínico

Paciente femenino de 56 años de edad que acudió de manera espontánea al hospital provincial docente Arnaldo Miliàn Castro en junio 2018 a consulta de medicina general por manchas color pardo negruzco en la cara de varios años de evolución. Fue enviada al servicio de Dermatología para su valoración conjunta en la Universidad de Ciencias Mèdicas en consulta multidisciplinaria.

Dr. Adrian Isacc Nieto Jiménez. Especialista en primer Grado en Medicina General Integral y Dermatología. Diplomado en Hematodermias. Profesor Asistente. Investigador Agregado. Universidad de Ciencias Médicas. Serafìn Ruiz de Zàrate Ruiz. Santa Clara. Cuba
Autor de correspondencia: adrianisacnj@gmail.com, adrianisacc.nieto@nauta.cu

Al interrogatorio, refirió como antecedente hipertensión arterial de 3 años en tratamiento médico con losartán 50 mg diarios.

El cuadro cutáneo inició tres años antes con manchas ligeramente negruzcas que fueron atribuidas a la exposición solar, por lo cual se indicó tratamiento tópico con diversas cremas a base de hidroquinona. Sin embargo, la medicación fue interrumpida tres meses previos a la visita hospitalaria aquí citada.

A la exploración física se observó dermatosis facial constituida por lesiones "maculopapulosas", negras, con aspecto de empedrado, que abarcaban mejillas,nariz, surcos nasogenianos y nasolabiales, pero respetaban la región periocular (Figuras 1,2 y 3).

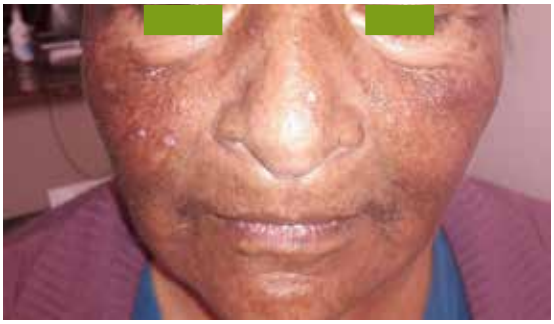

1

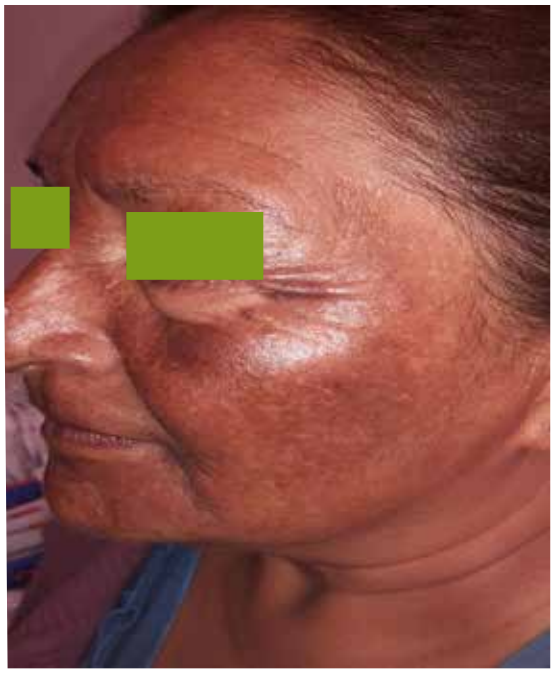

2

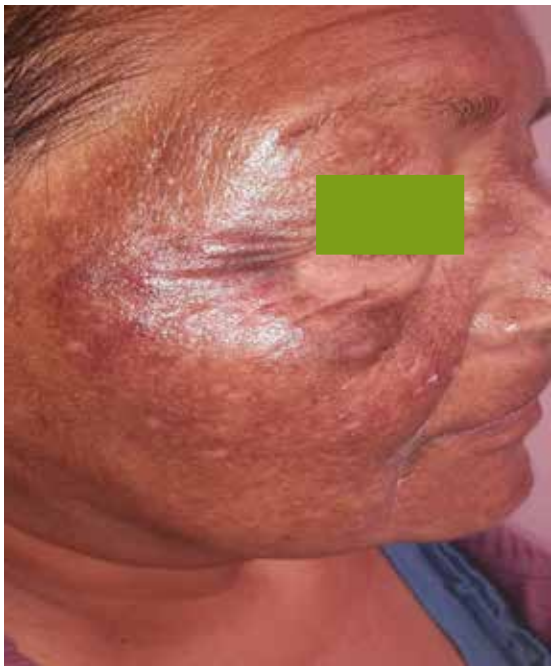

3

Figuras 1,2,3 Se observan lesiones maculo papulosas, negro parduzcas con aspecto empedrado, que abarcan mejillas, nariz, surcos naso genianos y naso labiales, pero respetaban la región peri ocular.

Se procedió a realizar biopsia cutánea con los posibles diagnósticos de Ocronosis exógena, hemocromatosis y pigmentación postinflamatoria.

El estudio histológico mostró estructuras redondas, de aspecto globular y color azul-gris, sugestivas de melanófagos por caída del pigmento. Otros hallazgos incluyeron piel reseca.

El diagnóstico es compatible con ocronosis figura 4 (histología)

Se realizaron exámenes complementarios de rutina que fueron normales.

Se inició tratamiento médico con esteroides tópicos no fluorados y tretinoina con excelentes resultados a corto plazo.

Comentarios

La ocronosis fue descrita inicialmente por Pick, en 1906, los primeros casos se asociaron, sobre todo, con la administración de fenoles hasta que, en 1976, se relacionó con el uso de hidroquinona en poblaciones de origen africano.[7, 8,9.]

Otros fármacos que se han asociado con el desarrollo de ocronosis exógena incluyen: fenol, inyecciones de quinina, resorcinol y uso prolongado de hidroquinona (en concentraciones superiores a

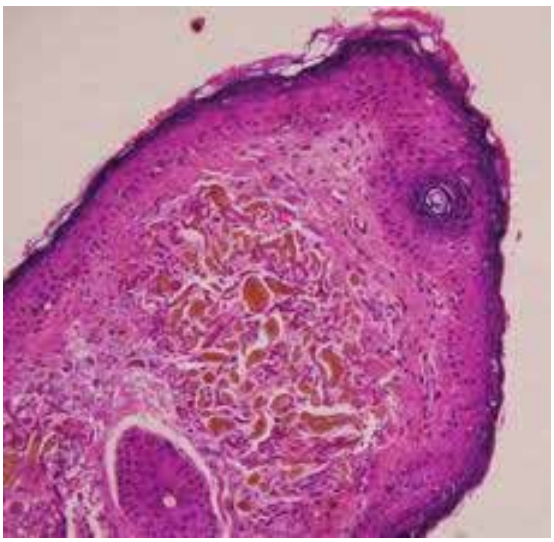

Figura 4. Estructuras redondas, de aspecto globular y azul gris, sugestivas de melanófagos por caída del pigmento.

6%), todos los cuales conducen a una alteración de la superficie corporal, particularmente en el sitio de aplicación.[6, 12]

El diagnóstico diferencial de ocronosis exógena abarca un grupo heterogéneo de trastornos que causan máculas faciales hiperpigmentadas, entre ellas: melasma; nevo de Ota bilateral; algunos tipos de hiperpigmentación inducida por fármacos como amiodarona, minociclina o metotrexato; hiperpigmentación post-inflamatoria; y dermatosis papulosa nigra.[13]

Como parte del procedimiento diagnóstico es conveniente recurrir a la dermatoscopia e histología pues permite diferenciar entre melasma y los estadios II/III de Dogliotti.

En la población latinoamericana, el padecimiento ha sido documentado sobre todo en fenotipos oscuros (III-V), con antecedentes de abuso en la cantidad y/o tiempo de administración de hidroquinona, coincidiendo con el caso planteado.[9]

En la histología con las tinciones de hematoxilina y eosina la forma exógena de ocronosis muestra la presencia de depósitos de color marrón amarillento u ocre lo cual da origen a su nombre.[1, 5]

Como parte del tratamiento, es indispensable interrumpir la administración del agente causal. El uso de ácido retinoico, corticosteroides tópicos y protectores solares puede beneficiar a algunos pacientes, aunque su eficacia es variable.[2] Algunos autores sugieren que la dermoabrasión (combinada o no con láser) y el uso de láser CO2 son buenas opciones; [14] no obstante, los mejores resultados, hasta el momento, se han logrado con el láser Q-switch de Alexandrita 755 nm. [14]

Conclusiónes

El presente caso ilustra una complicación del uso prolongado de hidroquinona tópica. Siempre que el médico utilice esta sustancia, deberá especificar la duración del tratamiento y realizar controles periódicos, pues es frecuente que los pacientes continúen la administración sólo porque "se siente bien" y pueden adquirir el producto sin receta.

Referencias

1. Snider R, Thiers B. "Exogenous Ochronosis". J Am Acad Dermatol 2017; 28(1): 662-664.
2. Zawar VP, Mhaskar ST. "Exogenous ochronosis following hydroquinone for melasma". J Cosmet Dermatol 2017; 3: 234-236.
3. Kundu R. "Consideraciones especiales para el tratamiento tópico de la piel de determinados grupos étnicos". En: Wolf K, Goldsmith L, et al. Dermatología en Medicina General, 7ª ed, Buenos Aires, Editorial Médica Panamericana, 2016, pp. 2142-2143.
4. Vélez H, Borrero J. Restrepo J, Rojas W. "Diccionario dermatológico. Dermatología Fundamentos de Medicina". 7ª ed., Corporación para investigaciones Biológicas, Medellin, Colombia, 2015, p. 93.
5. Vélez H, Borrero J. Restrepo J, Rojas W. "Diccionario dermatológico. Dermatología Fundamentos de Medicina". 7ª ed., Corporación para investigaciones Biológicas, Medellin, Colombia, 2014, p. 93.
6. Levyn C, Maibach H. "Exogenous ochronosis: an update on clinical features, causative agents and treatment options". Am J Clin Dermatol 2014; 2(4): 213-217.
7. Jordan H, Van Niekerk D. "Transepidermal elimination in exogenous ochronosis. A report of two cases". Am J Dermatopathol2013; 13: 418-424.
8. Picardo M, Carrera M. "New experimental treatments for melasma and other hyperpigmentations". Dermatol Clin 2013; 25: 353-362.
9. Olumide Y, Akinkugbe A, Altraide D. "Complications of chronic use of skin lightening cosmetics". Int J Derm 2015; 47: 344-353.
10. Dogliotte M, Liebowitz M. Granulomatous ochronosis –a cosmetic- induced skin disorder in blacks. S Afr Med J 2014; 56:757-60.
11. Findley G, Morrison J, Simon I. "Exogenous ochronosis and pigmented colloidmilium from hydroquinone bleaching creams". Br J Dermatol 2015; 93: 613-622.
12. Kundu R. "Consideraciones especiales para el tratamiento tópico de la piel de determinados grupos étnicos". En: Wolf K, Goldsmith L, et al. Dermatología en Medicina General, 7ª ed, Buenos Aires, Editorial Médica Panamericana, 2016, pp. 2142-2143.
13. Vargas F, Valdez P, Arenas R. "La ocronosis exógena: ¿Qué tanto la diagnosticamos o la diferenciamos del melasma?" Dermatol CMQ 2014; 10(2): 143-147.
14. Rivas J, Schettini A, Cavalcante M. "Exogenous ochronosis hydroquinone induced: a report of four cases". An Bras Dermatol 2014; 85(5): 699-703.

Recibido: 2 abril 2019
Aceptado:2 mayo 2019

NEWS AND VIEWS / NOTICIAS Y OPINIONES

Hormonal signaling factors produced by brown adipose tissue as regulators of metabolism of carbohydrates and lipids

Francisco Santacruz-Hidalgo[1], Eliana Viscarra-Sanchez[1].

DOI. 10.21931/RB/2019.04.02.11

Abstract: Brown adipose tissue is one of the principal generators of heat in the body; due to the activation of many hormones and receptors, it takes a fundamental role in thermogenesis. However recent studies have proved that this is not its only function. Brown adipose tissue could also act as an endocrine organ, which means that it releases chemical substances to the blood and regulate some activities in the organism. This cell communication process is momentous, since allowing cells to exchange physicochemical information with the environment and other cells in the body could be a relevant field of study in treatments of obesity, diabetes and other diseases related with body weight. This paper offers an overview of different transcriptional factors, endocrine regulation and therapeutic applications of the brown fat tissue, and also the distinctions that it has with white adipose tissue and beige adipose tissue.

Keywords: thermogenesis, brown adipose tissue, endocrine regulation, transcriptional factors.

Introduction

Brown adipose tissue (BAT) is considered as an endocrine organ because besides it causes oxidation of products to generate heat, it also secretes signaling factors to all the body that activate metabolism of lipids and carbohydrates. This factor is studied to treat diseases like obesity, that according to Centers for Disease Control and Prevention (CDC), it is estimated that in 2015–2016, 93.3 million (39.8 percent) American adults and 13.7 million (18.5 percent) American children and teens are clinically obese [1].

Brown Adipose Tissue (BAT) is made of brown adipocytes and progenitor cells of adipocytes as well. It has a significant number of mitochondria, which give it this brown coloration. It was thought that this tissue is only present in newborns, but it has been proved that is still present in adults as a response of cold, generating thermogenesis and it is activated principally by exercise that helps irisin releasing, which is a hormone that can convert white adipose tissue to brown adipose tissue [2].

One of the principal functions of brown adipose tissue is the activation of thermogenesis through decoupling protein UCP-1 (thermoginin), which is the protein principally involved in generating heat through thermogenesis. For this to happen, norepinephrine must be released first, to obtain the fatty acids from the triglycerides that activate UCP-1, the mitochondria will import the fatty acids that remain and here the thermogenesis will take place with the dissipation of energy as heat [3]

What is brown adipose tissueInformal definitions, the Brown adipose tissue it´s a conformation of adipocytes with rich content of mitochondria, which is inherent to mammals and could represent an evolutionary advantage to survive during the early stages of life, nocturnal and hibernal cold, among others. The development of this tissue probably took place during the early development of mammals, and in contrast to other mammalian organs it could be considered as "new organ". [4]
It also is related to non-shivering thermogenesis and endocrine control of metabolism, that is directly associated to the pathophysiology of distinct fat depots. Unlike white fat, this organ can dissipate significant amounts of chemical energy through uncoupled respiration and heat production [5].

Different types of adipocytes

We can distinguish between 2 significant groups of adipocytes, classified as white, beige and brown. White adipose tissue (WAT) consist mainly of white adipocytes, which are rounded cells that serve as storage of triglycerides, which are capable of save the excess energy obtained by ingesting food. Also, they function as thermal insulators, protection against mechanical damage and secretion of adipokines. The metabolic functions of WAT are associated with inflammation, insulin resistance and type 2 diabetes [5]. In the other hand brown adipose tissue (BAT) was discovered in hibernating mammals and newborns, where it helps to maintain adequate core temperature. It differs from WAT principally in the number of mitochondria present per cell and a central nucleus (in white adipose tissue the nucleus is located in the periphery). Brown adipocytes can emerge in white adipose depots by the action of prolonged cold exposure, this arising of BAT is called "browning" or "beiging". It's known that the high thermogenic capacity of the tissue contributes to energy expenditure [5]. The term beige adipose tissue is used to describe an intermediate state between white adipose tissue and brown adipose tissue.

Development and location of BAT

Expression of a thermogenic program in adipose tissue is orchestrated by a piece of sophisticated transcriptional machinery that involves a plethora of transcription factors, co-activators, and co-repressors [5].

In the following list, we are going to mention some of the transcriptional regulators in the brown/beige adipose tissue function.

Francisco Santacruz-Hidalgo1, Eliana Viscarra-Sanchez1.

1School of Biology Science and Applications, Yachay Tech University of Technology and Research, Ecuador.

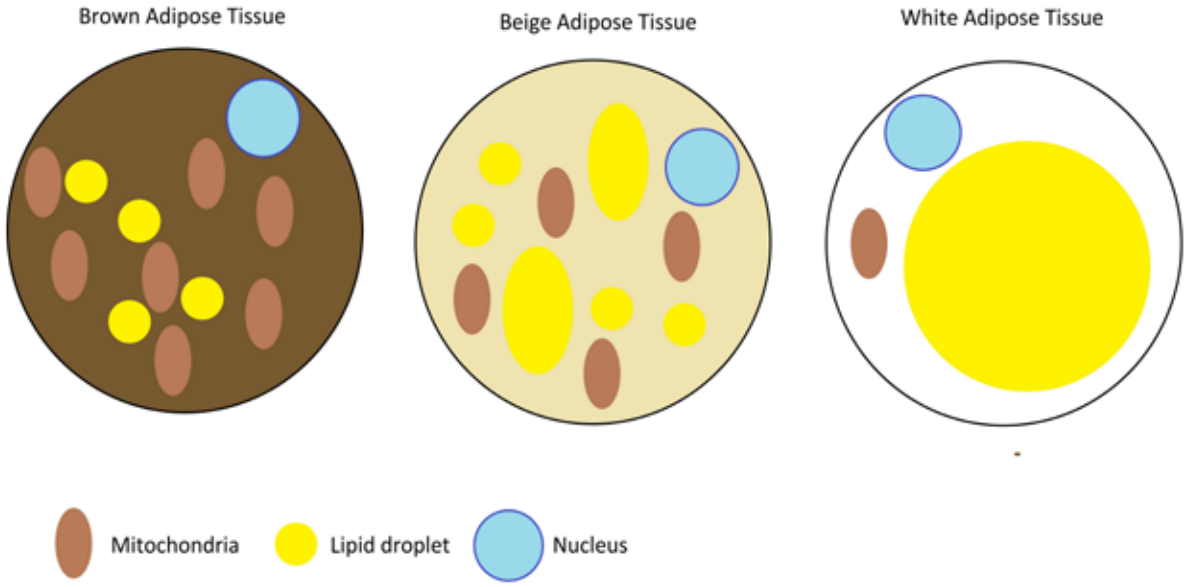

-Figure 1 Representation of the different type of adipocy

	White adipose tissue	Beige adipose tissue	Brown adipose tissue
Localization (humans)	Subcutaneous, intra-abdominal	Cervical, parasternal, supraclavicular, para- and prevetebra	Cervical, parasternal
Mitochondrial content	Low	Low to high	High
UCP1 expression	Low	Basal: Low Stimulated: high	High
Adaptive thermogenesis	Negative	Basal: Low Stimulated: high	High
Energy metabolism	Energy storage	Stimulated: energy dissipation	Energy dissipation
Obesity and diabetes	Positive correlation	Negative correlation	Negative correlation

Table 1 Characteristics of white, beige and brown adipose tissue

PPARγ complex (peroxisome proliferator-activated receptor gamma)

Is one transcriptional regulator of adaptive thermogenesis, it regulates its function by cold exposure, during exercise or fasting periods inducing the activation of PGC1α co-activator or by thyroid hormone receptors. The overexpression of PGC1α promotes the expression of UCP1 and mitochondrial enzymes in the respiratory chain

PRDM16

It is a transcriptional co-regulator. In a study, the overexpression of this molecule in myogenic precursor cells was enough to reprogram these cells to brown adipogenesis. It is related also in the control of muscle generation. The PRDM16 molecule interacts with PPARα/PPARγ and CCAAT/enhancer binding protein, leading to an induction of brown fat genes and the repression of fat white genes. [5]

Retinoids

Other transcriptional activators of BAT are the vitamin A metabolites or also called retinoids. This molecule induces the expression of UCP1 in adipocytes through nuclear receptors of retinoic acid and retinoid X receptors; this response it has been identified as an enhancer of the UCP1 promoter. Experiments done with mice suggest that high administration of retinoids reduce the body weight in mice in a high-fat diet[5].

BAT in endocrine regulation

BAT is considered an endocrine organ due to substances it secretes, such as hormones and cytokines that coordinate a response in the immune system, also TNF alfa, adiponectin (a hormone involved in lipids and fatty acids metabolism), leptin (a hormone that regulates appetite and thermogenesis). BAT exclusively secretes Batokynes, and some of them are needed to maintain a stable temperature, such as FGF21 (fibroblast growth factor is a protein present in mammals that can pass through the hematoencephalic barrier and act in brain areas). IGF-1 (Insulin like growth factor 1), neuregulin 4, interleukin 6 and others like prostaglandins and adenosine that play an autocrine role, being the white adipose tissue, heart, liver and also brain the target organs for these released factors [2]

BAT in metabolism

Brown adipose tissue is also related to lipidic and glucidic metabolism, because it has a high absorbance of glucose in its mitochondria, through GLUT-1 and GLUT-4 transporters. Due to it is involved in the elimination of triglycerides in association with LPL (lipoprotein-lipase), which is a protein that hydrolyzes triglycerides into fatty acids, allowing them to be available for trans-membrane transporters like CD36, that identifies cell surface molecules [3].

Toll-like receptors (TRL), proteins that are part of immune system, are involved in the absorption of fatty acids in the adipose tissue to increase the HDL in co-working with Vascular Endothelial Growth Factor (VEGF), which is another protein that increases the permeability of lipoproteins, increasing the expression of LPL.

Batokynes have also been studied in animals, and it has been identified that they act in the same way as in humans. Because when brown adipose tissue was implanted in lab rats, there was an increase in the consumption of glucose and insulin sensibility, which implies a healthier metabolism. For this reason, in the future, they could be used to create new medicines and drugs against diseases like diabetes and actually, nowadays, scientists are developing cellular models of human brown adipocytes cultures in vitro to be studied and allow the creation of treatments with this molecules to be consumed by people as medicine [6].

Sympathetic neural and gastrointestinal control of BAT

The sympathetic nervous system innervates the BAT, and it controls the activation of the thermogenesis. BAT thermogenesis is triggered by releasing epinephrine, stimulating β3-adrenoreceptors that later in a cascade of events ends with the activation of the UCP1. It has a sensory innervation that functions responding to changes in temperature. SNS also monitor the lipolysis of the tissue [7]. Oxidation products as matured hop bitter acids (MHBA) induce the secretion of gastrointestinal hormone cholecystokinin in the digestive tracts, elevating the Calcium ions levels in the enteroendocrine cells and activating the innervation by SNS, increasing the temperature of the BAT in mice [8].

Therapeutic applications of BAT

Activation of brown/beige adipose tissue is a strategy for treatments against obesity and promote metabolic health. There are many methodologies used to carry out this activation, including:

BMP8b and adrenergic-induced remodeling of neurovascular network

Overexpression of bmp8b gene in adipose tissue enhances browning of subcutaneous depots and maximal thermogenic capacity. This experiment carried out in genetically modified mice, demonstrate that the sympathetic innervation in fat has increased. An increase in innervation as we have seen it's fundamental to trigger the metabolism of fatty acids [9]BMP8b-induced browning, increased sympathetic innervation and vascularization of AT were maintained at 28 °C, a condition of low adrenergic output. This reinforces the local trophic effect of BMP8b. Innervation and vascular remodeling effects required BMP8b signaling through the adipocytes to 1.

PR domain zinc finger protein 16

It is one of the few transcriptional components that differ from brown and white adipose tissue, the overexpression of this gene in fibroblast or adipocyte precursors could lead into a stimulation a gene programming for mitochondrial biogenesis [10].

Conclusion

BAT is present in all the stages of human life; this discovering had great importance in the development of new strategies against metabolic and weight-related diseases.

BAT is considered an endocrine organ, which is involved in the metabolism of white fat and control of the body temperature.

There are some different forms to stimulate the activation of this tissue, including cold exposure, exercising and fasting. Also, WAT can be encouraged by genetic engineering by the use of BMP8b, PRDM16 and some others.

Most of the BAT experiments have been done in rodents and used cold stimulation. These studies demonstrate that it does not contribute in high amounts to overall metabolism, meaning that weight loss is not significant, but more research is needed to give meaningful conclusions.

References

1. Cereijo R, Giralt M, Villarroya F. Thermogenic brown and beige/brite adipogenesis in humans. Ann Med. 2015;47(2):169–77.

2. Benito M. Papel del tejido adiposo blanco, marrón y perivascular. 2015;303. Available from: https://www.analesranf.com/index.php/mono/article/viewFile/1575/1659

3. Olsen JM, Sato M, Dallner OS, Sandström AL, Pisani DF, Chambard JC, et al. Glucose uptake in brown fat cells is dependent on mTOR complex 2-promoted GLUT1 translocation. J Cell Biol. 2014;207(3):365–74.

4. CANNON B. Brown Adipose Tissue: Function and Physiological Significance. Physiol Rev [Internet]. 2004;84(1):277–359. Available from: http://physrev.physiology.org/cgi/doi/10.1152/physrev.00015.2003

5. Fenzl A, Kiefer FW. Brown adipose tissue and thermogenesis. Horm Mol Biol Clin Investig. 2014;19(1):25–37.

6. Enerba S, Bat H. Minireview Human Brown Adipose Tissue Minireview. Cell Metab [Internet]. 2010;11(4):248–52. Available from: http://dx.doi.org/10.1016/j.cmet.2010.03.008

7. Bartness TJ, Vaughan CH, Song CK. Sympathetic and sensory innervation of brown adipose tissue. Int J Obes [Internet]. 2010;34(S1):S36–42. Available from: http://dx.doi.org/10.1038/ijo.2010.182

8. Yamazaki T, Morimoto-Kobayashi Y, Koizumi K, Takahashi C, Nakajima S, Kitao S, et al. Secretion of a gastrointestinal hormone, cholecystokinin, by hop-derived bitter components activates sympathetic nerves in brown adipose tissue. J Nutr Biochem [Internet]. 2019;64:80–7. Available from: https://doi.org/10.1016/j.jnutbio.2018.10.009

9. Pellegrinelli V, Peirce VJ, Howard L, Virtue S, Türei D, Senzacqua M, et al. Adipocyte-secreted BMP8b mediates adrenergic-induced remodeling of the neuro-vascular network in adipose tissue. Nat Commun [Internet]. 2018;9(1):4974. Available from: http://www.nature.com/articles/s41467-018-07453-x

10. Yuan X, Dong M, Lee HJ, Jin W. Brown adipose tissue and its therapeutic application. Sci Bull. 2016;61(19):1498–503.

Received: 10 January 2019
Approved: 20 April 2019

NEWS AND VIEWS / NOTICIAS Y OPINIONES

The structure of Neurexin 1α (n1α) and its role as synaptic organizer

Marjorie Zambonino[1] and Pamela Pereira[2]

DOI. 10.21931/RB/2019.04.02.12

Abstract: α - and b-neurexins (NRXNs) are transmembrane adhesion protein complexes localized in presynaptic membranes into neurons and interact with the postsynaptic neuroligins (NLGNs). Our findings indicate that the neurexin 1α (n1α) is a synaptic organizer that directs postsynaptic development in neurons, evidenced in GABAergic neurons and trials with Knock-out Mice. Also, the interactions between hypervariable surfaces of n1α and ligands (neurexophilin, a-dystroglycan, and GABAA) promotes a proper protein-binding recognition, and consequently, a better synaptic adhesion.

There is a direct relationship between mental disorders and the n1α assemblage because NRXN1 gene encodes for n1α proteins which are involved in the transmission of information into the brain. For this reason, damage in this complex-protein or some neurexin gene variations causes pathological abnormalities and neuropsychiatric diseases such as schizophrenia, autism spectrum disorders, and intellectual disabilities.

Keywords: neurexin 1α, transmembrane adhesion protein, neuropsychiatric alterations, Knock-out mice, synaptic adhesion.

Introduction

The molecular dynamic of neurons consists of projections between several postsynaptic partners trough different connections. In neural circuits, the structure of n1α carries out connectivity through a synaptic adhesion and directs the neural postsynaptic development such as the interconnection of GABAergic neurons (neurons that use GABA as its neurotransmitter)[1].

N1α are a type of synaptic organizers anchored mostly to the pre-synaptic membranes that promote synapse formation through signaling and trans-synaptic adhesion.[2] The global organization of n1α is a combination of flexible and rigid binding domains, which composition promote the allosteric regulation of protein partner binding and the synaptic cleft. The singular shape of n1α is produced by interplay the structural elements within modules of laminin, neurexin or globulin, and with other postsynaptic arrangements like NLGNs.[3]

On the other hand, diseases linked to the malfunction of the n1α have a broad spectrum. This protein-complex is directly linked to the synapses of neurons and the subsequent processing of information into neural circuits.[4] This review will explain the architecture and the functioning of the n1α, and likewise, its impact both in synapsis organization and in the development of some types of pathologies such as autism and schizophrenia. As a result of any malfunction, damage, mutation or deletion in the NRXN1 gene.

Definition and structure of Neurexin 1α

Neurexins are important synaptic cell adhesion molecules (CAMs) from a family of mostly presynaptic adhesion proteins involved in neuronal networks.[5] They form trans-synaptic complexes with postsynaptic neuroligins and other binding partners in the synaptic cleft such as endogenous ligands including LRRTM family members (a transmembrane protein that leads presynaptic differentiation in contacting axons), neurexophilin (neurexin-binding proteins), a-dystroglycan and GABAA receptors[2]. The

Illness	NRXN1α Damage	Neurological Effects
Schizophrenia	• Deletion of many parts of the gene that codifies for the protein. [17] • The copy number variation (this affect the neurocognitive skills, personality determinants, etc.) [4]	Patients present a distorted perception of reality, for example, hears voices that are not there or thing that someone wants to hurt them.[14]
Autism spectrum Disorder	• Missense mutations and deletions that occur in the exons of genes that codify for the protein.[17,19] • Variation of copy numbers occurred in NRXN1 are associated with cognitive capability and language development disorders related to autism. [4]	People with this illness have difficulty in engaging in social relationships and presenting repetitive and restrictive behaviors.[16]
Intellectual Disability	• Copy number variation/Deletion of a part of the gene that encodes for the protein. [19]	Patient presents a difficulty for learning and has an intellectual IQ under the normal standards.[18]

Table 1: (Pereira J. Some diseases related to variations of neurexin1α. Ibarra; 2018). The table shows 3 of the most severe neurological illness related to the variations into neurexin1α. We can see that (CNV) is the constant factor that concern to the majority of neurological illness linked to variations of NRXN1α.

Universidad de Investigación de Tecnología Experimental Yachay Tech
[1,2] School of Biological and Applied - Biomedical Engineering Department.
https://orcid.org/0000-0001-8519-02261, https://orcid.org/0000-0002-0708-54792

extracellular domain consists of three neurexin repeats (I, II and III) containing the LNS-EGF-LNS modules. Three EGF-like repeats intersperse the six LNS domains, and six splice inserts SS1-SS6 which interact with proteins as the Figure 1A shows and the cytoplasmic tails that interact with exocytotic machinery.[2,5]

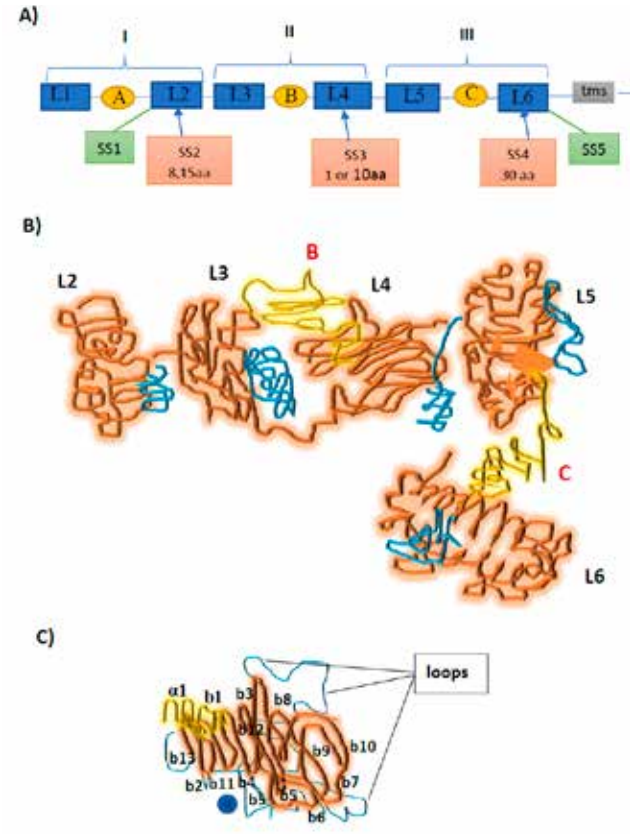

Figure 1. A) N1α is composed of six LNS or LG domains (blue squares) interspersed by three EGF like repeats (yellow ovals A, B, C). L6 is linked to a transmembrane segment (tms). Neurexin repeats I, II and III contains the splice inserts. B) A ribbon diagram of bovine n1a with domains L2–L6. The yellow compartments are b strands and α helices; loop b11-b12 is shown in blue, and the EGF-like repeats are in orange. There are imperceptible N-linked oligosaccharide chains attached to the complex. C) The n1α complex with b-loops and the ''hypervariable surface'' that carries a Ca2+-binding site (blue sphere).

The n1α is expressed by the NRXN1 gene located on chromosome 2p16.3 that spans 1.12 Mb and contains 23 exons, being one of the most significant known human gene.[6] It is exposed to relatively frequent damage including mutations, missense changes, translocation, complete gene deletion, and intragenic copy number alterations.[7]

Moreover, they contain an O-linked carbohydrate attachment sequence and a cysteine loop domain. Therefore, α NRNXs are diversified synaptic organizers with alternative mRNA splicing, which allows the formation of the ''transsynaptic dialog'' and the synapse maturation for a transmission efficiency[6,8].

To solve the structure of n1α, an X-ray crystallography of bovine neurexin is used to obtain a resolution of 2.65 A° and n1a+SS3 to 2.95 A°. The crystal structure reveals an L-shaped molecule separated in repeats I, II and III. The first one is flexible due to the L1 and EGF-A are nonvisible; the second repeat is a horseshoe-shaped L3-EGF-B-L4 globular structure and repeats III adopts an L5-EGF-C-L6 extensive configuration. Furthermore, they contain a hypervariable surface with loops conformed by a Ca2+-binding site and splice inserts SS2, SS3, and SS4. [3,8] (Figure 1 C)

Synaptic functioning

Due to the hypervariable surfaces of L2, L3, L4, L5, and L6 are putative binding sites of one side of the molecule, interacting ligands would assemble on just one side of the extracellular domain. This characteristic facilitates presynaptically tethered n1α to select multiple conventions of protein-partner recognition.[9] (Figure 1B)

Spatial n1α architectures suggest a sizeable macromolecular complex in the synaptic cleft, where protein partners interact with two LNS domains. By this way, they are capable of acting in a cell-specific way. One evidence is the synapses formed between GABAergic-cholinergic motor neurons of the motor circuit of nematode Caenorhabditis elegans and the body wall muscles.[1] The n1α directs the outgrowth of dendritic spine-like structures due to post-synaptic morphological development, but it is not necessary for synaptic connectivity with muscles.

Furthermore, the assemblage of cascades of synapses in overlapping neural circuits is significant for an organism's survival, by integrating and processing sensory inputs to motor outputs. The communication between neurons via synapses is essential for the transformation of information and cognitive performance in the brain.[10] N1α is also required for calcium-triggered neurotransmitter release and the correct working of voltage-gated calcium channels in the synapses of the brainstem and neocortex.[19]
Technics for studying n1α:

To understand the synaptic protein network, the levels of α neurexins and their ligands have to be manipulated in animal models. In the first place, the methods to analyze the conformational structure and flexibility of n1α, are based on the configuration of the LNS domains, L2 and L6 (which contain protein binding sites):

- Individual particle electron tomography (IPET), allows the 3D reconstruction of 110 n1α protein molecules L1-L6 at ~15 Å. These individual particles are large, multi-domain synaptic organizers like contactin-associated, protein-like-2 (CNTNAP2) and calsyntenin-3 (CLSTN3)[1].

- X-ray crystallography to analyze the structure of n1 α L2-L3 to 2.8 Å.

- SAXS, to determine the impact of splice insert SS6 on the flexibility of n1 α repeat III (L5-EgfC-L6), and consequently in neuronal activity.

This kind of methods determines the allosteric control and protein partner biding of n1 α architecture platform. On the other hand, scientist do some experiments with a knock out rats using techniques of molecular biology. This method of knockout (KO) animals is useful to demonstrate the essential role of the NRXN genes in synaptic transmission, extracellular synaptic interactions and the regulation of N- and P/Q-type Ca2+ channels.[11]

They produce a heterozygous partial deletion in the n1α gene (NRXN1, 2p16.3) and make comparisons between the behavior of knock out individuals and normal ones, to show that alterations in n1α cause ASD.[12] The behavioral testing of mice consists of multiple deletions of the a-isoforms of NRXN to analyze the phe-

notypes of relevance to human disorders. Mice have exposed to anxiety, cognitive, social and buried food tasks, which alterations are symptoms of autism in some human patients. The investigators perform three trials with an open field, light/dark box, and elevated plus maze in both male and female individuals.[10,11]

The results of genotype-phenotype correlation present in Nrxn1α KO Mice (with the absence of NRNX1), shows that knock out mice present some behavioral symptoms highly associated with ASD.[12] Also, the male population suffer more of reduced locomotor activity, reduced nest building, abnormal pattern of spatial memory and an increase of anxiety/altered social behaviors like aggression, social impairment and inflexibility/stereotype.[12,13]

Neuropsychiatric disorders

The dysfunction of n1α protein and alterations in genes encoding neurexins or neuroligins cause variations in excitatory and inhibitory transmission. The hemizygous exonic deletions within the NRNX 1 gene is involved in neuropsychiatric diseases and cognitive illnesses such as intellectual disability, developmental delay, autism spectrum disorder (ASD) and schizophrenia (SZ).[8] For the proper study in human, mammals contain three neurexin genes (NRXN1-3), which encodes for two isoforms, an extracellularly longer α -neurexins and shorter b-neurexins.[3]

Schizophrenia

Schizophrenia is a severe mental illness that affects the perception of the individual by altering the reality[14] directly. There are some critical factors that affect the correct function of n1α: the copy number variations, the single nucleotide polymorphism (SNP), point mutations and gene deletions.[4]

The development of this disease is due to interactions between n1α and the isoforms of neuroligin and neurexin-attach organic compounds that form neurexophilins. This complex is involved in the mechanism of the differential electric potential of calcium channels, which is essential in the synaptic transmission of information on the brain.[15] On the other hand, the chromosomal copy number variations (CNV) include genes involved mainly in sensory perception. Therefore, any n1α gene deletion affects neurocognitive skills/deficits and cause psychiatric disorders.[4]

Autism

Autism spectrum disorder (ASD) covers many symptomatologies and phenotypic expression that make social interactions difficult.[16] One strong evidence is the missense mutations and deletions in exons which produce abnormal n1α. Besides, scientific studies showed that CNVs in n1α are associated with cognitive capability alterations and language development disorders related to autism[17]

In this sense, CNVs are a vital source of genetic variation resulted in phenotypic diversity and evolution; but its high amount leads a copy number polymorphism (an indicator of genomic instability) and pathogenesis like cancer disease. Experimental trials with computational programs demonstrate that many mutations and abnormal frequencies in CNVs, during transmission between generations, change the secondary structure and the functionality of n1α protein, and consequently, produce ASD. [4]

Intellectual disabilities

Intellectual disability is a term used when a person has some limitations in their brain functioning. This illness prevents a healthy development in communication and social skills because it produces a slow learning process and a minor intellectual coefficient.[18] The leading cause is a deletion of a part of the gene that codifies for n1α protein, making difficult the transmission of information into the brain.[19,20]

Conclusions

Neurexins 1α is essential transmembrane cell-adhesion proteins that modulate synaptic activity in the central and peripheral nervous system. The n1α architecture influences the transmission of information on the brain and the proper recruitment and organization of n1α protein partners. This is essential for better performance in regulation and synaptic transmission between neural circuits.

NRXNs damage represents a synaptic failure that affects immediately their proper releasing of full potential and contributes to a broad spectrum of neuropsychiatric disorders such as autism and schizophrenia. The variation in CVG that encode for α-NRXN1 is the most critical factor because of duplications, deletions or mutations in the gene that can be catastrophic for the individual.

There are some new methods in the molecular biology field to study the conformation and the functionality of the neurexin 1α, such as the tomography IPET, X-ray crystallography, SAXS, and knockout animals. The last one (KO), has allowed the modification of the genome of rats in order to make advances in studies of pathologies that affect the human's neuronal activity directly, and help to perform more reliable clinical trials to improve the quality of patients.

References

1. Philbrook A, Ramachandran S, Lambert C, Oliver D, Florman J, Alkema M et al. Neurexin directs partner-specific synaptic connectivity in C. elegans. Neuroscience. 2018;5.

2. Liu J, Misra A, Reddy M, White M, Ren G, Rudenko G. Structural Plasticity of Neurexin 1α: Implications for its Role as Synaptic Organizer. Journal of Molecular Biology. 2018;430(21):4325-4343.

3. Miller M, Mileni M, Comoletti D, Stevens R, Harel M, Taylor P. The Crystal Structure of the α-Neurexin-1 Extracellular Region Reveals a Hinge Point for Mediating Synaptic Adhesion and Function. Structure. 2011;19(6):767-778.

4. Wang, K. (2017). The influence of neurexin 1 gene variants on cognitive ability in multiplex schizophrenia families. 1st ed. Tunku Abdul Rahman, p.133.

5. Chen F, Venugopal V, Murray B, Rudenko G. The Structure of Neurexin 1α Reveals Features Promoting a Role as Synaptic Organizer. Structure. 2011;19(6):779-789.

6. Jenkins A, Paterson C, Wang Y, Hyde T, Kleinman J, Law A. Neurexin 1 (NRXN1) splice isoform expression during human neocortical development and aging. Molecular Psychiatry. 2015;21(5):701-706.

7. Ching M, Shen Y, Tan W, Jeste S, Morrow E, Chen X et al. Deletions of NRXN1 (neurexin-1) predispose to a wide spectrum of developmental disorders. American Journal of Medical Genetics Part B: Neuropsychiatric Genetics. 2010;:n/a-n/a.

8. Chen L, Jiang M, Zhang B, Gokce O, Südhof T. Conditional Deletion of All Neurexins Defines Diversity of Essential Synaptic Organizer Functions for Neurexins. Neuron Article. 2017.

9. Rabaneda L, Robles-Lanuza E, Nieto-González J, Scholl F. Neurexin Dysfunction in Adult Neurons Results in Autistic-like Behavior in Mice. Cell Reports. 2014;8(2):338-346..

10. Neuroligins and neurexins link synaptic function to cognitive disease. Nature [Internet]. 2008 [cited 25 November 2018];455:903-911. Available from: https://www.nature.com/articles/nature07456

11. Grayton H, Missler M, Collier D, Fernandes C. Altered Social Behaviours in Neurexin 1α Knockout Mice Resemble Core Symptoms in Neurodevelopmental Disorders. PLoS ONE. 2013;8(6):e67114.

12. Esclassan F, Francois J, Phillips K, Loomis S, Gilmour G. Phenotypic Characterization of Nonsocial Behavioral Impairment in Neurexin 1 Knockout Rats. Behavioral Neuroscience. 2014;Volumen 129(1):12.

13. Laarakker M, Reinders N, Bruining H, Ophoff R, Kas M. Sex-Dependent Novelty Response in Neurexin-1α Mutant Mice. PLoS ONE. 2012;7(2):e31503.

14. National Institute of Mental Health Office of Science Policy, Planning, and Communications Science Writing, Press, and Dissemination Branch. SCHIZOPRENIA. United States; p. 6.

15. Borna G, Breuer D, Wang S, Rohlmann A, Coulon P, Vakili P. Modulation of synaptic function through the α-neurexin–specific ligand neurexophilin-1. aInstitute of Anatomy and Molecular Neurobiology, Westfälische Wilhelms-University. 2014;10.

16. U.S. Department of Health and Human Services National Institutes of Health National Institute of Mental Health. Autism Spectrum Disorder. United States; 2015 p. 8.

17. Enas K, Taiga K, Katsuhiko T. Neurexins and neuropsychiatric disorders. 1st ed. Shinshu, Japan; 2017.

18. Lujambio A, Sáenz A, Nava L, Piña C, Escobar M, etc al. Discapacidad intelectual. Mexico D.F; 2010 p. 59.

19. Supaporn Y, Oradawan P, Thanya S, Rawiwan R, Tippawan H. Mutation Screening of the Neurexin 1 Gene in Thai Patients with Intellectual Disability and Autism Spectrum Disorder. GENETIC TESTING AND MOLECULAR BIOMARKERS. 2014; Volume 18:6.

20. Sudhof T. Synaptic Neurexin Complexes: A Molecular Code for the Logic of Neural Circuits. Leading Edge Review. 2017;25.

Received: 9 April 2019

Accepted: 11 May 2019